

DEVELOPMENT OF SUPERIOR ASPHALT RECYCLING AGENTS

Phase I: Technical Feasibility

Technical Progress Report

By
Jerry A. Bullin
Charles J. Glover
Richard R. Davison
Moon-Sun Lin
Jay Chaffin
Meng Liu
Clint Eckhardt

April 1996

Work Performed Under Contract No. DE-FC04-93AL94460

For
U.S. Department of Energy
Office of Industrial Technologies
Washington, DC

By
Texas Transportation Institute
College Station, Texas

DISCLAIMER

This report was prepared as an account of work sponsored by an agency of the United States Government. Neither the United States Government nor any agency thereof, nor any of their employees, makes any warranty, express or implied, or assumes any legal liability or responsibility for the accuracy, completeness, or usefulness of any information, apparatus, product, or process disclosed, or represents that its use would not infringe privately owned rights. Reference herein to any specific commercial product, process, or service by trade name, trademark, manufacturer, or otherwise does not necessarily constitute or imply its endorsement, recommendation, or favoring by the United States Government or any agency thereof. The views and opinions of authors expressed herein do not necessarily state or reflect those of the United States Government or any agency thereof.

This report has been reproduced directly from the best available copy.

Available to DOE and DOE contractors from the Office of Scientific and Technical Information, P.O. Box 62, Oak Ridge, TN 37831; prices available from (615)576-8401.

Available to the public from the U.S. Department of Commerce, Technology Administration, National Technical Information Service, Springfield, VA 22161, (703)487-4650.

DEVELOPMENT OF SUPERIOR ASPHALT RECYCLING AGENTS

Phase I: Technical Feasibility

Technical Progress Report

By

**Jerry A. Bullin
Charles J. Glover
Richard R. Davison
Moon-Sun Lin
Jay Chaffin
Meng Liu
Clint Eckhardt**

April 1996

Work Performed Under Contract No. DE-FC04-93AL94460

**Prepared for
U.S. Department of Energy
Office of Industrial Technologies
Washington, DC**

**Prepared by
Texas Transportation Institute
College Station, Texas**

PREFACE

This report documents the technical progress made on the DOE funded project "Development of Superior Asphalt Recycling Agents" for the time period covering August 2, 1994 through August 1, 1995. Cost sharing for this study is being supplied by the Texas Department of Transportation and the Texas Advanced Technology Program. Bruce Cranford and Merrill Smith are the Program Managers for the DOE Office of Industrial Technologies. Porter Grace and Ken Lucien are the Technical Managers for the DOE Albuquerque Operations Office. Frank Childs, the Project Technical Monitor, is on the staff of Sciencetech, Inc., Idaho Falls, Idaho. Professors Jerry A. Bullin, Charles J. Glover and Richard R. Davison are the Co-Principal Investigators and are co-authors of this report along with post-doctoral researcher Moon-Sun Lin, current PhD candidates Jay M. Chaffin and Meng Liu, and technician Clint Eckhardt.

Work supported by the U.S. Department of Energy, Assistant Secretary for Energy Efficiency and Renewable Energy, Office of Industrial Technologies, under DOE Albuquerque Operations Office Cooperative Agreement DE-FC04-93AL94460.

This is the second annual progress report for the project. This report and the previous report can be obtained as indicated by the notice inside the front cover. The description of the initial report is similar to this report except, the report number is DOE/AL/94460-1, it is dated July 1995, and it has the DOE assigned-identification number DE95016702.

TABLE OF CONTENTS

	Page
Preface	i
Table of Contents	ii
List of Figures	vii
List of Tables	x
Chapter	
1 Introduction and Summary	1
Chapter	
2 Materials Production	6
Asphalt Fractionation	6
Background	6
Fractionation	9
Aged Asphalt Production	10
3 The Effect of Asphalt Composition on the Formation of Asphaltenes and Their Contribution to Asphalt Viscosity	12
Experiments	13
Methodology	13
Blend Preparation	14
Oxidative Aging	15
Results and Discussion	15
Effects of Saturates in the Absence of Original Asphaltene	15
Effects of Saturates in the Presence of Original Asphaltene	22
Conclusions	27
4 Compositional Optimization for a Superior Asphalt Binder	28
Experiments	30
Methodology	30

	Oxidative Aging	31
	Results and Discussion	31
	Aromatic and Supercritical Fraction Compositions	31
	Hardening Susceptibility (HS)	33
	Asphaltene Formation Susceptibility (AFS) and Viscosity-Asphaltene Relationship	35
	Viscosity-Temperature Susceptibility	40
	Conclusions	42
5	The Use of HPLC to Determine the Saturate Content of Heavy Petroleum Products	45
	Materials	48
	Methods	49
	HPLC Standards Preparation	49
	Instrumentation and Sample Preparation	49
	Response Factor Determination	50
	Results and Discussion	51
	Pure Saturates	51
	Asphalt Saturate Contents	53
	Conclusions	55
6	The Kinetics of Carbonyl Formation in Asphalt	56
	Experimental Design	58
	Results and Discussion	59
	Stage 1	59
	Stage 2	62
	Activation Energies and Reaction Orders	72
	The Initial Rapid Rate Region	73
	Implications of the Results	73
	Conclusions	75
7	Preliminary Experiments Using Supercritical Fractions as Asphalt Recycling Agents	77

Materials	77
Asphalts for Supercritical Fractionation	77
Industrial Supercritical Fractions	78
Commercial Recycling Agents	78
Experimental Methods	79
Supercritical Fractionation	79
Aged Asphalt Production	79
Recycled Blend Comparison	81
Properties Testing	82
Results and Discussions	82
RTFO and PAV Test Comparison	82
POV Test Comparison	84
Conclusions	91
8 The Use of Lime and Amines in Recycling Asphalt	92
Experimental Design	93
Experimental Methods	95
Lime-Asphalt Blending	95
Recycled Asphalt Blending	95
Results and Discussion	95
Lime Treated Asphalts	95
Lime Treated Recycled Material	97
Amine Experiments	98
Lime Additive Data Manipulation	101
Conclusions	108
9 Development of a Microductility Test	110
Experimental Methods	110
Original Method	110
Modifications	111
Results and Discussion	111

	Conclusions	112
10	Economic Summary	114
	The Rose Refining Process	115
	Superior Asphalt Pavement	116
	Capital Cost	116
	Maintenance	116
	Energy Use	117
	Waste	117
	Recycled Asphalt Pavement	118
	Capital Cost	118
	Maintenance	118
	Energy Use	119
	Waste	119
	Other Supporting Calculations	120
	Baseline Energy Consumption	120
	Amount of Pavement Material Repaired, per year	120
	Amount of Binder in the Pavement Repaired, per year	120
	Market Penetration	121
	Miles/year of Pavement Recycled	121
	Energy Efficiency Improvement	121
	Binder Saved by Recycling	121
	Energy Savings Associated with the Recycled Binder	121
	Energy Cost of the Recycling Agent (Excluding Processing Cost)	121
	Energy Cost of Processing the Recycle Agent	122
	Energy Efficiency Improvement	122
	Energy Savings Result	122
	Capital Investment	122
	Bbl of Recycle Agent Required per Mile of Pavement	122

Size or Capacity of a Typical RA Production Unit	123
Installed Cost/Bbl of Recycle Agent	123
Installed Cost/mile	123
References	124
Abbreviations	131
Notation	132
Appendix A: Experimental Methods	133
Supercritical Fractionation	133
Process Description	133
Aged Asphalt Production	136
Pressure Oxygen Vessel (POV)	137
Corbett Analysis	139
Corbett Analysis Using N-Hexane Precipitation and High Performance Liquid Chromatography (HPLC)	139
Fourier Transform Infrared Spectroscopy (FTIR)	140
Dynamic Mechanical Analysis (DMA)	140
Gel Permeation Chromatography (GPC)	141
Microductility Measurements	141
Appendix B: DOE-OIT Spreadsheets	142

LIST OF FIGURES

	Page
Figure 2-1. Giant Corbett Apparatus	8
Figure 3-1. HS of SHRP AAA-1 Saturates/Aromatics Blends	16
Figure 3-2. HS of SHRP AAA-1 Naphthene Aromatics	16
Figure 3-3. AFS of SHRP AAA-1 Saturates/Aromatics Blends	17
Figure 3-4. $\eta_{0,60C}^*$ Versus %AS for Aged SHRP AAA-1 Saturates/Aromatics	18
Figure 3-5. E_{VIS} Versus %AS for Aged SHRP AAA-1 Saturates/Aromatics	19
Figure 3-6. $E_{VIS}/\%$ AS for Unaged SHRP AAA-1 Asphaltene/Saturates/Aromatics	21
Figure 3-7. HS Versus $1/T$ for SHRP AAA-1 Saturates/Aromatics Blends	22
Figure 3-8. HS Versus $1/T$ for SHRP AAG-1 Saturates/Aromatics Blends	23
Figure 3-9. AFS of SHRP AAA-1 Asphaltenes/Aromatics/Saturates	24
Figure 3-10. $\eta_{0,60C}^*$ Versus %AS for SHRP AAA-1 Blends Containing 7% Original Asphaltenes	24
Figure 3-11. $\eta_{0,60C}^*$ Versus %AS for SHRP AAA-1 Blends Containing 15% Original Asphaltenes	25
Figure 3-12. $\eta_{0,60C}^*$ Versus %AS for SHRP AAG-1 Blends Containing 7% Original Asphaltenes	26
Figure 3-13. $\eta_{0,60C}^*$ Versus %AS for SHRP AAG-1 Blends Containing 15% Original Asphaltenes	26
Figure 4-1. SHRP Asphalt Naphthene Aromatic Hardening Susceptibilities	33
Figure 4-2. AAF-1 Fraction Hardening Susceptibilities	35
Figure 4-3. AFS for SHRP Asphalt Naphthene Aromatics	36
Figure 4-4. AFS for SHRP Asphalt Polar Aromatics	36
Figure 4-5. Comparison of AAA-1 NA and PA Carbonyl Growth Rates	37
Figure 4-6. AFS for AAF-1 Fractions	38
Figure 4-7. SHRP Asphalt NA Viscosity/Asphaltene Relationships	39
Figure 4-8. AAF-1 Fraction Viscosity/Asphaltene Relationships	41

Figure 4-9.	Viscosity Activation Energy Versus Carbonyl Area for NA and PA	41
Figure 4-10.	Viscosity Activation Energy Versus Carbonyl Area for AAF-1 Fractions	43
Figure 4-11.	Correlation of Andrade Equation Parameters	43
Figure 5-1.	Refractive Index Versus n-Alkane Carbon Number	47
Figure 5-2.	SHRP AAC-1 Chromatogram	51
Figure 6-1.	Oxygen Content Versus Carbonyl Content for AAA-1 and AAG-1	57
Figure 6-2.	Pressure Dependence of Carbonyl Formation for Lau3 Asphalt	60
Figure 6-3.	Temperature Dependence of Carbonyl Formation for Lau3 Asphalt	60
Figure 6-4.	Pressure Dependence of Carbonyl Formation for All Stage 1 Asphalts	63
Figure 6-5.	Temperature Dependence of Carbonyl Formation for All Stage 1 Asphalts	64
Figure 6-6.	Carbonyl Formation for AAA-1 at All Stage 2 Conditions	67
Figure 6-7.	Carbonyl Formation for AAF-1 at All Stage 2 Conditions	67
Figure 6-8.	Carbonyl Formation for AAG-1 at All Stage 2 Conditions	68
Figure 6-9.	Isokinetic Diagram for All 15 Asphalts	70
Figure 6-10.	Arrhenius Plot for the First 5 Stage 2 Asphalts	70
Figure 6-11.	Arrhenius Plot for the Second 5 Stage 2 Asphalts	71
Figure 6-12.	Reaction Order Versus Activation Energy for All 15 Asphalts	71
Figure 6-13.	Initial Jump Pressure Dependence Versus Constant Rate Reaction Order	74
Figure 7-1.	Dimensionless Log Viscosity for Blends Studied	83
Figure 7-2.	Carbonyl Formation Rates for POV Aged PAV Aged AAF-1	86
Figure 7-3.	Arrhenius Plot for POV Aged PAV Aged AAF-1	86
Figure 7-4.	HS for POV Aged PAV Aged AAF-1	87
Figure 7-5.	HS Versus Approximate Material Saturate Content	89
Figure 7-6.	Arrhenius Plot for Atmospheric Aging of AAF-1	90
Figure 8-1.	Hardening Susceptibility Plot for Ca(OH) ₂ -Treated SHRP AAA-1	96

Figure 8-2.	Arrhenius Plot for Amine Treated Rejuvenated AAA-1/ABM F2	100
Figure 8-3.	Oxidation Rates of CaO-Treated AAF-1/YBF-F2	102
Figure 8-4.	Hardening Susceptibility Plot for CaO-Treated AAF-1/YBF-F2	102
Figure 8-5.	Arrhenius Plot for CaO-Treated AAF-1/YBF-F2	104
Figure 8-6.	Carbonyl Formation Rates for AAF-1/YBF-F2 at Three Temperatures	107
Figure 9-1.	Temperature Dependence of Microductility for AAD-1	113
Figure 9-2.	Temperature and Hole Size Dependence of Microductility for AAB-1	113
Figure A-1.	Supercritical Unit Process Diagram	134
Figure A-2.	Legend for Supercritical Extraction Unit Diagram	135
Figure A-3.	Pressure Oxygen Vessel Control Panel	138
Figure A-4.	Pressure Oxygen Vessel and Control Panel	138

LIST OF TABLES

		Page
Table 1-1.	Work Plan	3
Table 2-1.	Inventory of Aged Asphalts	11
Table 3-1.	Corbett-type Composition of Blends for Four Asphalts Studied	14
Table 4-1.	Initial Properties of NA, PA Fractions and Supercritical Fractions	32
Table 4-2.	Content of NA and PA in Aromatics Fractions of Five SHRP Asphalts	32
Table 4-3.	Hardening Susceptibilities (HS) of SHRP Asphalts and Their NA, PA and Aromatics Fractions	34
Table 4-4.	Comparison of Calculated and Measured AFS of Aromatics of SHRP Asphalts	37
Table 4-5.	Comparison of Solvation Power Parameters of Fractions of SHRP Asphalts	39
Table 5-1.	GPC Molecular Weights and HPLC Refractive Index Response Factors for 13 Saturate Fractions	52
Table 5-2.	Average Refractive Index Response Factors for Saturate Groups	52
Table 5-3.	Saturate Content of SHRP Core Asphalts Using Various Calibrations Standards	54
Table 6-1.	Aging Conditions Applied in the Stage 2 Experiments	58
Table 6-2.	CA Growth Rate for All Asphalts and POV Conditions in the Stage 1 Experiments	61
Table 6-3.	$CA_0 - CA_{\text{unk}}$ for All Asphalts and POV Aging Conditions in the Stage 1 Experiments	61
Table 6-4.	α for All POV-Aged Asphalts at Different Temperatures in the Stage 1 Experiments	63
Table 6-5.	E for All POV-Aged Asphalts at Different Pressures in the Stage 1 Experiments	64
Table 6-6.	Kinetic Model Parameters for All POV-Aged Asphalts in the Stage 1 Experiments	65

Table 6-7.	CA Growth Rate for All POV-Aged Asphalts in the Stage 2 Experiments at All Conditions	65
Table 6-8.	$CA_0 - CA_{\text{tank}}$ of All POV-Aged Asphalts in the Stage 2 Experiments at All Aging Conditions	66
Table 6-9.	Kinetic Model Parameters of All POV-Aged Asphalts Studied in the Stage 2 Experiments	69
Table 6-10.	β and γ Values of All Asphalts in the Stage 1 and Stage 2 Experiments	74
Table 7-1.	Industrial Supercritical Fraction and Commercial Rejuvenating Agent Properties	78
Table 7-2.	Representative Texas A&M Supercritical Fraction Properties	80
Table 7-3.	Composition and Viscosity Data for Asphalts Subjected to PAV Test	84
Table 7-4.	POV Aging Results	87
Table 7-5.	Saturate Content and Hardening Susceptibility Rankings	88
Table 8-1.	Materials Properties	94
Table 8-2.	Hardening Susceptibilities of Lime-Treated Tank Asphalts	96
Table 8-3.	Aging Indexes of Lime-Treated Tank Asphalts	97
Table 8-4.	Aging Data for Untreated Rejuvenated Asphalts at 90°C	99
Table 8-5.	POV Aging Parameters for Amine Treated Rejuvenated Asphalts	100
Table 8-6.	Aging Data for CaO Treated AAF-1/YBF-F2 at 90°C	101
Table 8-7.	The Effect of CaO on Oxidative Aging Parameters of Asphalt Blends	103
Table 8-8.	Calculation of Critical Time at 50°C	109
Table 10-1.	Estimated Cost to Produce Recycling Agent Using a Supercritical Fractionation Unit	115
Table 10-2.	Superior Asphalt (SA) Pavement versus Conventional Asphalt Pavement Comparison	117
Table 10-3.	Recycled Asphalt Pavement versus Conventional Asphalt Pavement Comparison	120

CHAPTER 1

INTRODUCTION AND SUMMARY

About 27 million tons of asphalt and nearly twenty times this much aggregate are consumed each year to build and maintain over two million miles of roads in this country. Over a cycle of about 12 years on the average, these roads must be reworked and much of these millions of tons of rock and asphalt cannot be reused with present recycling technology. Instead, much of the maintenance is accomplished by placing thick layers (hot-mix overlays) of new material on top of the failed material. This results in considerable waste of material, both in terms of quality aggregate (which is diminishing in supply) and in terms of asphalt binder. In addition, the new asphalt binder represents a significant source of potential energy (greater than that of a similar amount of coal).

The main impediment to recycling asphalt binder is the poorly developed science of recycling agent composition and, as a result, optimum recycling agents are not available. An excellent recycling agent should not only be able to reduce the viscosity of the aged material, but it must also be able to restore compatibility. The properties of the old material and recycling agent must be compatible to give both good initial properties and aging characteristics, and this must be understood. Many currently available commercial recycling agents address only the need to reduce viscosity and may in fact exacerbate problems with material compatibility.

The agent must also be inexpensive and easily manufactured. A large quantity of potential feedstock for the production of recycling agents is available and much of it is now fed to cokers. This material could be recovered by supercritical extraction which is an existing refinery technology. A supercritical pilot plant is available at Texas A&M and has been used to produce fractions for study.

The objective of this research is to establish the technical feasibility (Phase I) of determining the specifications and operating parameters necessary to produce high quality recycling agents which will allow most, if not all, of old asphalt-based road material to be

recycled. The initial and aged properties of the recycled road material should be comparable to that of new material. It is expected that supercritical fractionation of asphalt can be utilized to fractionate material available at refineries, establish operating parameters, and to reblend these fractions, if necessary, to produce superior recycling agents and to systematically study the effect of varying composition on properties. The advanced road aging simulation procedure, developed at Texas A&M, will be used to determine the aging characteristics of blends of old asphalt and recycling agents so as to relate aging to blend composition.

To accomplish this objective, this study has been broken down into several tasks. The proposed original time line for completion of all tasks is listed in Table 1-1.

Chapter 2 details work accomplished during the second year of this project on asphalt fractionation (Task 1). The fractionation experiments discussed in Chapter 2 were performed using column chromatography techniques and not supercritical fractionation. These fractionation experiments were performed to produce pure materials for further investigation of the contribution that various chemical groups have on asphalt performance. The fractions produced as a result of these experiments were used extensively in the work detailed in Chapters 3, 4 and 5.

Chapter 2 also details work accomplished during the second year on Aged Asphalt Production (Task 2). The apparatus constructed during the first year of this project is described once again. In addition, the inventory of aged asphalts is listed in Chapter 2. Essentially, all of the aged asphalt production required for this project has been completed.

Chapter 3 details additional work accomplished during the second year on Preliminary Recycling Agent Formulation (Task 3). Specifically, the influence of asphaltenes and saturates was investigated. The study detailed in Chapter 3 of this year's technical progress report differs from the studies performed last year in that this year's experiments were designed to investigate the interactions between saturates and asphaltenes in a more controlled manner. The objective of the work described in Chapter 2 was to determine how these interactions may influence asphalt performance. Asphaltenes, saturates, and aromatics from a given asphalt were recombined in varying ratios to determine these interactions. This study indicates that all saturates act in nearly the same manner in all asphaltic materials. At higher temperatures, the saturates have little

Table 1-1. Work Plan

Task	Year 1	Year 2	Year 3	% Time
1. Supercritical Fractionation	_____			10
2. Aged Asphalt Production	_____			5
3. Preliminary Recycle Agent Formulation and Recycle Blend Testing	_____	_____		15
4. Expanded Recycle Blend Testing	_____	_____	_____	20
5. Rejuvenated Material Aging and Testing		_____	_____	20
6. Mixing Rules Development		_____		5
7. Lime Additive Testing		_____	_____	5
8. Other Additives Testing		_____	_____	5
9. Processing Schemes Development			_____	5
10. Projection Update and Commercialization Plan	_____		_____	5
11. Reports	_____		_____	5

detrimental effect on the rheological properties of asphalts; however, at low temperatures and in the presence of asphaltenes, the saturates have a highly detrimental influence. Therefore, to reduce this harmful influence in recycled asphalts, which are high in asphaltenes, the saturate content of the recycling agent should be minimized.

Chapter 4 describes additional studies on Preliminary Recycling Agent Formulation (Task 3). The studies in Chapter 4 were performed to determine if, and how, the naphthene aromatics behave differently than the polar aromatics in asphaltic materials. Pure naphthene aromatic and pure polar aromatic fractions were aged in the Pressure Oxygen Vessels (POV) to determine the aging characteristics of each fraction. Because any recycling agent is going to contain some mixture of these fractions, several supercritical fractions from SHRP AAF-1 were also investigated. The supercritical fractions investigated contain varying ratios of naphthene and polar aromatics, with little to moderate contamination of saturates and asphaltenes. The data in Chapter 4 indicate that a high naphthene aromatic content is desirable in a recycling agent, although some polar aromatics are necessary.

Chapter 5 details the development of a superior method for determining the saturate content in heavy petroleum materials such as asphalt, asphalt supercritical fractions, and asphalt recycling agents. Pure saturate fractions isolated from several asphalts and industrial supercritical fractions were analyzed using High Performance Liquid Chromatography (HPLC) to determine if the saturates present in heavy petroleum products are all similar. The experiments described in Chapter 5 indicate that they are in fact similar and that HPLC can be used to rapidly accelerate saturate determination in asphaltic materials. This has direct bearing on Preliminary Recycling Agent Formulation (Task 3) in that it is now possible to quickly and accurately screen potential recycling agents on the basis of both asphaltene and saturate content.

Chapter 6 details intensive studies on asphalt aging in general, which obviously impacts Rejuvenated Material Aging and Testing (Task 5). The experiments performed in this chapter allowed the determination of the oxidation kinetics of fourteen asphalts. The work detailed in Chapter 6 shows conclusively that the aging of asphalt is time, pressure, and temperature dependent. This casts long shadows over the currently accepted practice of aging asphalts at a single high temperature and high pressure for a single period of time and trying to predict asphalt

performance from this test.

A preliminary experiment to compare the aging performance of recycled asphalts (Task 5) rejuvenated with supercritical fractions and with commercial recycling agents is described in Chapter 7. Unaged SHRP AAF-1 and aged AAF-1 recycled with nine different rejuvenating agents (3 industrial supercritical fractions, 3 laboratory supercritical fractions, and 3 commercial recycling agents) were subjected to a slightly modified Pressure Aging Vessel (PAV) test. The residues from the PAV test were then POV aged to determine oxidation aging kinetics. The study indicates that supercritical fractions are no worse than commercial recycling agents as rejuvenating agents. In fact, supercritical fractions may be superior, if they are manufactured properly.

Experiments investigating the use of lime as an additive for recycling (Task 7) and the use of amines as additives for recycling (Task 8) are described in Chapter 8. Two different aged asphalts were rejuvenated with three different supercritical fractions. Three different levels of lime in the form of calcium oxide (CaO) and three different amines were investigated as additives for the recycled asphalts rejuvenated with one of the supercritical fractions in a preliminary experiment. The results of this study indicated that amines had little to no positive influence on the aging characteristics of the recycled asphalts and would not be cost effective. Thus, for the other rejuvenating agents, it was decided that the amines would not be investigated. This effectively completes work on Task 8. The experiments with lime indicate that lime is beneficial and will be examined further in the remaining recycled asphalt studies performed under this DOE project.

Chapter 9 details work on the development of a meaningful microductility test for use in testing the performance of unaged and aged, original and recycled asphalt binders. Thus, this test is relevant to Expanded Recycle Blend Testing (Task 4) and it is also relevant to Rejuvenated Material Aging and Testing (Task 5).

Finally, Chapter 10 summarizes the potential waste and energy savings associated with this project for both the recycling agent producer (refiner) and the recycling agent consumer (DOTs across the nation). Economic analyses for all parties affected by this project are also included in Chapter 10.

CHAPTER 2

MATERIALS PRODUCTION

It is necessary to have idealized components to perform many of the experiments described in this report. Because these idealized components cannot be purchased on the open market, it is necessary to perform fractionation experiments to produce these materials. This fractionation can be accomplished by a wide variety of methods, as described below. To perform asphalt recycling experiments, it is also necessary to use aged asphalt. Rather than obtain asphalts whose original properties are unknown from pavement samples using time consuming, labor intensive extraction procedures which are complicated greatly by the extraction process, a large scale oxidation apparatus was employed to produce artificially aged asphalts.

ASPHALT FRACTIONATION

Background

Much effort has been expended in determining the chemical composition of asphalt and other heavy petroleum products. At least one method for determining composition based on chemical reactivity (Rostler and Sternberg, 1949) is routinely used. However, this chemical reactivity classification method irreversibly alters the structure of the compounds in the separation process (White et al., 1970). To produce idealized, unaltered asphalt fractions several chromatographic techniques for asphalt group-type fractionation have been proposed. The most well known of these methods is the method of Corbett (1969), which has since been adapted by the American Society for Testing and Materials (ASTM D4124) as the standard method for determining asphalt composition.

The Corbett (1969) method and the method of Rostler and Sternberg (1949) both entail performing a binary fractionation of the material based on solubility in n-heptane. The insoluble fraction, if present, is separated by filtration and is referred to as the asphaltene fraction, or simply asphaltenes. The soluble fraction is called maltenes or petrolenes. In the Corbett method,

the maltenes are then fractionated through adsorption-desorption chromatography. A detailed description of the Corbett method follows.

In the standard method, approximately 10-14 grams of asphalt are dissolved in a 100:1 (vol% n-C₇:wt% sample) solution. The asphaltenes are separated by precipitation and filtration and the maltene solution is then separated into saturates, naphthene aromatics, and polar aromatics by elution chromatography using an open column containing activated alumina. The maltenes are loaded onto the column and solvents of increasing solvent strength are used to elute the various fractions. N-heptane (n-C₇) is added to the column, followed by toluene, a mixture of 50:50 (vol%:vol%) toluene:methanol (MeOH), and finally trichloroethylene (TCE). The saturate-like molecules, having little affinity for the alumina, are eluted first with n-C₇ up to the elution of the n-C₇/Toluene solvent front. The polar aromatics, which are highly retained on the alumina, concentrate at the TCE/Toluene:MeOH solvent front and elute last. The naphthene aromatics elute between the saturates and the polar aromatics. The difficulty of this separation arises from the fact that the solvent fronts are not distinct. In fact, the solvent fronts rarely, if ever, travel down the column uniformly. This is crucial as the separation cut-points are determined by visual inspection and can be highly subjective. Each individual fraction is collected in a tared beaker and the solvent is allowed to evaporate in order to determine the mass of each fraction.

Because the Corbett fractionation is only capable of fractionating up to 14 g of material, Peterson et al. (1994) developed a "Giant" Corbett procedure capable of fractionating up to 150 g of material. This procedure is similar to the Corbett method in that the asphaltenes are removed by filtration from a 20:1 (vol% n-C₇:wt% sample) solution and the maltenes are fractionated by elution from a column containing activated alumina. However, the maltenes are eluted using only two solvents with continuous recycle. A diagram of the "Giant" Corbett apparatus is shown in Figure 2-1. Briefly, n-heptane is passed over the column initially to elute what Peterson called the paraffins. As the solvent and dissolved maltene elute from the column, it enters a flask where the solvent is distilled and the paraffin fraction remains in the flask. The distilled solvent is then recycled to the top of the apparatus. After two to three hours of n-heptane recycle, the n-heptane and the flask are removed. A new flask is placed in the heating mantle and a 85:15 mixture of TCE:ethanol is added to the column to elute what Peterson called the aromatics

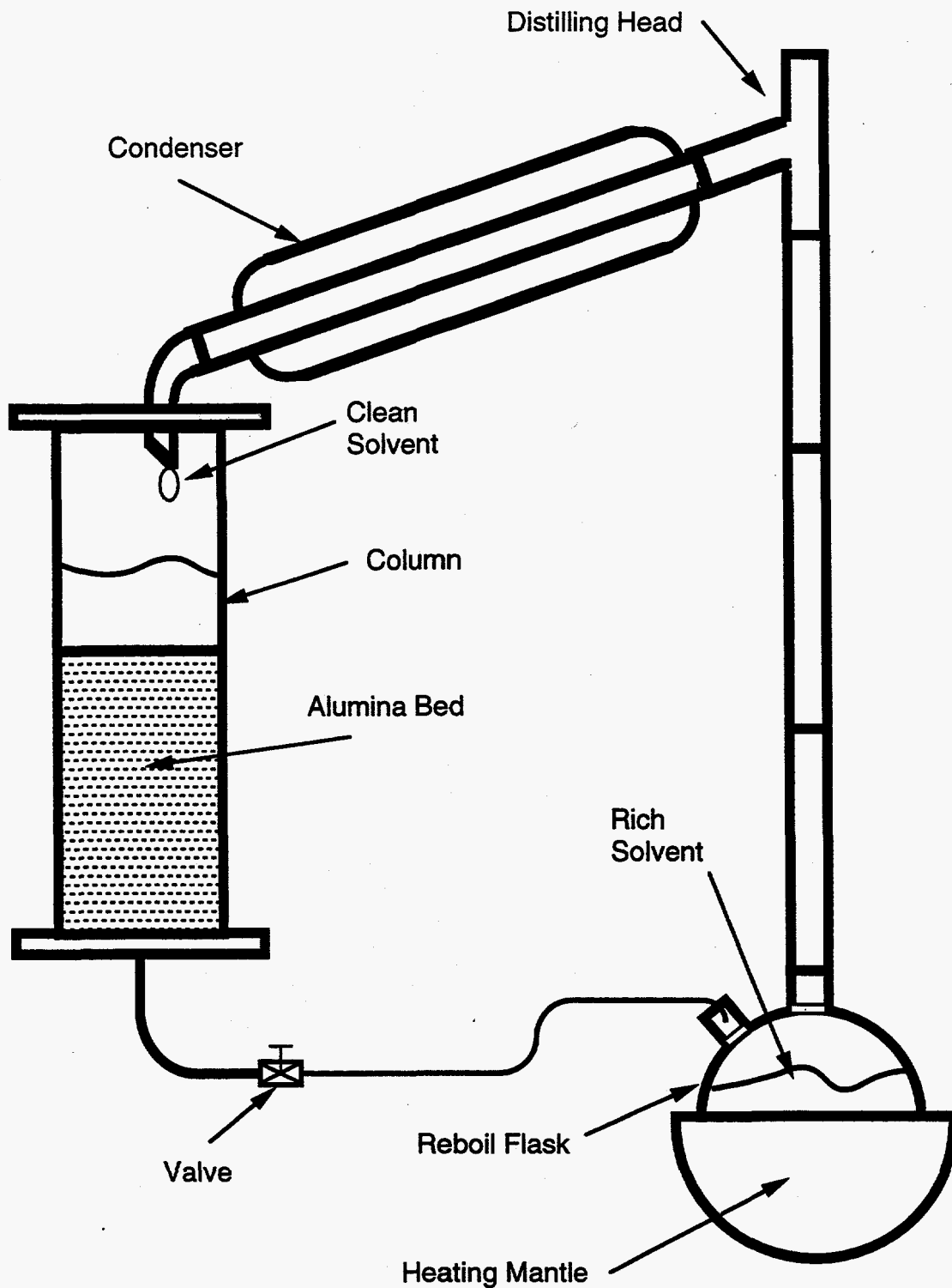


Figure 2-1. Giant Corbett Apparatus

fraction. Thus, the "Giant" Corbett procedure is capable of fractionating up to 150 g of maltene material into two fractions, paraffins and aromatics. The paraffin fraction contains all of the saturates and some lighter naphthene aromatics and the "Giant" Corbett aromatic fraction contains all of the polar aromatics and some heavier naphthene aromatics.

Fractionation

To produce the quantities of idealized fractions necessary for the experiments performed in this study, it was necessary to use the "Giant" Corbett procedure to prefractionate the asphalts and then perform traditional Corbett fractionation of both the paraffin fraction and the "Giant" Corbett aromatic fraction. These procedures were modified by using n-hexane instead of n-heptane so that fractions compatible with the High Performance Liquid Chromatography (HPLC) system, which uses n-hexane as the mobile phase (See Chapter 5).

Because the Corbett fractionation of the paraffins and "Giant" Corbett aromatics also suffered from indistinct, non-uniform solvent fronts, it was necessary to make a judgement about which fraction(s) should be as pure as possible. It was decided that the saturate fraction is the only one where purity is critical (See Chapter 5), so the saturate/naphthene aromatic cut-point was somewhat conservative. Thus, the light naphthene aromatics contained a small amount of saturates. If the light naphthene aromatics from traditional Corbett fractionation of the paraffin fraction were added to the heavy naphthene aromatics from the traditional Corbett fractionation of the "Giant" Corbett aromatics fraction, the naphthene aromatic fraction was produced. If the light naphthene aromatics from the paraffin fraction were added to the "Giant" Corbett aromatics fraction, a fraction that is referred to as "the aromatics" throughout the remainder of this report was produced.

Instead of allowing the solvent to evaporate from tared beakers, the fractions were recovered using a tared sample tin and a rotary evaporation apparatus. The recovered fractions were analyzed by Gel Permeation Chromatography (GPC, See Appendix A) to confirm complete solvent removal (Burr et al., 1990). Typical recoveries using the rotary evaporation technique were around 96%.

Five of the core asphalts from the Strategic Highways Research Program (SHRP), AAA-1,

AAD-1, AAF-1, AAG-1, and AAM-1 were fractionated in this manner. Asphaltenes, aromatics and saturates from AAA-1, AAD-1, AAF-1, and AAG-1 were used in the experiments described in Chapter 3. Polar aromatics, naphthene aromatics, and saturates from AAA-1, AAD-1, AAF-1, AAG-1, and AAM-1 were used for the experiments described in Chapter 4. The saturates from AAA-1, AAD-1, AAF-1, and AAM-1 were used for the experiments described Chapter 5. Eight industrial supercritical fractions (ISCF) were also fractionated using only the n-hexane modified traditional Corbett procedure to produce pure saturate fractions which were used in the experiments detailed in Chapter 5.

AGED ASPHALT PRODUCTION

For the project to avoid unreasonable delays, it was necessary to determine a suitable method of rapidly producing, in the laboratory, large amounts of asphalts comparable to asphalt aged over many years in pavement service. A new apparatus was developed during the first year of this DOE effort for aging a large quantity of asphalt by bubbling air through a well mixed asphalt sample at moderate temperature. The air-bubbling (AB) apparatus consists of a variable speed 1/4 horsepower motor which drives a 2" diameter mixing shaft placed in a half-full gallon can of asphalt. A less powerful mixer with a 1/15th horsepower motor is also available for use.

The can containing the asphalt is wrapped with a heating tape connected to a variable transformer and a thermocouple actuated on/off controller. Building air passes through a surge tank and a filter before being fed to the asphalt. The air is introduced to the asphalt through a 5" diameter sparging ring made from 1/4" stainless steel tubing with 14 nearly uniformly-spaced 1/16" holes. The operating temperature of the air-bubbled reaction vessel must be high enough for the oxidation to proceed at an appreciable rate, but not so high as to drastically alter the reaction mechanism or reaction products. Additionally, the temperature must be high enough to soften the asphalt so that the asphalt can be well mixed by the mixing paddle.

To produce pavement-like materials, the reaction temperature is targeted at 93.3°C (200°F) initially. However, as the aging proceeds, the temperature rises as a result of increased viscous dissipation. This is not critical but the temperature should not be allowed to exceed 110°C (230°F).

Over the course of this project, several materials have been produced in the AB apparatus described above. These materials along with their 60°C low frequency limiting viscosities (See Appendix A) are listed in Table 2-1. The asphalts are listed according to asphalt type (eg. AAA-1) and sample number (eg. AB1). Several additional materials have been produced in the air bubbling apparatus; however, the supply of these materials has been exhausted (eg. AAF-AB1). Other materials produced either in the POV or in a laboratory oven are also listed in Table 2-1. It is clear from Table 2-1 that materials having a wide range of viscosities are available for study in the remainder of this DOE effort.

Table 2-1. Inventory of Aged Asphalts

Sample	$\eta_{0,60^\circ\text{C}}^*$ (poise)
AAA-AB8	37,500
AAA-AB10	228,000
AAA-AB11	55,000
AAB-AB1	114,000
AAB-AB2	85,000
AAB-AB3	38,000
AAD-AB1	250,000
AAD-AB3	28,000
AAD-AB4	39,000
AAF-AB2	21,000
AAF-AB4	85,000
AAM-AB1	18,000
JG33-AB1	44,000
XON14-1	100,000
XON14-2	60,000
JRSC-1	100,000

CHAPTER 3

THE EFFECT OF ASPHALT COMPOSITION ON THE FORMATION OF ASPHALTENES AND THEIR CONTRIBUTION TO ASPHALT VISCOSITY

Because asphalt binders can age differently over time, properties of the original material usually give an uncertain assessment of long term performance. Therefore, the oxidation characteristics of asphalt binders must be considered to be part of asphalt performance. Lau et al. (1992) showed that the logarithm of the 60°C low frequency limiting viscosity ($\eta_{0,60^\circ\text{C}}^*$) increases linearly with the growth of the infrared carbonyl peak area (CA) as an asphalt oxidizes. On the basis of this observation, Lau et al. (1992) defined the hardening susceptibility ($\text{HS}_{60^\circ\text{C}}$) to be the slope of this linear relationship.

$$\text{HS}_{60^\circ\text{C}} = \frac{d \ln \eta_{0,60^\circ\text{C}}^*}{d \text{CA}} \quad (3-1)$$

Furthermore, Lau et al. (1992) showed that $\text{HS}_{60^\circ\text{C}}$ is a characteristics "property" for a given asphalt and is independent of aging temperature up to 93.3°C. However, the HS determined at this single measurement temperature (60°C) may not be representative of performance at lower temperatures.

Asphaltenes repeatedly have been shown to have a major influence on the viscosity of asphalt (Traxler, 1961; Anderson et al., 1976; Plancher et al., 1976; Lee and Huang, 1973). Lin et al. (1996) confirmed this through blending asphaltenes with unaged maltenes at multiple asphaltene levels. The viscosity increased without a corresponding increase in carbonyl area. Therefore, Lin et al. (1995) suggested that the $\text{HS}_{60^\circ\text{C}}$ should be divided into two quantities.

$$\text{HS}_{60^\circ\text{C}} = \left(\frac{d \ln \eta_{0,60^\circ\text{C}}^*}{d \text{CA}} \right) = \left(\frac{d \ln \eta_{0,60^\circ\text{C}}^*}{d \% \text{AS}} \right) \left(\frac{d \% \text{AS}}{d \text{CA}} \right) \quad (3-2)$$

where %AS represents the weight percentage of asphaltenes. The first term represents the viscosity/asphaltene relationship. Although the asphaltenes originally present in an asphalt are chemically different from those produced through oxidative aging (Girdler, 1965), all asphaltenes were shown to have a similar effect on the viscosity of an asphalt (Lin et al., 1995). This viscosity/asphaltene relationship, which is the manifestation of the interactions between the asphaltenes and the rest of constituents in asphalts, can be described using several suspension or colloidal models (Lin et al., in press; Eilers, 1948; Heukelom et al., 1971; Sheu et al., 1991). The second term in Equation (3-2), $(d\%AS/dCA)$, is defined as asphaltene formation susceptibility (AFS). The AFS is a characteristic of the reactive components of asphalt which describes the susceptibility for asphaltene formation as carbonyl functional groups form.

The effects of asphalt composition on the viscosity/asphaltene relationship can provide valuable information on the colloidal nature of asphaltenes in asphalt. The understanding of factors affecting AFS will give a further insight into the asphaltene formation due to oxidative aging. This work was undertaken to understand and explain the effects of asphalt composition on viscosity/asphaltene behavior and AFS and to provide a basis for optimizing the performance based on composition.

EXPERIMENTS

Methodology

To study the effects of the maltene phase composition on the viscosity/asphaltene relationship and on the AFS, several experiments were designed to systematically control both asphaltene and saturate content in asphaltic materials. Four SHRP asphalts (AAA-1, AAD-1, AAF-1, and AAG-1) representing a wide variety of crude sources were examined in this study. Each asphalt was fractionated into asphaltenes, aromatics, and saturates by the procedures described in Chapter 2. Blends of asphaltenes/aromatics/saturates in varied ratios were produced using fractions from the same asphalt, and these blends were then aged in a pressurized oxygen vessel (POV, see Appendix A). Fourier transform infrared spectroscopy (FTIR, see Appendix A) and dynamic mechanical analysis (DMA, see Appendix A) were used to monitor the chemical and physical property changes induced by oxidative aging. In addition, the n-hexane asphaltene

content of the aged samples was determined by precipitation as described in Appendix A.

Blend Preparation

Because of the miscibility of the components, saturate/aromatics blends were produced by simple mixing. Blends containing asphaltenes were obtained by dissolving and mixing the components in toluene and then recovering the asphaltic material. This was the best way to maximize homogeneity of the blend. Solvent recovery was performed at relatively low temperatures to eliminate potential solvent aging (Burr et al., 1994). Complete solvent removal was confirmed by GPC (Burr et al., 1990). The approximate composition in terms of weight percent asphaltene and weight percent saturates for all blends produced are tabulated in Table 3-1.

Table 3-1. Corbett-type Composition of Blends for Four Asphalts Studied

		% Asphaltenes		
		0	7	15
% Saturates	0	SHRP AAA-1	SHRP AAA-1	SHRP AAA-1
		SHRP AAD-1	SHRP AAG-1	SHRP AAG-1
		SHRP AAF-1		
		SHRP AAG-1		
	7	SHRP AAA-1	SHRP AAA-1	SHRP AAA-1
		SHRP AAD-1	SHRP AAG-1	SHRP AAG-1
		SHRP AAF-1		
		SHRP AAG-1		
	15	SHRP AAA-1	SHRP AAA-1	SHRP AAA-1
		SHRP AAD-1	SHRP AAG-1	SHRP AAG-1
		SHRP AAF-1		
		SHRP AAG-1		
20	SHRP AAA-1			
	SHRP AAD-1			
	SHRP AAF-1			
	SHRP AAG-1			

Oxidative Aging

Several $1.5 \text{ g} \pm 0.05 \text{ g}$ samples of each blend were aged in a pressurized oxygen vessel (POV) under atmospheric air pressure. The blends, which were initially asphaltene free, were aged at 87.8, 93.3, and 98.8°C for up to four weeks, and the blends which originally contained asphaltenes were aged only at 98.8°C for three weeks. Note that the blends which were initially asphaltene free formed asphaltenes upon aging.

RESULTS AND DISCUSSION

Effects of Saturates in the Absence of Original Asphaltene

Peterson et al. (1994) reported that increased paraffin fraction content, in the absence of original asphaltenes, improves the oxidative characteristics of asphalt material in terms of decreased $HS_{60^\circ\text{C}}$. However, several other researchers have concluded that saturates have a negative influence on the performance of asphalt binder (Que et al., 1991; Manheimer, 1933). Figure 3-1 shows the viscosity versus carbonyl area for aged SHRP AAA-1 saturates/aromatics blends for saturates content ranging from 0% to 20%. The slopes of the regression lines, which are defined as $HS_{60^\circ\text{C}}\text{s}$, appear to be the same for all levels of saturates. The blends from SHRP AAD-1, AAF-1, and AAG-1 show the same behavior (data not shown). This result is in direct contrast to Peterson's conclusion (Peterson et al., 1994). The decrease in $HS_{60^\circ\text{C}}$ with the addition of paraffins noted by Peterson might be due to the residual light naphthenes in his paraffin fractions.

To understand the effect of low molecular weight naphthene aromatics, the $HS_{60^\circ\text{C}}$ of a naphthene aromatic fraction was measured. Figure 3-2 shows that the $HS_{60^\circ\text{C}}$ of the SHRP AAA-1 naphthene aromatic fraction is extremely low. In other words, the naphthene aromatics do not harden, even with appreciable carbonyl formation. The $HS_{60^\circ\text{C}}$ for pure saturates, on the other hand, cannot be determined because saturates neither harden nor oxidize upon aging. Thus, if it assumed (correctly or incorrectly) that $\ln \eta_{0,60^\circ\text{C}}^*$ is additive and CA is additive, then the decreasing $HS_{60^\circ\text{C}}$ with increasing paraffin content, as reported by Peterson et al. (1994), can be explained.

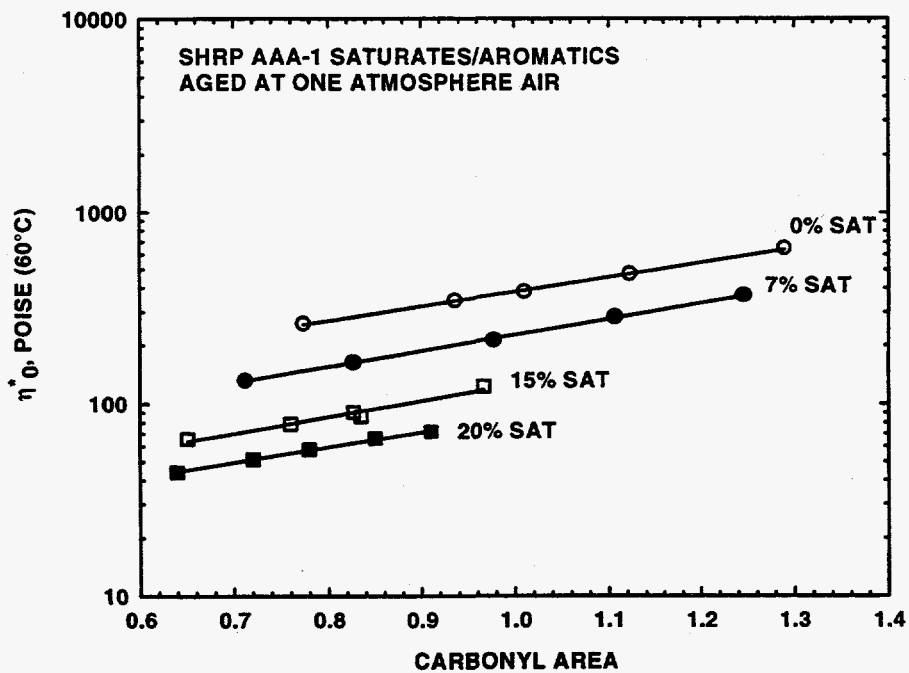


Figure 3-1. HS of SHRP AAA-1 Saturates/Aromatics Blends

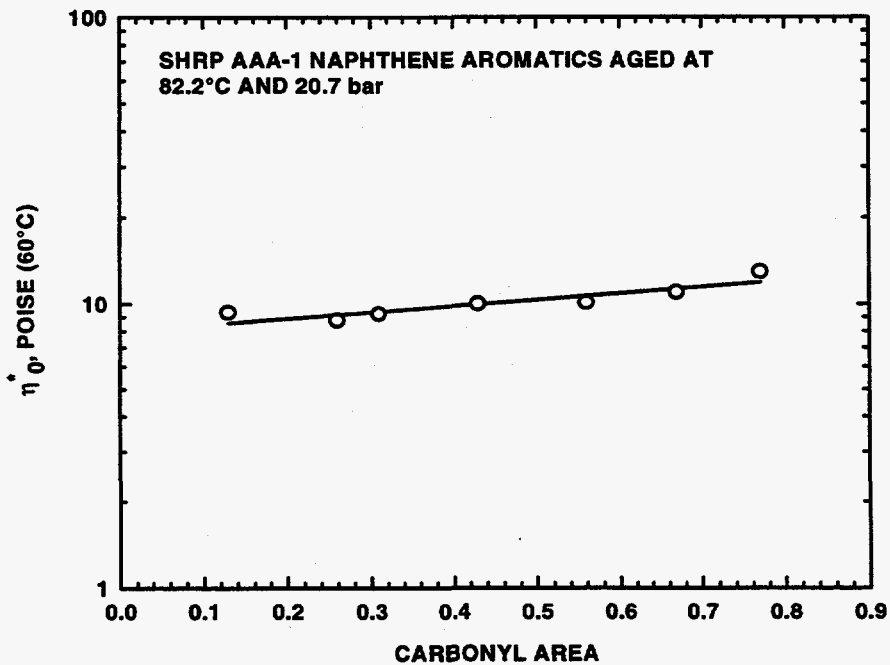


Figure 3-2. HS of SHRP AAA-1 Naphthene Aromatics

As proposed by Lin et al. (in press), HS can be divided into two separate effects, as described in Equation 3-2. Figure 3-3 shows that the presence of saturates has little, if any, effect

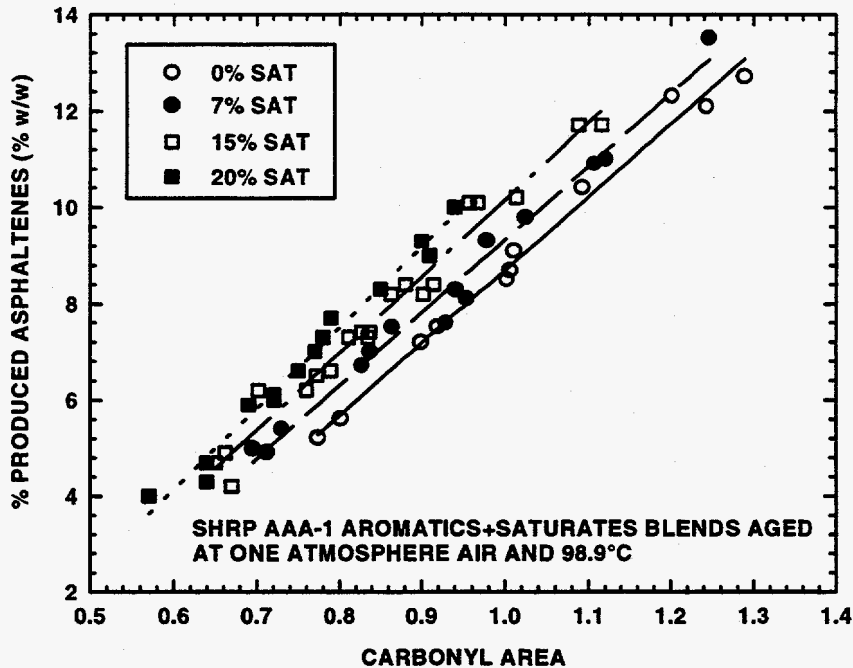


Figure 3-3. AFS of SHRP AAA-1 Saturates/Aromatics Blends

on AFS ($d\%AS/dCA$) for SHRP AAA-1 aromatics/saturates blends. The same behavior was observed for the aromatics/saturates blends from three other asphalts studied (data not shown). Previously, Lin et al. (1995) showed that the presence of original asphaltene also has no effect on AFS. Therefore, the AFS is strictly a function of the composition of reactive aromatics fraction, and the AFS of an asphalt binder can be reduced by changing the composition of the aromatics fraction. The reduction of asphaltene formation due to oxidation (AFS) is a very important concern in asphalt performance (Lin et al., 1995) due to the large influence that asphaltene formation has in increasing the asphalt's viscosity.

Figure 3-4 shows that the amount of saturates present in SHRP AAA-1 saturates/aromatics blends has no effect on the 60°C viscosity/asphaltene relationship. This is a reasonable consequence from the results shown in Figures 3-1 and 3-3. The same behavior was observed

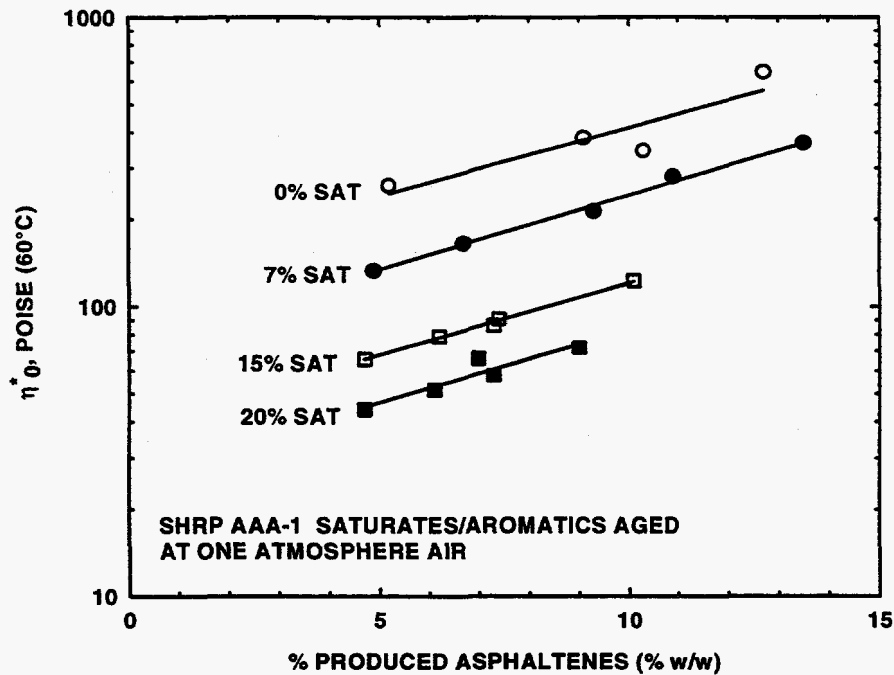


Figure 3-4. $\eta_{0,60C}^*$ Versus % AS for Aged SHRP AAA-1 Saturates/Aromatics

for the aromatics/saturates blends from three other asphalts studied (data not shown). However, this is somewhat unexpected due to the incompatibility of asphaltenes and saturates. It is well documented that saturates cause damage to asphalt binders at low temperatures, such as 0°C (Que et al., 1991; Manheimer, 1933). Thus, the measurement at 60°C might not be able to reveal the detrimental effects of saturates.

To further study how saturates affect hardening behavior, the viscosities of each aged and unaged saturates/aromatics sample were measured at temperatures of 0, 10, 25, and 40°C in addition to 60°C. The viscosity dependence on temperature can be described by a simple two-parameter Andrade equation where A_{vis} and E_{vis} , which are obtained by fitting Equation 3-3

$$\ln \eta_0^* = A_{vis} + \frac{E_{vis}}{RT} \quad (3-3)$$

to the data, are frequency factor and activation energy, respectively. R and T are the universal gas constant and absolute temperature, respectively. Figure 3-5 shows that the formation of

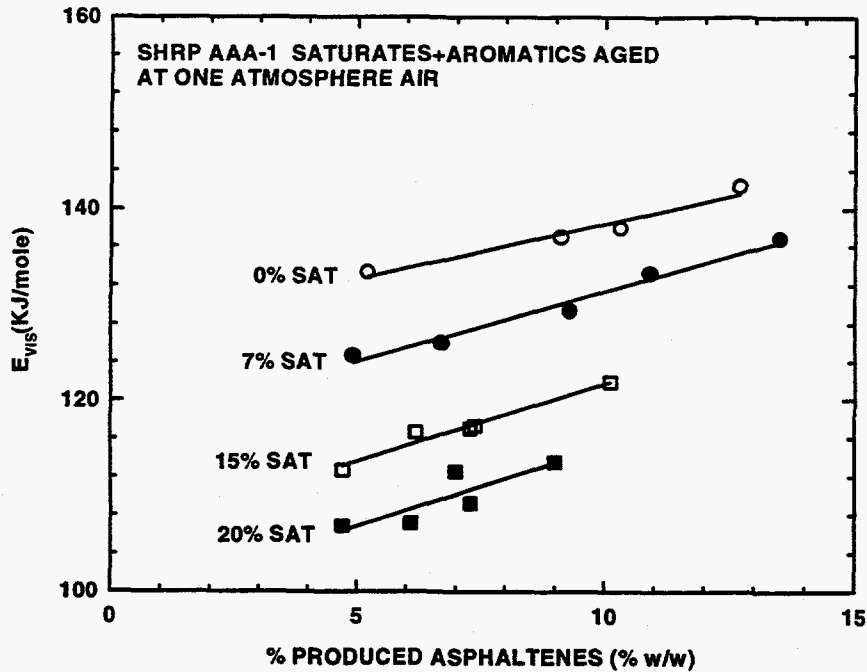


Figure 3-5. E_{vis} Versus % AS for Aged SHRP AAA-1 Saturates/Aromatics

asphaltenes increases the viscosity activation energy, E_{vis} . Furthermore, the blend containing 20% saturates has slightly stronger viscosity activation energy dependence on asphaltene formation than the blend containing 0% saturates. Although increased saturate contents reduce the absolute values of E_{vis} , the comparison should be made based on the change of E_{vis} with respect to oxidative aging (i.e. the slopes of the linear regression lines in Figure 3-5).

This phenomenon can be explained by semi-colloidal models. For asphaltic materials, the asphaltenes which constitute the dispersed phase are dispersed by the maltene which is composed of aromatics (or resins) and saturates. The state of dispersion is dependent upon the affinity between maltene and asphaltene molecules. Altgelt et al. (1975) showed that the solvation power of the maltene has a large effect on the viscosity/asphaltene relationship. Increased asphaltene content caused a sharper viscosity increase in poorer solvents, indicating that strong aggregation

of asphaltene molecules occurred. In contrast, good solvents for asphaltene show a relatively small increase in viscosity on the addition of asphaltene. It also has been shown that aromatics or resins have very good solvency with asphaltene molecules, while saturates are virtually incapable of solubilizing asphaltene (Corbett, 1979). At temperatures above the crystalline formation temperature for saturates, saturates and aromatics form one homogenous liquid phase which provides reasonable solvation for asphaltenes. However, at low temperature, saturates may crystallize and exhibit local phase separation from the aromatic phase. The solvent power of aromatics/saturates mixtures will drop significantly due to this crystalline formation. This reduced solvent power due to saturate crystallization is further compounded by a relatively small decrease in solvent power for pure aromatics due to the decrease in temperature (Eilers, 1948).

Therefore, the large viscosity activation energy dependence on asphaltene content for high saturates content can be explained largely as a result of a relatively large reduction in solvation power of aromatics/saturates mixture due to saturate crystalline formation.

To further verify this concept, original asphaltenes rather than those asphaltenes produced by oxidation were blended into aromatics/saturates mixtures. Figure 3-6 shows that the original asphaltenes have an effect similar to that of asphaltenes produced by oxidative aging. This agrees with previous research (Traxler, 1960; Peterson et al., 1994) that the coexistence of asphaltene and saturates induce a poor state of dispersion and consequently produce material with low performance.

With this in mind, effort was directed toward determining the effect saturates may have on the hardening susceptibility. By combining Equations (3-1) and (3-3), Equations (3-4a) and (3-4b) are obtained.

$$HS_T = \frac{d \ln \eta_{0,T}^*}{dCA} = \frac{dA_{vis}}{dCA} + \frac{1}{RT} \frac{dE_{vis}}{dCA} \quad (3-4a)$$

$$HS_{T_0} = \frac{d \ln \eta_{0,T_0}^*}{dCA} = \frac{dA_{vis}}{dCA} + \frac{1}{RT_0} \frac{dE_{vis}}{dCA} \quad (3-4b)$$

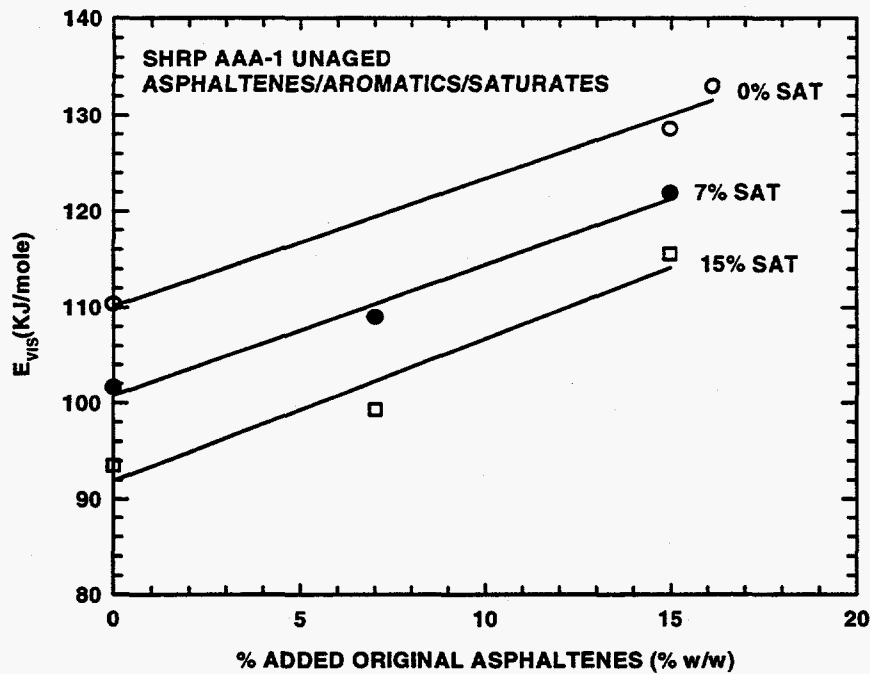


Figure 3-6. $E_{vis}/\%$ AS for Unaged SHRP AAA-1 Asphaltene/Saturates/Aromatics

Equation (3-4a) shows the relationship between the hardening susceptibility at any temperature, T , (HS_T) and the parameters A_{vis} and E_{vis} in the Andrade equation. Equation (3-4b) shows that same relationship for the HS at a reference temperature, T_0 . Subtracting Equation (3-4b) from Equation (3-4a) gives Equation (3-5).

$$HS_T = HS_{T_0} + \left(\frac{1}{R}\right) \left(\frac{dE_{vis}}{dCA}\right) \left(\frac{1}{T} - \frac{1}{T_0}\right) \quad (3-5)$$

Equation (3-5) shows the relationship between HS_T , HS_{T_0} , T , and the parameter E_{vis} in the Andrade equation. HS_T is proportional to reciprocal temperature with a proportionality constant equal to $(1/R)(dE_{vis}/dCA)$. Figure 3-7 shows a linear increase in HS with increasing $1/T$ (decreasing T) for SHRP AAA-1 saturates/aromatics blends. Therefore, (dE_{vis}/dCA) is positive

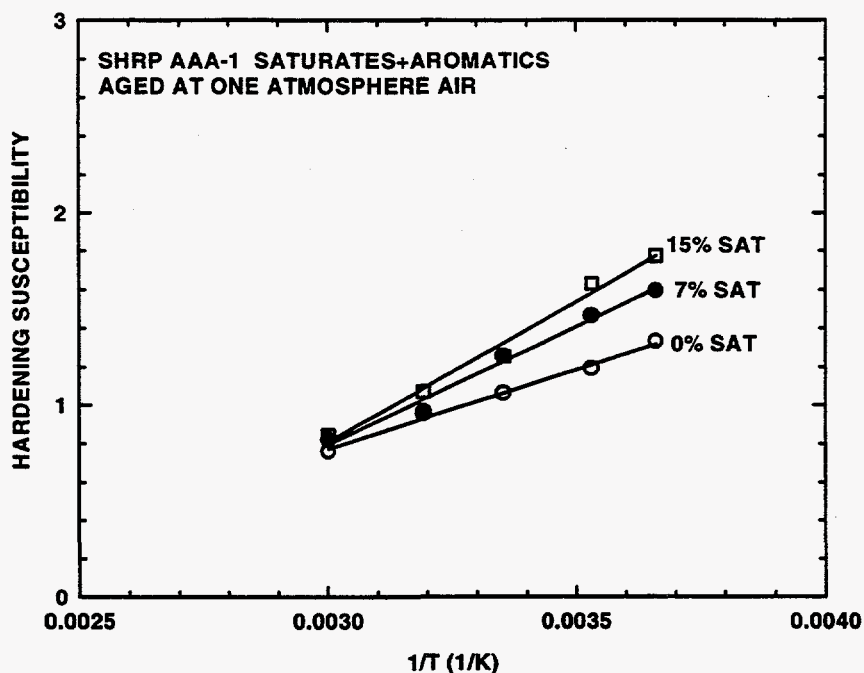


Figure 3-7. HS Versus 1/T for SHRP AAA-1 Saturates/Aromatics Blends

and HS_T will become worse as measurement temperature decreases. Furthermore, the linear slope of the $(E_{vis}/R)/\%AS$ relationship increases as saturates content increases, indicating that (dE_{vis}/dCA) increases with saturate content as shown in Figure 3-5 (CA is related to %AS through AFS which is independent of saturates and asphaltenes content as shown in Figure 3-3 and Lin et al., 1995). The same behavior was observed for SHRP AAG-1 saturates/aromatics blends (Figure 3-8). In conclusion, saturates may have little influence on the performance of an asphalt at higher temperatures but may have significant harmful effects at lower temperatures, especially as the asphalt oxidizes.

Effects of Saturates in the Presence of Original Asphaltene

For the initially asphaltene free aromatics/saturates blends, the highest asphaltene content achieved after oxidative aging for one month is approximately 13% which is typical of the initial asphaltene content of common AC-20 asphalts. To study the oxidation behavior of blends which have asphaltenes initially present, blends were produced by adding original asphaltenes into

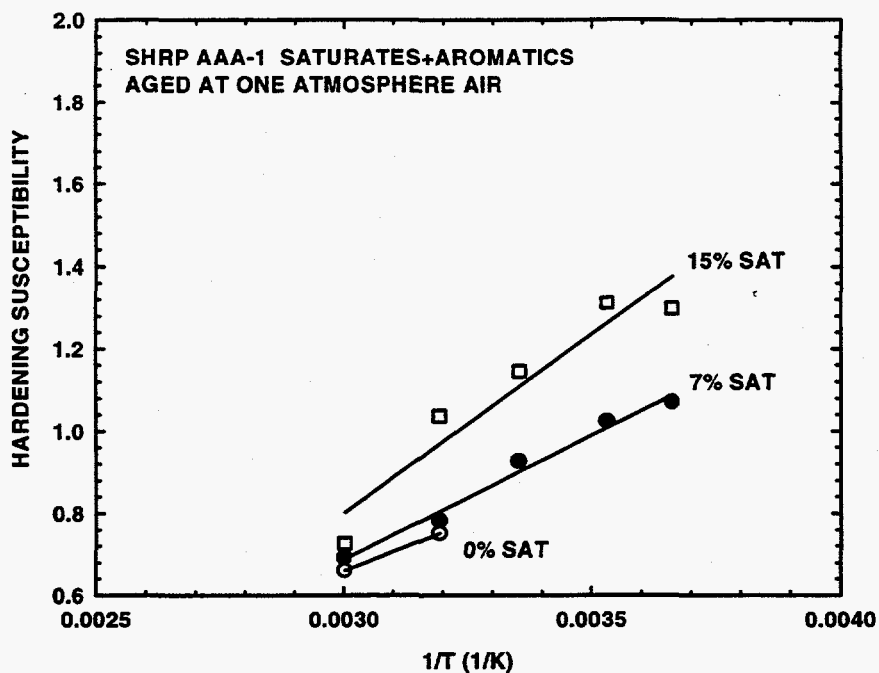


Figure 3-8. HS Versus 1/T for SHRP AAG-1 Saturates/Aromatics Blends

aromatics/saturates blends at several desired levels as shown in Table 3-1. These ternary blends were then aged in the POV. Figure 3-9 shows the asphaltene content versus carbonyl area (slope=AFS) for blends containing various initial asphaltene and saturate contents. The data shown in Figure 3-9 confirm that neither the quantity of saturates nor the quantity of asphaltenes present in the unaged blends appear to have an effect on the AFS. Once again, this implies that the AFS is only a function of the composition of the reactive aromatics fraction, which is the only fraction that produces new asphaltenes as a result of oxidative aging.

Figure 3-10 shows the $\ln \eta_{0.60^\circ\text{C}}^*$ as a function of total asphaltene content for blends with 7% original asphaltenes and saturate contents of 0%, 7%, and 15%. As illustrated in Figure 3-10, the effect of asphaltene content on $\ln \eta_{0.60^\circ\text{C}}^*$ increases as saturates content increases. Compared to Figure 3-5, the stronger effects of saturates on the $\ln \eta_{0.60^\circ\text{C}}^*/\%AS$ function shown in Figure 3-10 might be due to the higher initial asphaltene level. Figure 3-11 shows the $\ln \eta_{0.60^\circ\text{C}}^*$ as a

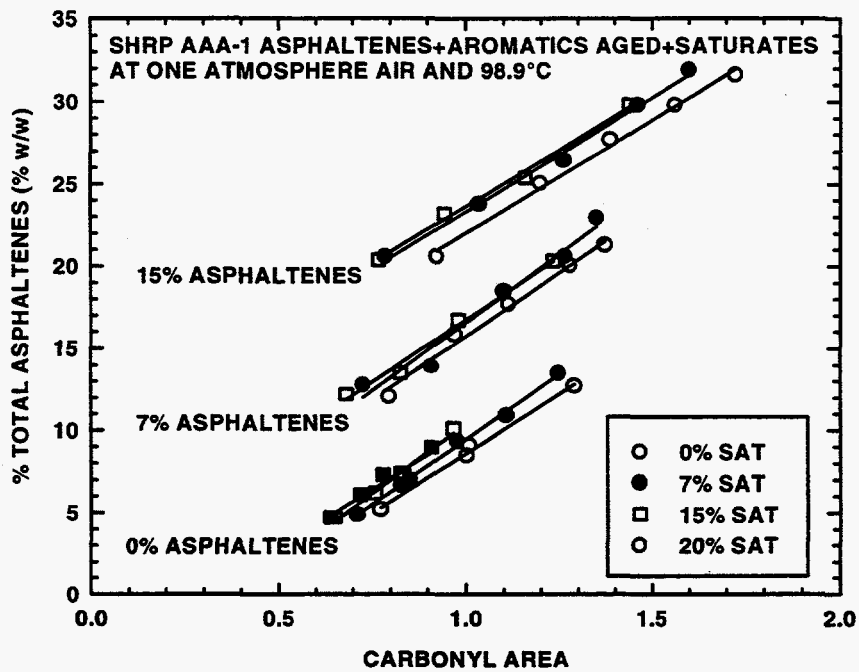


Figure 3-9. AFS of SHRP AAA-1 Asphaltenes/Aromatics/Saturates

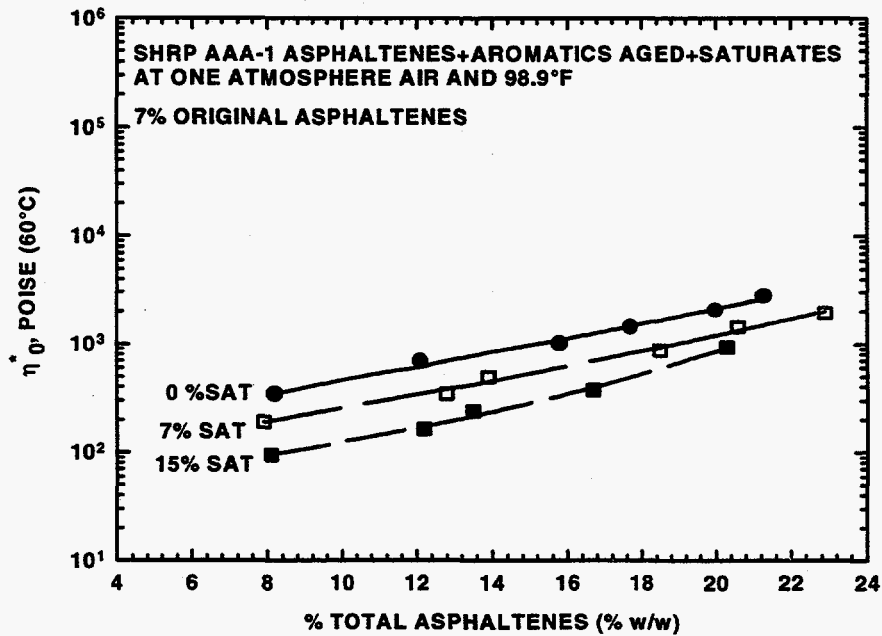


Figure 3-10. $\eta_{0,60}^{\circ}$ Versus % AS for SHRP AAA-1 Blends Containing 7% Original Asphaltenes

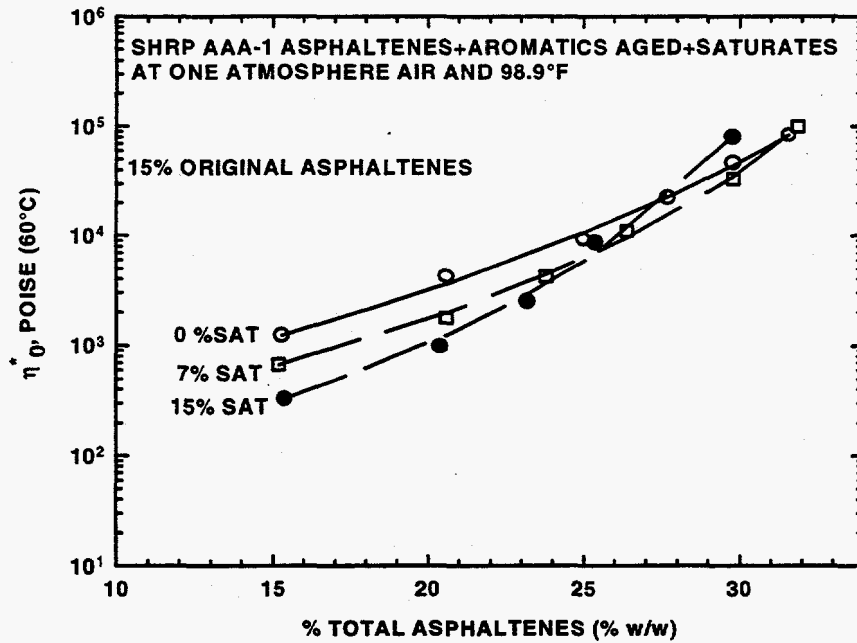


Figure 3-11. $\eta_{0,60C}^*$ Versus % AS for SHRP AAA-1 Blends Containing 15% Original Asphaltenes

function of total asphaltene content for blends with 15% original asphaltenes and saturate contents of 0%, 7%, and 15%. In Figure 3-11, the effect of saturates on $\ln \eta_{0,60C}^*/\%AS$ relationship is substantial for the blend containing 15% saturates and 15% original asphaltenes. Although the blend containing 15% original asphaltene and 15% saturates possesses the lowest initial viscosity due to the presence of 15% saturates, after aging and producing asphaltenes, this blend has a sharper increase in viscosity than the lower saturate content blends. This sharp increase in viscosity with increased asphaltenes is due to the low solvation power of the dispersing media with excessive amount of saturates. As described by colloidal models (Altgelt et al, 1975), asphaltene molecule aggregation is strongly influenced by the solvent power of the maltene phase. Maltenes with low solvent power favor aggregate formation while maltenes with good solvent power easily disperse asphaltene molecules and pull aggregates apart into smaller size. Furthermore, Pal and Rhodes (1989) showed that the formation of aggregates in suspensions increases the effective volume of dispersed phase (associated phase), which leads to an increase in suspension viscosity. Figures 3-12 and 3-13 show similar behavior for blends made from

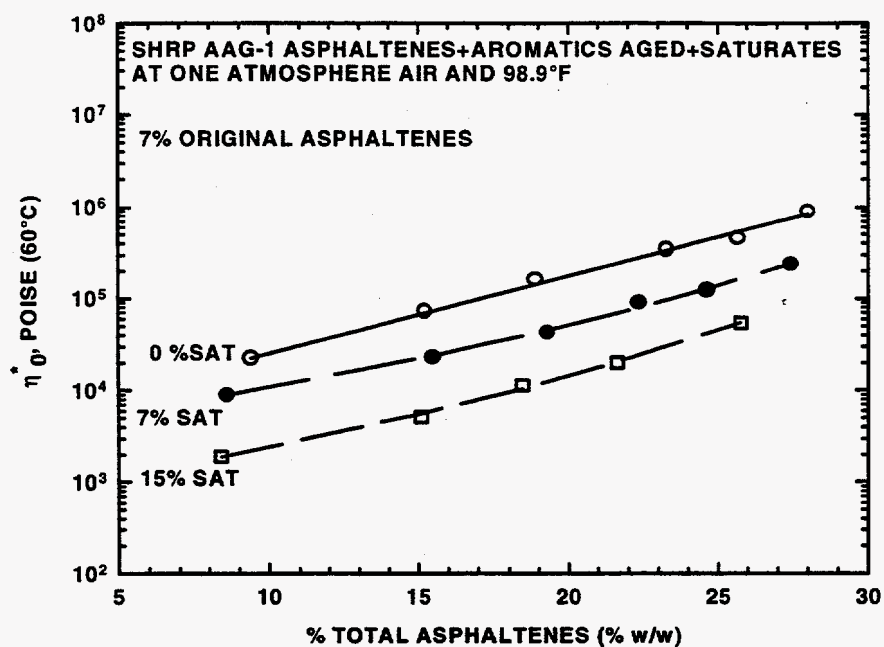


Figure 3-12. $\eta_{0,60C}^*$ Versus % AS for SHRP AAG-1 Blends Containing 7% Original Asphaltenes

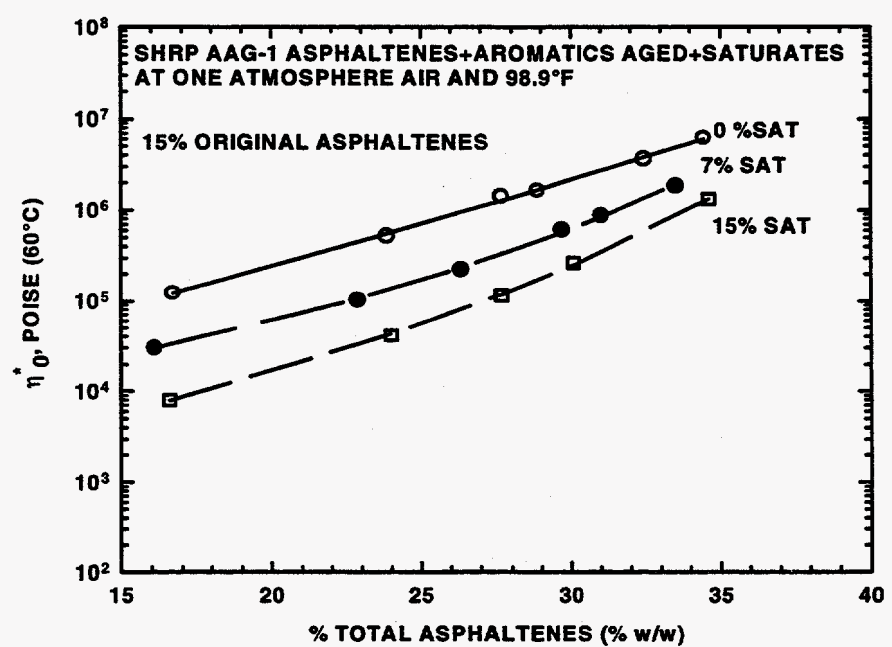


Figure 3-13. $\eta_{0,60C}^*$ Versus % AS for SHRP AAG-1 Blends Containing 15% Original Asphaltenes

SHRP AAG-1. However, the effects for SHRP AAG-1 blends are less pronounced than for SHRP AAA-1 blends, indicating that the composition of asphaltenes, aromatics, and saturates also play a significant role in determining the interaction among fractions.

CONCLUSIONS

It has been demonstrated in this study that composition has significant effects on the aging performance of asphalts. The data collected in this study support other researchers findings that asphaltenes and saturates are incompatible. Furthermore, the data collected in this study suggest that asphaltene/saturate incompatibility increases as either asphaltene or saturate content increases. Several specific conclusions that can be drawn from this study follow:

- (1) The AFS, or asphaltene formation as a function of carbonyl formation, is not affected by the presence of saturates. This, in combination with the previous study on the influence of asphaltenes on the AFS, implies that the AFS is a function only of the composition of reactive aromatics.
- (2) Asphaltenes, both original and those produced through oxidation, increase the viscosity activation energy (E_{vis}). For aged asphalt, the increase in E_{vis} with the increase in asphaltene content through aging can be characterized using $\left(\frac{dE_{vis}}{dCA}\right)$ which is a characteristic aging parameter of an asphalt.
- (3) Saturates increase $\left(\frac{dE_{vis}}{dCA}\right)$, indicating that high saturate content does serious damage to the performance of asphalt at low temperature.
- (4) The $(\ln \eta/\%AS)$ function is strongly dependent on the solvent power of the maltene phase. The presence of saturates reduces the solvation power of a maltene, which causes $\ln \eta$ to increase sharply with increasing asphaltene content. This effect is more pronounced as the initial asphaltene content increases.

CHAPTER 4

COMPOSITIONAL OPTIMIZATION FOR A SUPERIOR ASPHALT BINDER

One of the major causes of road failure is the fact that asphalt binders oxidize in service. Oxidative aging of an asphalt binder results in a higher carbonyl content and a higher viscosity, and thus renders the asphalt pavement more susceptible to damage from traffic load and thermal cycling. It has been reported (Lau et al., 1992) that during the aging of an asphalt binder, the log of the viscosity of the material has a linear relationship with its carbonyl content, and that the slope is asphalt dependent. This slope, the hardening susceptibility (Lau et al., 1992), is defined in Chapter 3 by Equation (3-1).

$$HS_{60^{\circ}\text{C}} = \frac{d \ln \eta_{0,60^{\circ}\text{C}}^*}{d \text{CA}} \quad (3-1)$$

Furthermore, Lau et al. (1992) showed that HS is a characteristic property of each individual asphalt binder and is independent of the aging temperature. A desirable asphalt binder will have a comparatively low value of HS.

Lin et al. (in press) suggested that the $HS_{60^{\circ}\text{C}}$ should be divided into two quantities which account for the fact that oxidation (carbonyl growth) increases asphaltene content which in turn increases viscosity.

$$HS_{60^{\circ}\text{C}} = \left(\frac{d \ln \eta_{0,60^{\circ}\text{C}}^*}{d \text{CA}} \right) = \left(\frac{d \ln \eta_{0,60^{\circ}\text{C}}^*}{d \% \text{AS}} \right) \left(\frac{d \% \text{AS}}{d \text{CA}} \right) \quad (3-2)$$

A modified Pal-Rhodes model (Pal and Rhodes, 1989) was used to describe the effect of asphaltenes on the viscosity, the first term in Equation (3-2) (Lin et al., in press). The influence of saturate content on the viscosity is discussed in Chapter 3 (Lin et al., 1995; Lin et al., 1996). Essentially all saturates have the same influence on the viscosity, except at low temperatures where wax content becomes important. Asphaltenes differ primarily in size which does have some effect

on hardening, with larger asphaltenes producing more hardening. In an asphalt, high initial levels of asphaltenes and saturates result in higher values of HS by increasing the first term in Equation (3-2). However, for different asphalts, the differences in the solvation power of the maltene phases override the differences between the asphaltenes.

The second term in Equation (3-2) relates the increase in asphaltene content to the corresponding increase in carbonyl content, and is defined as asphaltene formation susceptibility (AFS) (Lin et al., in press). It is reported that AFS is independent of saturate content and original asphaltene content but varies greatly from one asphalt to another. These findings imply that the maltene phase, or more specifically, the aromatic phase of an asphalt binder predominantly determines its hardening characteristics.

Jemison et al. (1995) reported that supercritical fractions and blends of supercritical fractions exhibited much improved hardening characteristics relative to their parent asphalts. In terms of Corbett fractions (Corbett, 1969), the supercritical fractions and blends are lower in saturates, asphaltenes and heavier polar aromatics. They are largely combinations of naphthene aromatics and lighter polar aromatics. This indicates that asphalts containing these aromatic fractions might show overall superior properties.

Many other researchers have investigated the relation between asphalt composition and its performance (Thenoux et al., 1988; Goodrich et al., 1986; Petersen, 1982; Corbett, 1979; Rostler and White, 1959). Since it is impossible to separate an asphalt binder into pure components, most of the studies have tried to identify the influence of generic fractions on asphalt behavior. Particularly, Corbett (1979) reported that a blend of naphthene aromatics and asphaltenes provided good properties. Since asphaltenes can be produced by aging naphthene aromatics, his results then suggests that an aged naphthene aromatics may act as a good binder. However, Corbett in his work did not show if the blend had favorable aging characteristics.

Equations (3-1) and (3-2) are both expressed in terms of a dynamic viscosity measured at 60°C. To ensure good performance at low temperatures, the viscosity temperature susceptibility (VTS) must be considered. This is conveniently expressed in terms of the Andrade Equation.

$$\ln\eta_0^* = A_{\text{vis}} + \frac{E_{\text{vis}}}{RT} \quad (3-3)$$

The viscosity activation energy, E_{vis} , is used as a measure of VTS.

There has been insufficient study of the predominant contribution of the aromatic portion of an asphalt to its properties and particularly to its property changes due to oxidative aging. This study is based on the Corbett separation of the aromatics into a naphthene aromatic (NA) fraction and a polar aromatic (PA) fraction. These fractions were aged and compared to the aging characteristics of the unseparated aromatics and to the aging characteristics of supercritical fractions separated from the asphalts. The parameters used for comparison are hardening susceptibility, HS, the asphaltene formation susceptibility, AFS, the viscosity asphaltene relationship (the second term in Equation (3-2)) and the viscosity temperature susceptibility, VTS (E_{vis} in Equation (3-3)).

EXPERIMENTS

Methodology

In addition to the NA and PA fractions of five SHRP core asphalts (AAA-1, AAD-1, AAF-1, AAG-1, and AAM-1), the aromatics fraction from four of these five asphalts and six supercritical fractions of AAF-1 were studied. As described in Chapter 2, the aromatics were separated from whole asphalts and further fractionated to produce the NA and PA fractions. The supercritical fractions were produced during the first year of this DOE effort and contain both naphthene and polar aromatics. For this study, fractions AAF F1 through AAF F4 and AAF F6 and AAF F7 were utilized. These fractions were renamed F1F, F2F, etc... for this study.

All of the materials were aged in POVs (see Appendix A) to assess age hardening. FTIR and DMA were used to monitor the chemical and physical property changes due to oxidative aging (see Appendix A). In addition, asphaltene content was determined by precipitation using n-hexane, as described in Appendix A.

Oxidative Aging

For each of the naphthene aromatics, polar aromatics and supercritical fractions, several samples, each having a mass of 0.7 ± 0.02 g were aged in the POVs under atmospheric pressure. The naphthene aromatic fractions from all five asphalts, together with the three light supercritical fractions from AAF-1 (F1F, F2F and F3F) were aged at 100°C for up to 55 days. The polar aromatic fractions, together with the three heavier supercritical fractions F4F, F6F and F7F were aged at 100°C and 95°C for up to 14 days. The aromatic fractions were aged previously (Lin, 1995). Samples were taken from the POVs periodically. Asphaltene content, carbonyl content, and viscosity all increase monotonically with aging time.

RESULTS AND DISCUSSION

Aromatic and Supercritical Fraction Compositions

Table 4-1 gives the initial CA and viscosity values of the five NA fractions, five PA fractions, and the six supercritical fractions. A dramatic difference between the initial viscosities of the PA fractions of the five asphalts are observed. Table 4-1 shows that the physical and chemical properties of NA and PA fractions are highly asphalt dependent. For the supercritical fractions, the initial CA and viscosity values increase with the fraction number. The composition of the supercritical fractions has a general trend (Stegeman et al., 1991) in that from fraction F1F to F7F, saturate content decreases from 30% to several percent, asphaltene content increases from negligible to above 10%. Naphthene and polar aromatics constitute the rest, with naphthene aromatics decreasing from 50% to 10%, and polar aromatics increasing from 20% to 70%, although not necessarily monotonically. For fractions from F2F to F7F, naphthene and polar aromatics are the major components. The composition of the aromatics in terms of naphthene aromatics and polar aromatics are shown in Table 4-2. Basically all the aromatics are about 50% in NA and PA, with AAA-1, AAD-1 and AAF-1 having slightly more NA than PA, while AAG-1 and AAM-1 having slightly more PA than NA.

Table 4-1. Initial Properties of NA, PA Fractions and Supercritical Fractions

Fraction	Initial CA	Initial Viscosity (poise)	Fraction	Initial CA	Initial Viscosity (poise)
ANA ^a	0.114	24.1	APA	1.23	74,540
DNA	0.117	15.5	DPA	1.60	39,600
FNA	0.158	57.1	FPA	1.20	806,200
GNA	0.215	364	GPA	2.01	2,227,000
MNA	0.154	116	MPA	1.31	4,800,000
F1F	0.167	<10	F4F	0.489	415
F2F	0.211	13.9	F6F	0.564	5,250
F3F	0.364	89.0	F7F	0.699	74,000

^a ANA represents naphthene aromatics of SHRP AAA-1. Likewise, DNA stands for naphthene aromatics of AAD-1, and APA represents polar aromatics of AAA-1.

Table 4-2. Content of NA and PA in Aromatics Fractions of Five SHRP Asphalts

Asphalt	Naphthene Aromatics (w%)	Polar Aromatics (w%)
AAA-1	58.6	41.4
AAD-1	55.1	44.9
AAF-1	57.5	42.5
AAG-1	44.0	56.0
AAM-1	46.3	53.7

Hardening Susceptibility (HS)

Lau et al. (1992) reported that the HS, as defined in Equation (3-1) is an important hardening characteristic for asphalts. A lower value of this parameter means a smaller increase in viscosity for the same amount of growth in carbonyl content due to oxidative aging, which is desirable. Figure 4-1 shows the viscosity-carbonyl area relationships for the five SHRP asphalt NA fractions. The HS values (slopes) for the NA fractions, PA fractions, and aromatics as well as these of the original whole asphalts (Davison et al., 1994) are listed in Table 4-3.

Several points are observed from Table 4-3. First, for each asphalt, the naphthene aromatic fraction has a smaller HS value than that of the aromatics and the whole asphalt, while polar aromatic fraction has larger HS value than that of the aromatics. Three out of the four aromatics have significantly smaller HS values than the whole asphalts. The exception, AAG-1, however, has nearly equal HS values for the aromatics and for the whole asphalt. Second, the HS values vary much more between the whole asphalts than between their fractions. The variation between

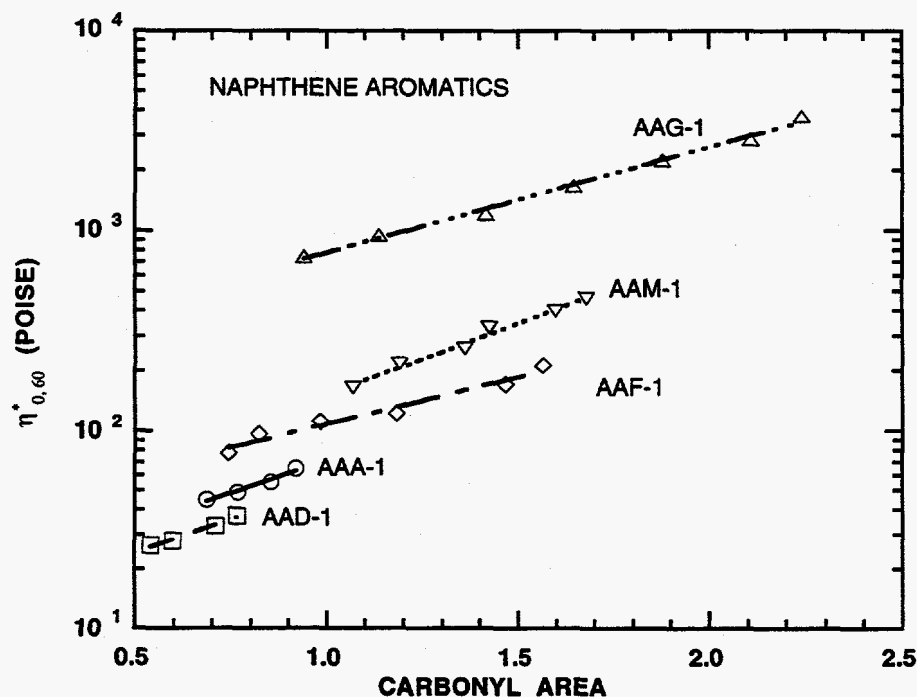


Figure 4-1. SHRP Asphalt Naphthene Aromatic Hardening Susceptibilities

Table 4-3. Hardening Susceptibilities (HS) of SHRP Asphalts and Their NA, PA and Aromatics Fractions

Asphalt	Naphthene Aromatics	Polar Aromatics	Aromatics	Whole Asphalt
AAA-1	1.53	3.13	1.73	6.93
AAD-1	1.56	2.88	2.34	8.00
AAF-1	1.08	2.07	1.60	4.47
AAG-1	1.21	2.30	1.58	1.35
AAM-1	1.65	3.01	--	4.91

asphalts is undoubtedly due to the different asphaltene and saturate contents in the whole asphalts. The lack of wide variation between the NA, PA, and aromatic fractions results from the relative compatibility due to the absence of the saturates and asphaltenes.

Figure 4-2 compares the HS of AAF-1 whole asphalt with the HS relationships of its fractions, both supercritical fractions and Corbett fractions. The data for F1F are not shown, as the extremely low viscosities require use of an alternative geometry for measurement, for which there was not enough material. Obviously, the whole asphalt has a much larger HS than its fractions. This is entirely due to the presence of asphaltenes and saturates in the whole asphalt. In the absence of asphaltenes, the saturates present in the lighter supercritical fractions have little effect on the HS.

The HS values of the supercritical fractions generally increase with increasing PA content and decreasing NA content. Fraction F3F is an exception, the reason for which is not currently understood. However, the HS of F3F is still less than the HS of either the polar aromatics or F7F, and far less than the whole asphalt. F7F has slightly larger HS than the polar aromatics because F7F is not only largely polar aromatics, but it also contains a measurable amount of asphaltenes. The conclusion is that to achieve a low HS, more NA are needed than PA in the targeted asphaltic material.

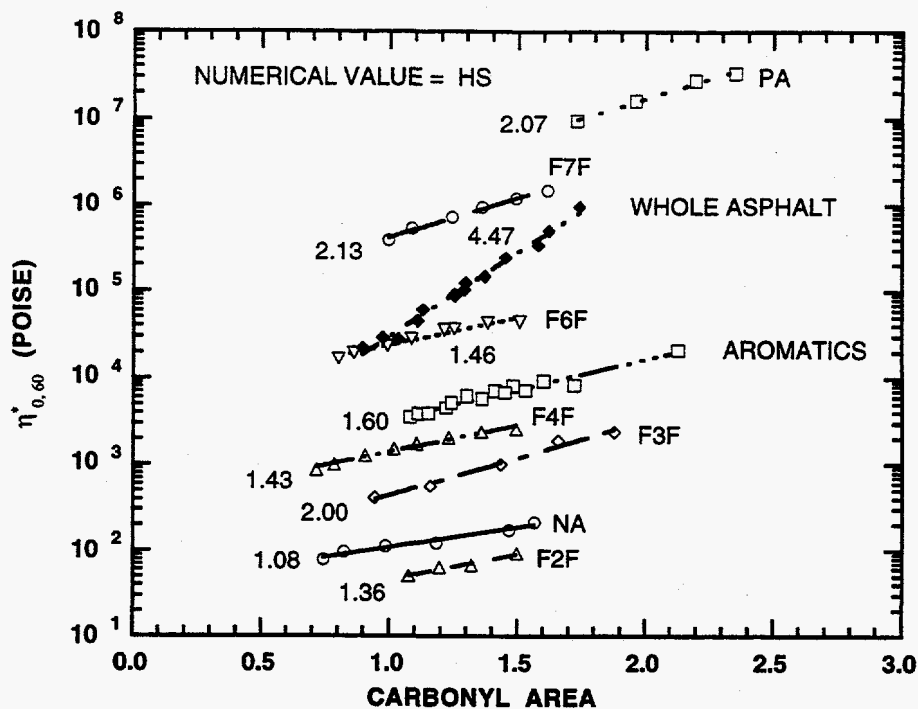


Figure 4-2. AAF-1 Fraction Hardening Susceptibilities

Asphaltene Formation Susceptibility (AFS) and Viscosity-Asphaltene Relationship

Figure 4-3 shows the relationship between asphaltene content and carbonyl area for the NA fractions. The AFS is the slope of the line. The AFS relationships of the PA fractions are shown in Figure 4-4. Naphthene aromatics have significantly lower AFS values than polar aromatics. The AFS values of the aromatics are listed in the third column of Table 4-4. The second column in the table contains the AFS values calculated from the NA and PA data assuming that the AFS is additive and using the composition data of the aromatics in Table 4-2. The AFS values for the NA and PA fractions are also listed in Table 4-4. The calculated AFS values are lower than the experimental AFS values except for AAA-1, for which the calculated and measured AFS for aromatics nearly equal. This can be explained by the relative reaction rate of the two pure fractions. Figure 4-5 is a plot of carbonyl growth versus aging time for naphthene aromatics and polar aromatics for one of the asphalts. Obviously the reaction rate for the polar aromatics is overwhelmingly larger than that for the naphthene aromatics. This is also true for other asphalts (data not shown). Therefore, during the aging of the aromatics fraction, most of the carbonyl

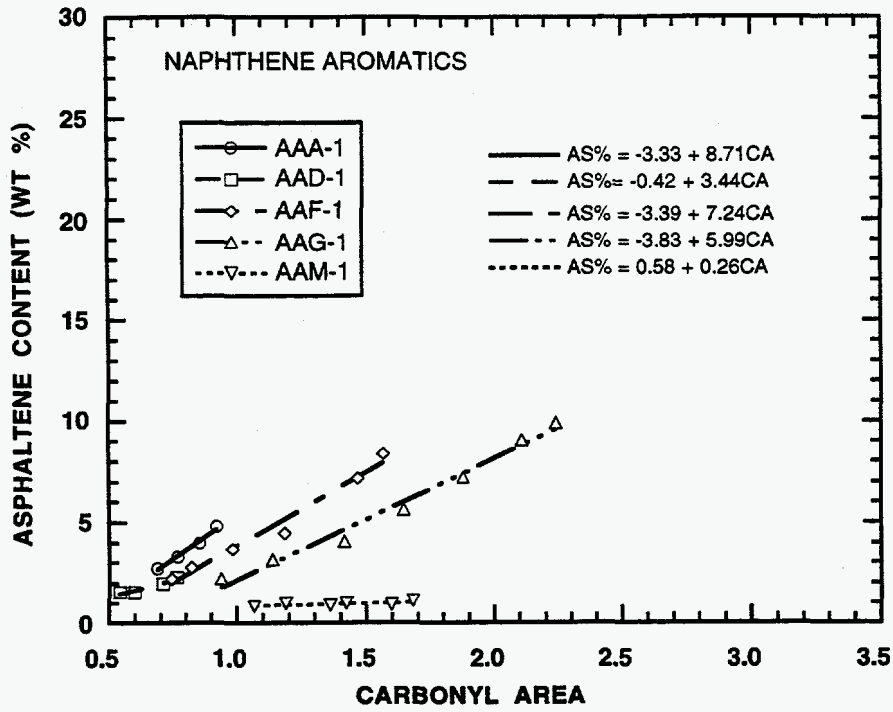


Figure 4-3. AFS for SHRP Asphalt Naphthene Aromatics

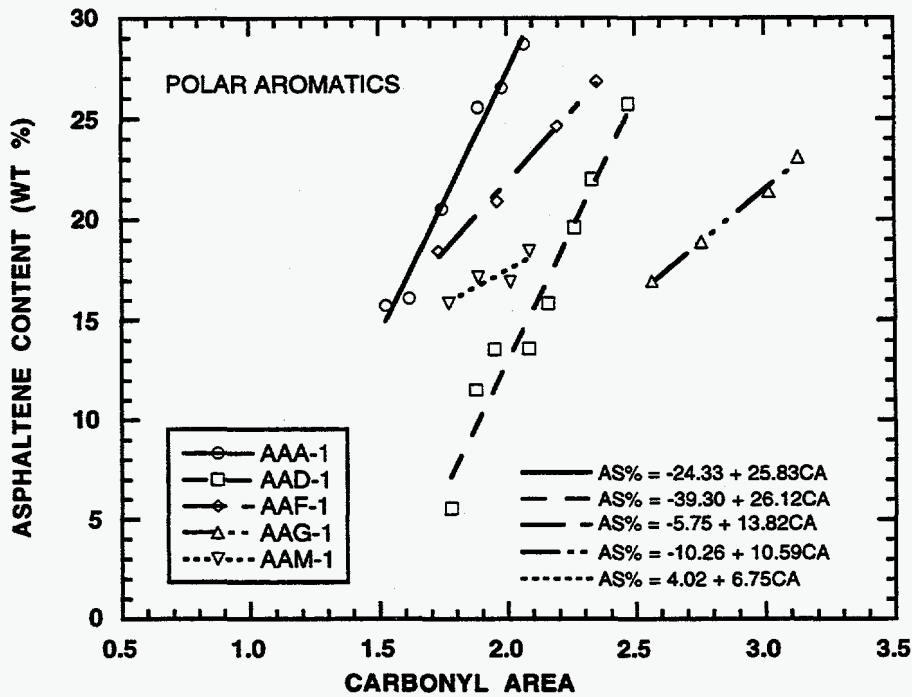


Figure 4-4. AFS for SHRP Asphalt Polar Aromatics

Table 4-4. Comparison of Calculated and Measured AFS of Aromatics of SHRP Asphalts

Asphalt	Calculated Aromatics ^a	Aromatics	Naphthene Aromatics	Polar Aromatics
AAA-1	15.80	15.13	8.72	25.83
AAD-1	13.62	19.72	3.44	26.12
AAF-1	10.04	11.75	7.25	13.82
AAG-1	8.57	9.55	5.99	10.59
AAM-1	3.75	--	0.26	6.75

^a Assume that AFS is additive.

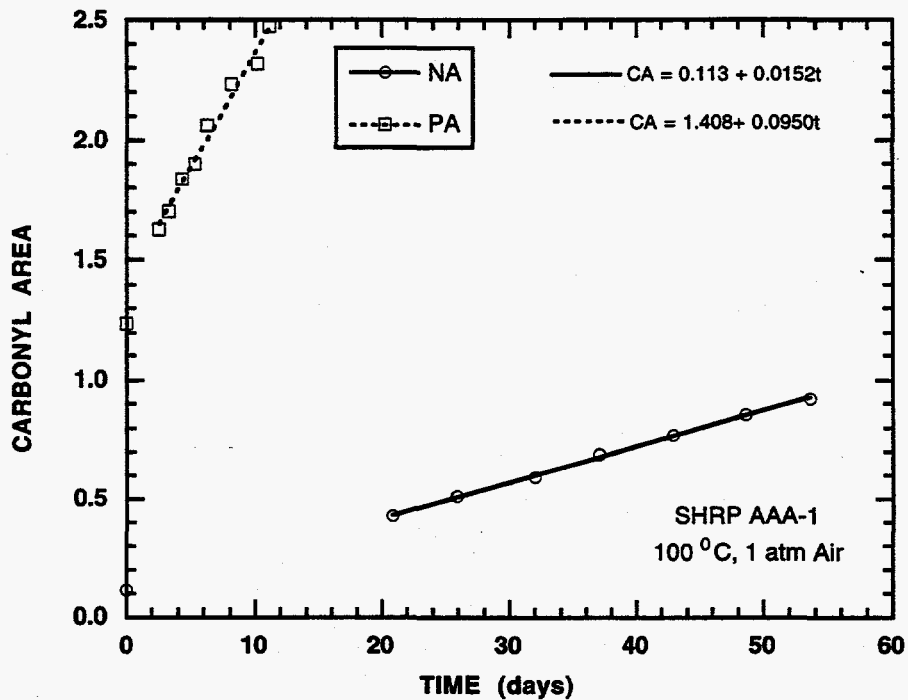


Figure 4-5. Comparison of AAA-1 NA and PA Carbonyl Growth Rates

growth and consequently most of the asphaltene increase comes from the polar aromatic portion. Thus, the AFS values of the aromatics are very close to those of the polar aromatics. Figure 4-6 shows the AFS for the supercritical fractions of asphalt AAF-1. Generally, the AFS increases as the polar aromatic content increases (fraction number increases).

Figure 4-7 is a plot of viscosity versus asphaltene content for the NA fractions. The slopes of the regression lines represent the abilities of the aromatic media to dissolve the asphaltenes. In this Chapter, the slope is called the solvation power parameter. A small solvation power parameter corresponds to a small increase in log viscosity with the same amount of asphaltene addition, and thus a strong solvation power. Lin et al. (1996) used a modified Pal-Rhodes model to describe the effect of the asphaltene content on the viscosity. However, the range of asphaltene content was much larger in their study than that shown in Figure 4-7. The regression lines in Figure 4-7 can be viewed as local approximations of the modified Pal-Rhodes model. Table 4-5 lists the solvation power parameters of the NA fractions, the PA fractions and the aromatics. It

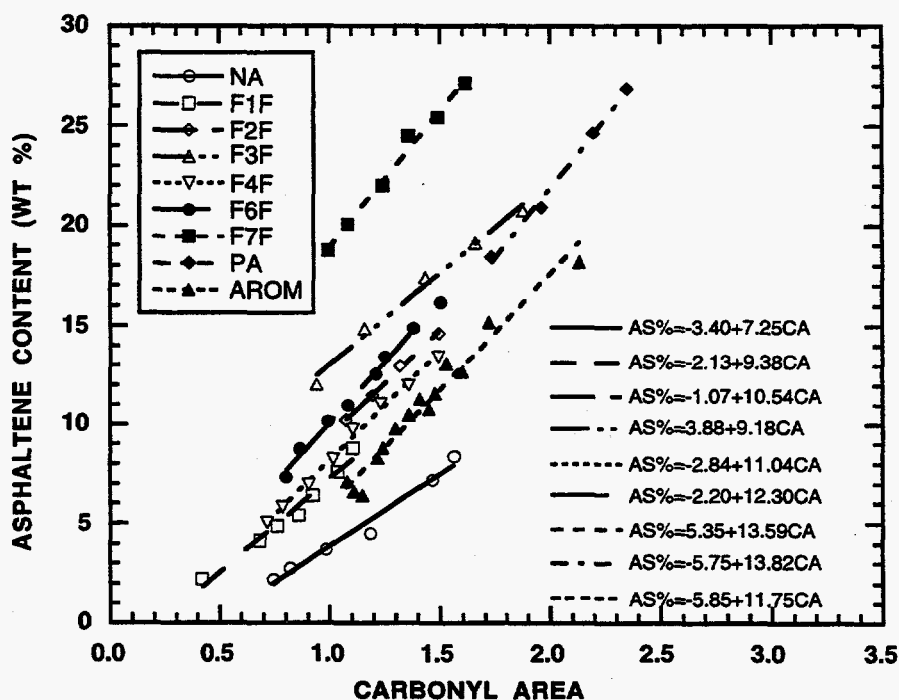


Figure 4-6. AFS for AAF-1 Fractions

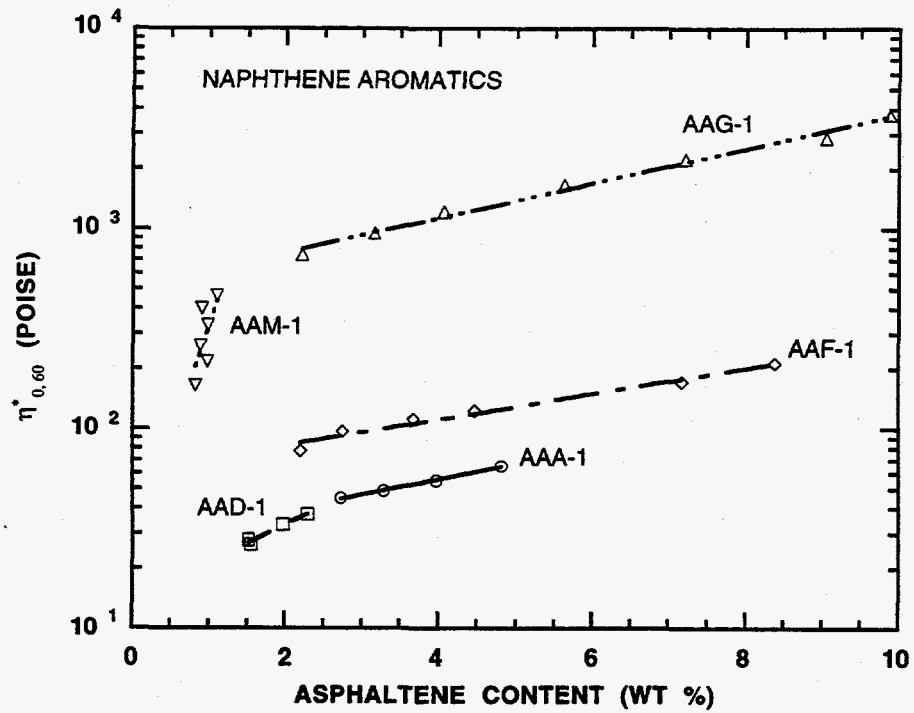


Figure 4-7. SHRP Asphalt NA Viscosity/Asphaltene Relationships

Table 4-5. Comparison of Solvation Power Parameters of Fractions of SHRP Asphalts

Asphalt	Naphthene Aromatics	Polar Aromatics	Aromatics
AAA-1	0.177	0.118	0.117
AAD-1	0.430	0.105	0.118
AAF-1	0.148	0.148	0.131
AAG-1	0.200	0.216	0.164
AAM-1	2.696	0.388	--

is evident for asphalts AAF-1 and AAG-1 that the solvation power parameters of the three fractions are similar. However, for asphalts AAA-1 and AAD-1, the solvation power parameters for the PA fractions and aromatics are slightly smaller than those of the NA fractions. For these two asphalts, this indicates that the PA fractions have stronger solvation power than the NA fractions. Furthermore, as long as the aromatics fraction contains a sufficient amount of polar aromatics, the solvation power approaches that of the pure polar aromatics. For asphalt AAM-1, the naphthene aromatics fraction has a far larger solvation power parameter than the polar aromatics fraction. The data also show that the AAM-1 naphthene aromatics fraction has a much larger solvation power parameter than the naphthene aromatics fraction of the other asphalts. One possible explanation for this is that the oxidation products from the naphthene aromatic fraction from AAM-1 are viscosity building components much like the oxidation products from the polar aromatics are viscosity building components for the other asphalts.

Figure 4-8 is a plot of viscosity versus asphaltene content for the fractions of AAF-1. As noticed previously, the whole asphalt has nearly identical solvation power parameters for its NA fraction, PA fraction, and aromatics. The solvation power parameters of the supercritical fractions of AAF-1 are all close to these values. Once again, F3F an exception to this general trend. The reasons for this are not clear.

From the analysis of the AFS values and solvation power parameters, it is seen that polar aromatics may have slightly stronger solvation power than naphthene aromatics, but the naphthene aromatics have much smaller AFS. As a combined effect, naphthene aromatics have a smaller HS, which is desirable.

Viscosity-Temperature Susceptibility

In order to describe viscosity-temperature susceptibilities of the fractions, the two-parameter Andrade equation, Equation (4-1), was used. Viscosities for a specific sample were measured at multiple temperatures to obtain its E_{vis} . Figure 4-9 shows the increase in E_{vis} with respect to carbonyl growth. The changes in E_{vis} during the aging experiment are around or below 20 kJ/mole. On the other hand, the differences between the E_{vis} of NA fractions of different asphalts may be as much as 50 kJ/mole. This indicates that the absolute value of E_{vis} is more

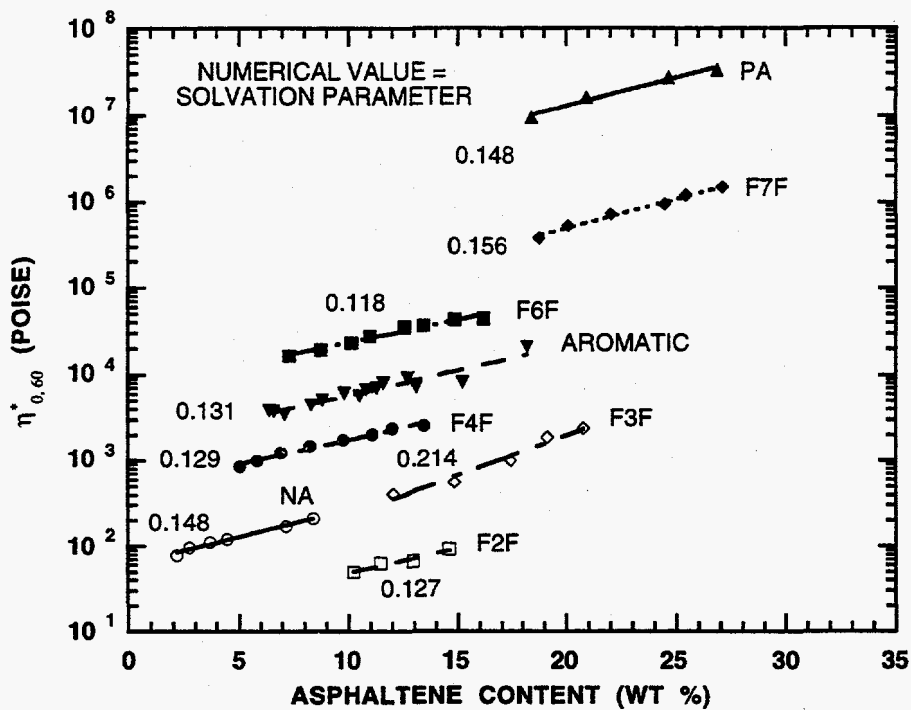


Figure 4-8. AAF-1 Fraction Viscosity/Asphaltene Relationships

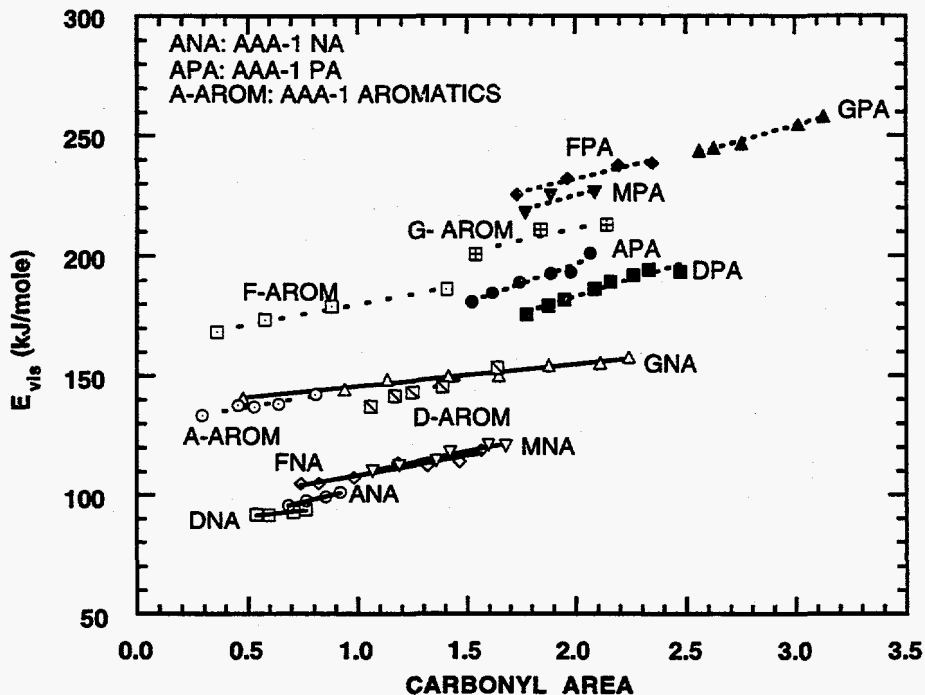


Figure 4-9. Viscosity Activation Energy Versus Carbonyl Area for NA and PA

important than its change due to oxidative aging. It is observed that E_{vis} of the NA fractions fall between 90 kJ/mole and 160 kJ/mole, while E_{vis} of the PA fractions fall between 170 kJ/mole and 260 kJ/mole. For each asphalt, the NA fraction has much smaller E_{vis} than the PA fraction, with the aromatics in between. This trend is again shown by Figure 4-10 where E_{vis} is plotted versus carbonyl area for the AAF-1 supercritical fractions. As the fractions contain more polar aromatics, their E_{vis} becomes larger. This means that in terms of viscosity-temperature susceptibility, a high content of naphthene aromatics is desirable.

Figure 4-11 shows a remarkable relation between A_{vis} and E_{vis} in Equation (4-1) that, if exact, makes a viscosity isokinetic temperature for all materials (a temperature at which all materials have the same viscosity value). The displacement between the polar aromatics line and the other line may arise because the polar aromatics, as well as, fractions F6F and F7F become so hard on aging that low temperature viscosities could not be measured. Thus, for these samples, the viscosity measurement temperature range was from 60°C to 90°C while for other samples, the viscosity was measured at temperatures from 10°C to 90°C. This suggests that the Andrade Equation may be only an approximation with E_{vis} varying with temperature. The displacement resulting from the difference between the two temperature ranges is about 20 kJ/mole, which is still less than the difference between the NA fractions and the PA fractions from the five different asphalts. Therefore, it is still likely that the PA fractions have much larger E_{vis} than the NA fractions.

CONCLUSIONS

The following conclusions are derived from this study:

1. The HS of each asphalt and its fractions follow the ranking NA < aromatics < PA < whole asphalt. For an asphalt's supercritical fractions, HS increases with fraction number.
2. For a given asphalt, the NA fraction has a much smaller AFS than its PA fraction; aromatics are intermediate. For supercritical fractions, the AFS increases with fraction number.
3. The NA fraction has a bit less solvation power than the PA fraction. However, the effect of a much smaller AFS overrides the effect of a bit less solvation power. Furthermore, the

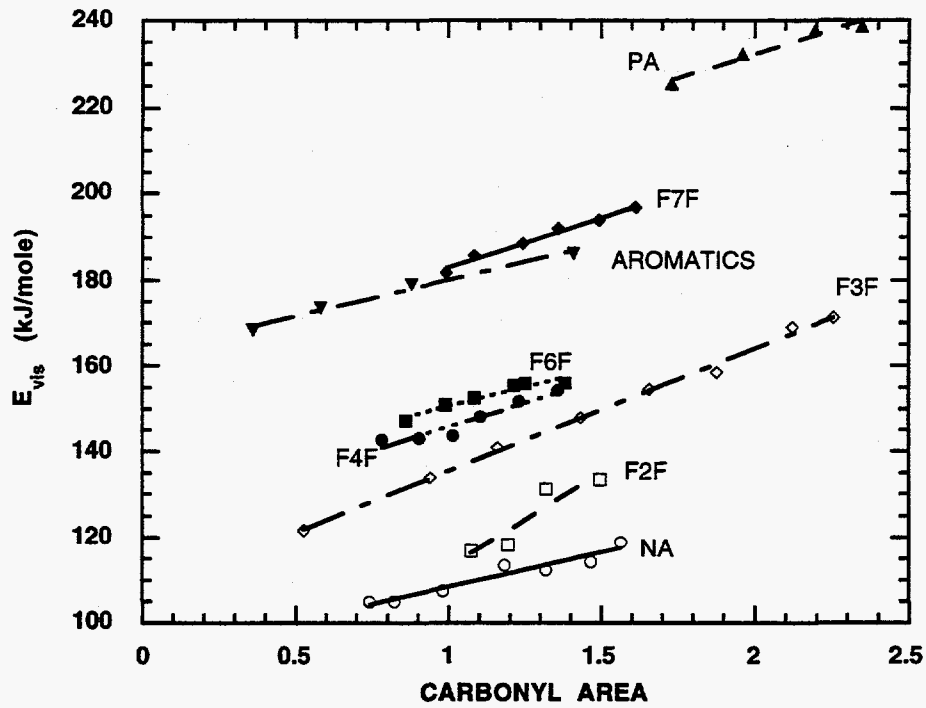


Figure 4-10. Viscosity Activation Energy Versus Carbonyl Area for AAF-1 Fractions

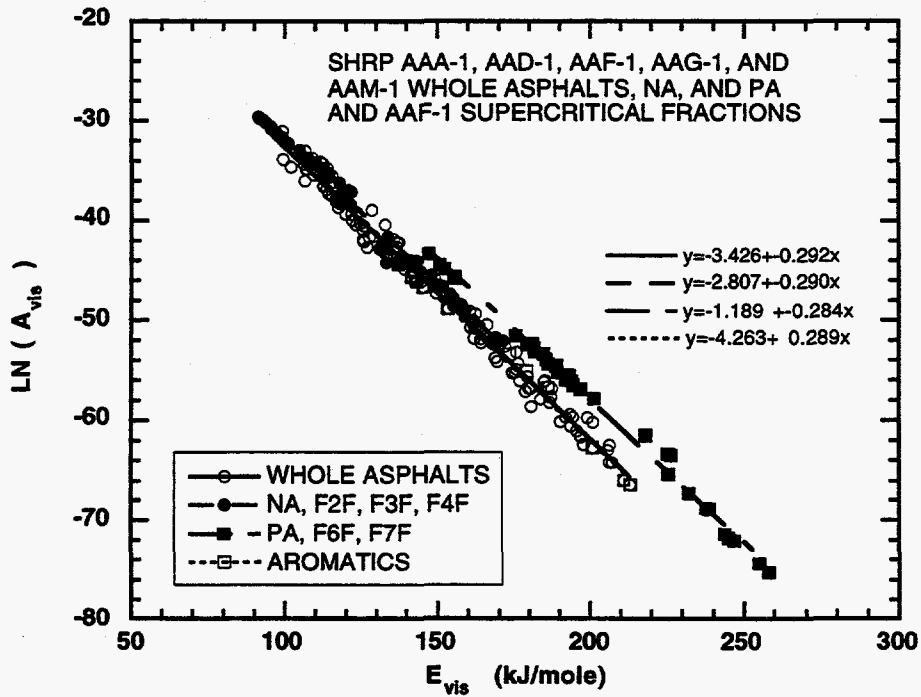


Figure 4-11. Correlation of Andrade Equation Parameters

presence of enough PA results in a solvation power as strong as a pure PA.

4. The NA fraction has smaller E_{vis} than the PA fraction.
5. A high naphthene aromatics content is desirable in the targeted aromatics asphaltic material.
6. A_{vis} correlates linearly with E_{vis} . The significance of this correlation is yet to be explored.

CHAPTER 5

THE USE OF HPLC TO DETERMINE THE SATURATE CONTENT OF HEAVY PETROLEUM PRODUCTS

Much effort has been expended in determining the chemical composition of asphalt and other heavy petroleum products. Composition data are required by refiners who wish to upgrade their residues. Residue upgrading by catalytic cracking requires that the metals (especially Ni and V) content of the feed be as low as possible so that the catalyst deactivation is minimized. It is widely known that the metals concentrate in the most highly condensed, most polar molecules in petroleum residues (Savastano, 1991; Branthaver et al., 1983; Branthaver et al., 1984). If the content of this highly polar fraction is too high, catalytic cracking may not be economical. In addition, chemical or group-type composition information is necessary because many residue processing parameters have been determined empirically based on the aromatic and paraffinic contents of the feedstock in order to maximize yield of high value products.

The chemical composition of petroleum residues is also important to the scientist, especially the asphalt chemist who is interested in correlating asphalt behavior to chemical composition. At least one method for determining composition based on chemical reactivity (Rostler and Sternberg, 1949) is routinely used. Generally, these chemical reactivity classification methods only allow for empirical correlations, since the fractionated components are irreversibly altered in the separation process (White et al., 1970). Although the fractions from such separations can be analyzed individually, the properties determined from individual analyses are undoubtedly not representative of their properties in the unfractionated asphalt.

To eliminate the irreversible changes that the chemical reactivity separation methods produce, several chromatographic techniques for asphalt group-type fractionation have been proposed over the past several decades. Many of the group-type fractionation methods, including the method of Rostler and Sternberg (1949), entail performing a binary fractionation of the material based on solubility in some arbitrary solvent. The solvents of choice typically have been paraffinic hydrocarbons. The insoluble fraction, if present, is separated by filtration and is

referred to as the asphaltene fraction, or simply asphaltenes. The paraffin-soluble fraction is called maltenes or petrolenes. It is widely known that the quantity of asphaltenes increases with decreasing carbon number and increased branching in paraffinic solvents. As discussed previously, the asphaltene fraction contains most of the metal-bearing species. The asphaltenes have been shown to be responsible for the highly viscous nature of asphalts (Lin et al., 1995; Lin et al., in press). More complicated separations focus on further separation of the maltene fraction. The most well known of these is the column chromatography method of Corbett (1969) described in Chapter 2.

In the mid 1970s to early 1980s, petroleum chemists began to use the relatively new analytical technique of high performance liquid chromatography (HPLC) for group-type analyses of petroleum and coal derived materials (Suatoni and Swab, 1975; Suatoni et al., 1975, Suatoni and Swab, 1976; Suatoni and Garber, 1976; Dark and McFadden, 1978; Dark and McGough, 1978; Gayla and Suatoni, 1980). One primary advantage of HPLC is the elimination of cut-point subjectivity. Low solvent volume (80 mL vs. 1500 mL), low solvent toxicity (n-C₆ vs. Toluene and TCE), and much shorter analysis times (10-40 min. vs. several days) are additional benefits of using HPLC.

Suatoni and Swab (1975) utilized a μ -PORASIL packing to perform group-type analyses on several high boiling compounds in one of their earlier works. They concluded that the saturate fractions from different materials with similar boiling points possessed nearly the same refractive index (RI) response factor (RF_s) regardless of crude source. Furthermore, they analyzed several compounds with a wide range of boiling points and they showed that the RF_s was a function of residue boiling point range. In essence, they were able to construct a calibration factor correlation based on sample boiling point. This is explained by inspecting Figure 5-1 which shows the refractive index of n-alkanes as a function of carbon number (handbook of Chemistry and Physics, 1987), which is intimately related to boiling point. It has been noted elsewhere that unlike the data of Suatoni and Swab, the data presented in Figure 5-1 suggest that the refractive index may approach a limiting value (Lundanes and Greibrokk, 1985). In a later experiment, Gayla and Suatoni (1980) reported data that indicated that the RF_s values for saturates obtained from coal

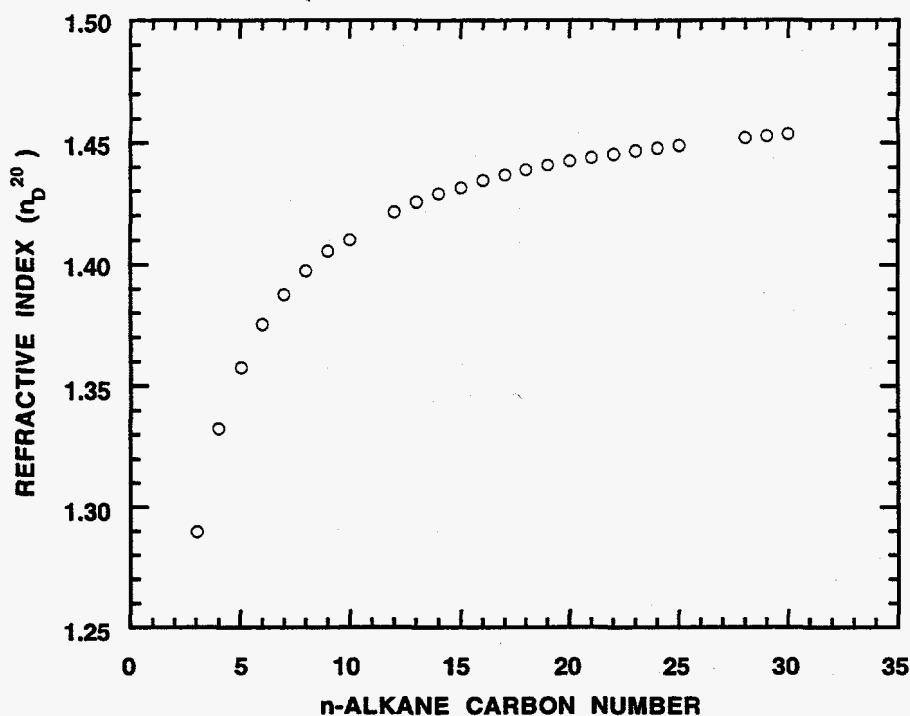


Figure 5-1. Refractive Index Versus n-Alkane Carbon Number

liquids with widely varying boiling points were *identical* for three out of the four materials studied.

Dark and McGough (1978) performed separation of asphalts using a μ -BONDAPAK column and multiple solvents to produce 9 separate fractions. They used RF_s values determined from crude oils rather than the RF_s values from the asphalts they investigated to quantify the various fractions. They indicated that the RF_s values were in error, but they concluded that relative comparisons could be made. The reason for this error is evident from Figure 5-1. Two different crude oils may have widely different average boiling points (average n-alkane carbon numbers), and thus, have widely different RF_s values. Furthermore, the average boiling point of a crude oil is significantly different from the average boiling point of its own residue.

Dark (1982) concluded that the best agreement between HPLC crude oil saturate content and open column saturate content was obtained when the HPLC saturate content was determined by difference, rather than by direct methods. This work is commonly cited in more recent publications and, as a result, most of the subsequent HPLC studies have focused on determining

the content of the aromatic components using various detectors and obtaining the saturate content by difference (Bishara and Wilkins, 1989; Beg et al., 1990, Ali and Nofal, 1994; Dark, 1983). In fact, some researchers have abandoned the use of detector calibration altogether and have instead relied on gravimetric methods (Carbognani and Izquierdo, 1990). Lundanes and Greibrokk (1985) were able to obtain calibration factors for saturates obtained from crude oil residues, but only after GPC fractionation was performed to narrow the molecular weight range (ie. boiling point range) of the sample.

This work is an attempt to determine if accurate quantitation of the saturate content in asphalt and asphalt related materials can be accomplished using refractive index response factors. Because most refiners typically operate their vacuum distillation towers at similar conditions, it is natural to assume that the highest boiling residues (asphalts) should all have similar RF_s values, as demonstrated by Suatoni and Swab. Furthermore, if the RF_s values for high boiling residues are similar, it may be possible to isolate a *suitable* standard saturate calibration material.

MATERIALS

This experiment involved the analysis of industrial supercritical fractions (ISCF) obtained from a number of different refiners and asphalts obtained from the Strategic Highway Research Program (SHRP) materials reference library (MRL). The other material analyzed in this study is petroleum jelly obtained from a local supermarket.

Supercritical fractions were analyzed because they are typically products of residue upgrading. They are also of interest due to their potential for use as either asphalt additives or asphalt recycling agents. Most currently available recycling agents are by-products of lube oil manufacture. To minimize the aromatic content in lube oils, the process conditions are typically quite conservative, resulting in recycling agents with high saturate contents. It is recommended that recycling agents contain no more than 30% saturates in order to produce good quality recycled asphalt mixtures (Epps et al., 1980). This is because saturates and asphaltenes are inherently incompatible. Supercritical fractionation is one potential industrial method for controlling the saturate content in recycling agents. Thus, it is essential to be able to accurately

quantify the saturate content in ISCFs. In this work, the ISCFs have been given arbitrary designations to protect the identities of the companies supplying material.

Several "standard" asphalts were obtained from the SHRP MRL. These SHRP asphalts have been studied extensively throughout the world and a large data base of chemical and physical properties exists for these asphalts. The SHRP reference included at the end of this paper is by no means an exhaustive compilation of available data (Mortazavi and Moulthrop, 1993).

METHODS

HPLC Standards Preparation

To perform quantitation of the saturate content in the heavy petroleum products, it was necessary to obtain standard materials. Because it is not possible to purchase "saturates" from chemical suppliers, it was necessary to perform preparative column chromatography to isolate saturate fractions from various petroleum products. As described in Chapter 2, several variations of the Corbett procedure were utilized. Initially, the "pure" saturates were prepared according to the procedure outlined in ASTM D4124. As the experiment continued, this procedure was modified first by substituting n-hexane for n-heptane and then by performing prefractionation according to the "giant Corbett" procedure described by Peterson et al. (1994) in order to produce larger quantities of the pure fractions. The paraffin fraction from the "giant Corbett" procedure was then fractionated following the method in ASTM D4124 to produce a pure saturate fraction and a slightly saturate- contaminated light naphthene fraction. Using these methods, pure saturate fractions were obtained for eight ISCF materials and four core SHRP asphalts.

Instrumentation and Sample Preparation

A WATERS 600E multisolvent delivery system was utilized for gel permeation chromatography (GPC) and HPLC analyses of the petroleum products investigated in this study. Injection was accomplished with a WATERS 700 WISP autoinjector. A WATERS 410 differential refractometer (RI) detector was utilized for sample detection. Data acquisition and processing were performed using Baseline 810 software.

For HPLC analyses, helium-sparged HPLC grade n-hexane was utilized as the mobile phase. The flow rate was controlled at 2 mL/min. A single column 7.8 mm ID × 300 mm long packed with 10 μm μ-BONDAPAK aminopropylmethylsilyl bonded amorphous silica was used for the analyses. The column was backflushed fifteen minutes after injection to speed the elution of the polar aromatics and shorten the analysis time. Samples were prepared by dissolving 0.20 ± 0.01 g of sample in 10 mL n-hexane. The "pure" saturate samples were prepared by dissolving 0.100 ± 0.005 g in 10 mL n-hexane due to the limited quantity of material. Even so, several of the "pure" saturate fractions were exhausted in this study. After the samples were filtered through preweighed 0.45 μm PTFE membrane syringe filters, 20 μL aliquots of the maltene fraction were injected onto the column. Sample elution was monitored by both the RI detector and a UV detector (WATERS 486 Tunable Absorbance Detector). The UV detector was utilized to monitor the purity of the saturate fractions and was operated at a wavelength of 254 nm. The columns and detectors were operated isothermally at 308.2 K. The saturate content was determined from the pure saturate refractive index RF_s , as described in the results and discussion section.

Molecular weights were determined using GPC, as described in Appendix A.

Response Factor Determination

A representative asphalt RI chromatogram is shown in Figure 5-2. Three peaks are evident. The first, sharp peak signifies elution of the saturates. The second, broader peak is produced by elution of the (naphthene) aromatics. The final peak, which elutes approximately 30 minutes after injection indicates elution of the polars (aromatics). The resolution between the saturates and aromatics, in general, is not sufficient to allow an accurate determination of the saturate peak area. As a result, the peak height is used rather than the peak area for quantitation purposes. The RF_s is calculated by dividing the peak height by the mass of the pure saturate fraction weighed into the scintillation vial.

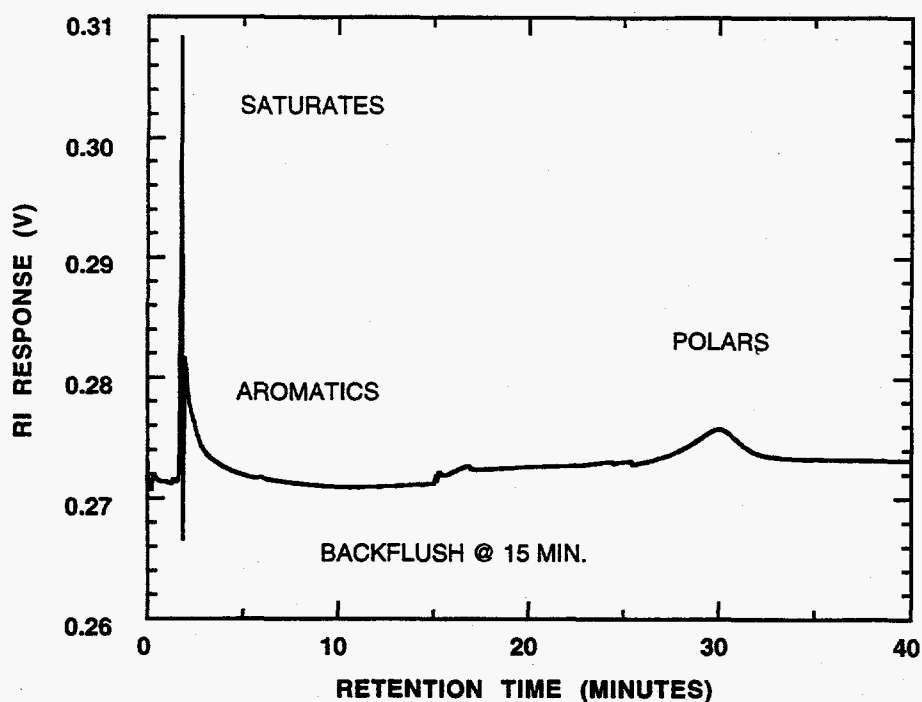


Figure 5-2. SHRP AAC-1 Chromatogram

RESULTS AND DISCUSSION

Pure Saturates

The RF_s values and molecular weights for pure saturates obtained from the 12 different petroleum materials and the petroleum jelly are listed in Table 5-1. Average RF_s values for asphalt saturates, ISCF saturates, all of the heavy petroleum product saturates studied in this work, and the petroleum jelly are listed in Table 5-2. It is immediately obvious from the data in Table 5-2 that the saturates from industrial supercritical fractions have a slightly higher overall RF_s than the asphalt saturates. Even though this is expected based on the slightly higher molecular weights of the ISCF saturates, this difference in average RF_s may be attributed to the fact that the ISCF saturates were produced nearly a year after the asphalt saturates and the fact that the two different groups were isolated by different researchers. Furthermore, the saturate fraction obtained from asphalt AAM-1 has the highest molecular weights of all samples analyzed but has one of the lowest response factors. Therefore, it is natural to conclude that the variations in RF_s values are due mainly to operator subjectivity (one of the main problems associated with the open

Table 5-1. GPC Molecular Weights and HPLC Refractive Index Response Factors for 13 Saturate Fractions

Saturate Source Material	M_n	M_w	RF _s (V/g)
AAA-1	611	842	1.10
AAD-1	515	706	1.02
AAF-1	914	1142	1.24
AAM-1	1576	2285	1.03 ^a
ISCF A	970	1328	1.16
ISCF B	934	1322	1.11
ISCF C	1157	1529	1.18
ISCF D	1215	1635	1.19
ISCF E	952	1220	1.09
ISCF F	906	1325	1.11
ISCF G	816	1218	1.13
ISCF H	901	1188	1.05
Petroleum Jelly	800	1164	1.05

^a three different "pure" saturate samples analyzed

Table 5-2. Average Refractive Index Response Factors for Saturate Groups

Group	RF _s (V/g)
Asphalt saturates ^a	1.06 ± 0.096
ISCF saturates ^a	1.13 ± 0.048
All saturates analyzed	1.10 ± 0.079
Petroleum Jelly	1.05

^a pure asphalt saturate fractions and pure ISCF saturate fractions isolated by different researchers at different times

column method) and are not indicative of any real difference between the saturates. This argument may naturally be extended to say that petroleum jelly is similar enough to the asphalt and ISCF saturate fractions that it has the potential for use as a "standard" saturate for the HPLC determination of saturate content in heavy petroleum products such as asphalts. Even if the petroleum jelly does not have *exactly* the same RF_s as the materials examined in this study, it may still be a suitable calibration standard. The petroleum jelly not only has approximately the same RF_s value as the asphalt and ISCF saturate fractions but it is also of similar molecular weight. It should be noted that the molecular weight values reported in Table 5-1 represent alkanes with carbon numbers between 37 and 112. The molecular weights reported in Table 5-1 may seem high, but they match values for saturate fractions obtained from both vapor pressure osmometry and field ionization mass spectrometry (Boduszynski et al., 1980). The UV chromatograms of all of the saturate fractions analyzed indicated approximately the same amount of UV active species in each fraction, including the petroleum jelly.

Asphalt Saturate Contents

Once it was determined that the saturates from the different asphalts, supercritical fractions, and the petroleum jelly were all similar, it was possible to determine the saturate contents of any unknown sample. This was done by injecting an unknown sample onto the columns and determining the peak height for the saturate fraction. The saturate content in the sample was determined by dividing the sample peak height by the appropriate RF_s , and then dividing by the sample mass used and multiplying by 100 to obtain saturate content in terms of weight percent (wt%).

The saturate contents, in wt%, of the eight SHRP core asphalts are listed in Table 5-3. This table shows the saturate contents of the asphalts determined using the asphalts own saturate RF_s , the average asphalt RF_s , the overall average RF_s , and the RF_s of the petroleum jelly in comparison with values obtained from Mortazavi and Moulthrop Appendix A (1993). The values obtained from HPLC calibration using the various response factors are remarkably similar but are, in general, not the same as those obtained from the literature. Upon closer investigation it is evident that the saturate contents determined by HPLC for all of the asphalts except AAD-1 are

Table 5-3. Saturate Content of SHRP Core Asphalts Using Various Calibration Standards

Asphalt	MRL %S	HPLC %S	HPLC %S	HPLC %S	HPLC %S
		Asphalt's Own RF _s	Asphalt Ave. RF _s	Overall Ave. RF _s	Petroleum Jelly RF _s
AAA-1	10.6	10.8	11.1	10.8	11.2
AAB-1	8.6	-	12.4	12.1	12.5
AAC-1	12.9	-	17.3	16.8	17.5
AAD-1	8.6	7.6	7.3	7.1	7.4
AAF-1	9.6	10.7	12.5	12.1	12.6
AAG-1	8.5	-	9.6	9.3	9.7
AAK-1	5.1	-	6.0	5.8	6.0
AAM-1	1.9	12.0	11.6	11.2	11.7

higher than the literature values. However, this does not mean that the HPLC values are incorrect. In fact, the HPLC saturate contents are probably much more accurate. The differences between the HPLC determined saturate contents and the saturate contents determined by the traditional method can be attributed to the use of different stationary phases for the different analyses. The aminopropylmethylsilyl bonded phase in the HPLC column retains the naphthene aromatics better than the naked alumina in the open column. The increased retention of the naphthene aromatics results in more saturates eluting before the naphthene aromatics elute in the HPLC separation. Data published by Dark (1982) support this belief and indicate that even more efficient separation of the saturates and (naphthene) aromatics may be possible using naked silica as the stationary phase. However, using silica as the stationary phase may cause irreversible adsorption of the polar (aromatic) fraction (Suatoni and Swab, 1975).

The increased retention of the naphthene aromatics and large deviation from the literature saturate value is most evident for asphalt AAM-1. While the use of an average RF_s or the petroleum jelly RF_s might possibly result in a large deviation from the "true" value, it is unlikely that the use of the RF_s for the saturates from AAM-1 would cause the deviations evident in

Table 5-3. That is, using the RF_s for the saturates from a given asphalt should result in accurate saturate contents for that given asphalt. Further support for the inaccuracy of the data obtained from the open column techniques can be seen in the variability of the literature values themselves. The literature saturate contents reported in Table 5-3 (Appendix A, Mortazavi and Moulthrop, 1993) differ from other values reported in the same reference (Table 3, Mortazavi and Moulthrop, 1993). This only substantiates the statement that the cut-points for the traditional open column technique are subjective, sometimes highly subjective. HPLC techniques eliminate most, if not all, operator subjectivity if a suitable calibration standard is used. The data collected in this study indicate that petroleum jelly may be a suitable standard.

CONCLUSIONS

All of the previous work on HPLC calibration has relied on the tacit assumption that the saturate data from the standard open column separation methods are correct and that the HPLC saturate contents must be determined in such a way as to minimize the difference between the two values even if this requires obtaining the saturate content by difference. This belief that the open column saturate contents represent the true saturate contents has undoubtedly hindered development of HPLC as an analytical tool in characterization of heavy petroleum products even though it has been known for over ten years that bonded-phase HPLC provides better separation of the naphthene aromatics from the saturates. A natural consequence of this is that the saturate contents determined by HPLC should be more representative of the "true" saturate content. Even with improved and/or complete resolution of the saturate and naphthenic fractions, accurate quantitation of the saturate *character* in the asphalt may never be possible as a molecule containing a benzene ring with an aliphatic side chain with thirty carbon atoms will be grouped as a naphthene aromatic even though it probably exhibits entirely saturate-like behavior in the material.

It has been shown in this study that the refractive index response factors for saturates obtained from heavy petroleum products are similar to each other and to the response factor for petroleum jelly. Therefore, petroleum jelly, with a response factor of 1.05 V/g, may be an *adequate* saturate calibration standard for asphalt and asphalt related materials.

CHAPTER 6

THE KINETICS OF CARBONYL FORMATION IN ASPHALT

Asphalt is a major by-product of the refining industry. About 28 million tons per year are produced for use primarily in road construction and repair. An important factor in road life is the oxidation and subsequent hardening of the asphalt binder with age. Many accelerated aging tests have been devised in an attempt to rank asphalts according to their tendency to oxidize and harden. These are invariably run at elevated temperatures and sometimes at elevated pressures. A recent test developed by the Strategic Highway Research Program (SHRP) specifies the use of air at a pressure of 20 atm and at a temperature of 373 K.

Although many aging tests exist, there have been few studies of asphalt oxidation kinetics and almost none to determine if the activation energies or oxygen reaction orders are different for different asphalts. This is an important practical question, for if asphalts are to be compared in tests run at temperatures and pressures significantly different from road conditions, there is a tacit assumption that all asphalts exhibit the same activation energy and reaction order.

Several authors have demonstrated that the formation of carbonyl containing compounds in an asphalt as a result of oxidative aging changes the physical properties of the asphalt in a predictable way (Lee and Huang, 1973; Martin et al., 1990; Lau et al., 1992; Petersen et al., 1993). This relationship is different for different asphalts, but for each asphalt the change in carbonyl content, CA, is an excellent surrogate for the total oxidative changes and a predictor of the resulting changes in physical properties. This is partly explained by the fact that for each asphalt there is a linear relation between carbonyl growth and total oxygen increase as seen in Figure 6-1 for two of the test asphalts.

Lau et al. (1992) showed that at 20 atm oxygen pressure and at temperatures from 333 K to 366 K (140- 200°F) the carbonyl formation rate became constant after an initial more rapid rate region. These constant rates varied linearly with reciprocal absolute temperature in the usual

Arrhenius form

$$r_{CA} = A' \exp(-E/RT) \quad (6-1)$$

For the five asphalts studied, there appeared to be minor variations in the slopes of $\ln r_{CA}$ versus $1/T$. In the present work, carbonyl formation kinetics are determined for a range of temperatures and pressures for 14 asphalts to determine definitively the effect of these variables on carbonyl formation rates. All rates are expressed in arbitrary carbonyl units as CA/day. These rates could be converted into units of percent oxygen per day using data such as shown in Figure 6-1. The units are immaterial for the purposes of this study, and carbonyl is much easier to measure.

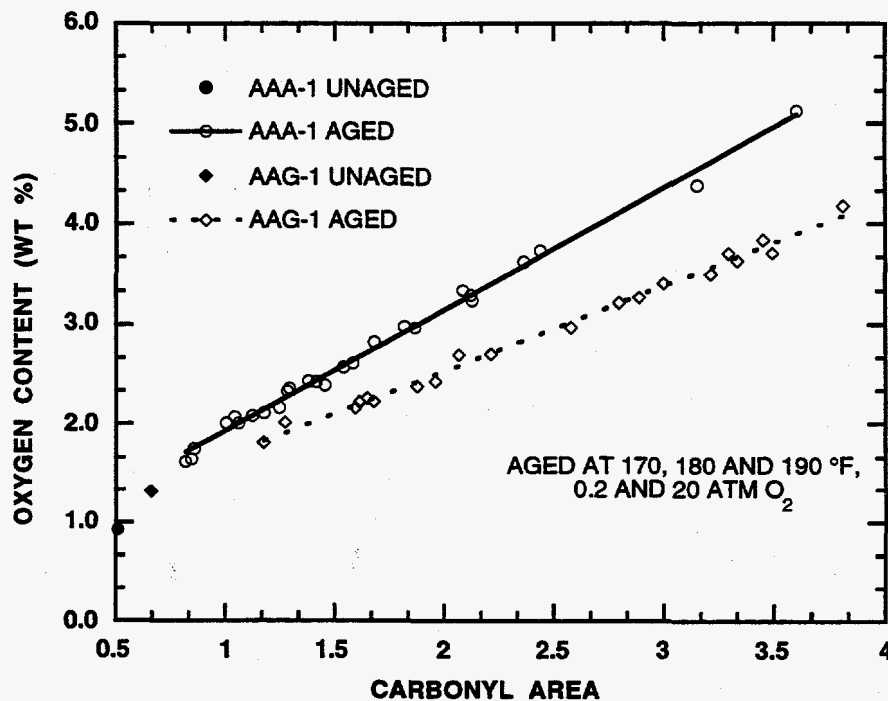


Figure 6-1. Oxygen Content Versus Carbonyl Content for AAA-1 and AAG-1

EXPERIMENTAL DESIGN

This research was conducted in two stages. In the first stage, the same asphalts studied by Lau et al. (1992) were oxidized at 0.2, 2 and 20 atm oxygen and at 333.3, 344.4 and 355.5 K (140, 160 and 180°F). The second-stage study involved ten asphalts with one, the Lau4, a repeat from the first stage. The rest of the stage-two material was comprised of two Texas asphalts (TX1 and TX2) and 7 asphalts from the SHRP project (AAA-1, AAD-1, AAF-1, AAG-1, AAM-1, AAB-1, AAS-1). The aging conditions used in this stage are listed in Table 6-1.

Table 6-1. Aging Conditions Applied in the Stage 2 Experiments

Condition	Temperature	Pressure
C1	170°F (349.8 K)	20 atm
C2	180°F (355.4 K)	20 atm
C3	180°F (355.4 K)	10 atm
C4	190°F (360.9 K)	20 atm
C5	190°F (360.9 K)	0.2 atm
C6	200°F (366.5 K)	0.2 atm
C7	210°F (372.0 K)	0.2 atm

In the SHRP aging procedure, asphalts are first aged in the Thin Film Oven Test (ASTM D-1754) to simulate hot mix aging. To see if this made any difference, many of the 2nd stage samples were run following the equivalent Rolling Thin Film Oven Test (ASTM D-2872). Many, but not all, were run in duplicate; i.e., both virgin asphalt and oven-aged asphalt were run at the same condition.

Asphalt samples weighing about 2 to 2.4 g were melted and placed in 4cm x 7cm aluminum trays. This gives a film thickness of 1 mm or less. Each POV holds 60-70 of these trays. For each asphalt a tray was removed every few days, depending on the temperature and pressure, with the maximum time ranging to 180 days at 333.3 K in the first stage. Oxygen

content (Figure 6-1) was obtained using a Fisons EA 1108 CHNS-O analyzer through direct oxygen measurement. Carbonyl content analysis was performed using FTIR, as described in Appendix A. Potential gas phase diffusion was eliminated by using pure oxygen. Diffusion in the asphalt was eliminated by placing the exposed surface directly on the prism. Since the reflected rays only penetrate about one micron, this is essentially a surface measurement. Some analyses were also made by mixing the film before placing on the prism. It was found that at 20 atm the results were indistinguishable from the surface measurements, and, since easier, the bulk measurements were used at this pressure.

RESULTS AND DISCUSSION

Stage 1

As determined by Lau et al. (1992), the rates of carbonyl formation became constant for all 5 asphalts after an initial higher rate period. This is seen in Figure 6-2, where results at all three pressures and at 355.5 K are shown for 1 asphalt, and in Figure 6-3 where results for all three temperatures are shown at 2 atm. The intercept of the constant rate portion regression line is defined as the initial jump CA_0 , while the slope of the line is the aging rate. From Figures 6-2 and 6-3, it is observed that 1) the initial jump is pressure dependent and not temperature dependent, 2) aging rate increases with pressure, and 3) aging rate increases with temperature. Rate data for all stage one conditions are shown in Table 6-2 and CA_0 - CA_{tank} in Table 6-3. Table 6-3 shows again that CA_0 is a function of pressure but, despite scatter, does not appear to be a function of temperature. Also, these conclusions are strongly supported by the stage 2 studies, which appear in the next section.

Figures 6-2 and 6-3 suggest that, as in classical kinetics, the aging rate can be expressed as

$$r_{CA} = A P^\alpha \exp(- E/RT) \quad (6-2)$$

where A is the frequency factor, α the reaction order with respect to oxygen pressure, and E the activation energy. For this expression to be valid, it is necessary to verify that α is temperature

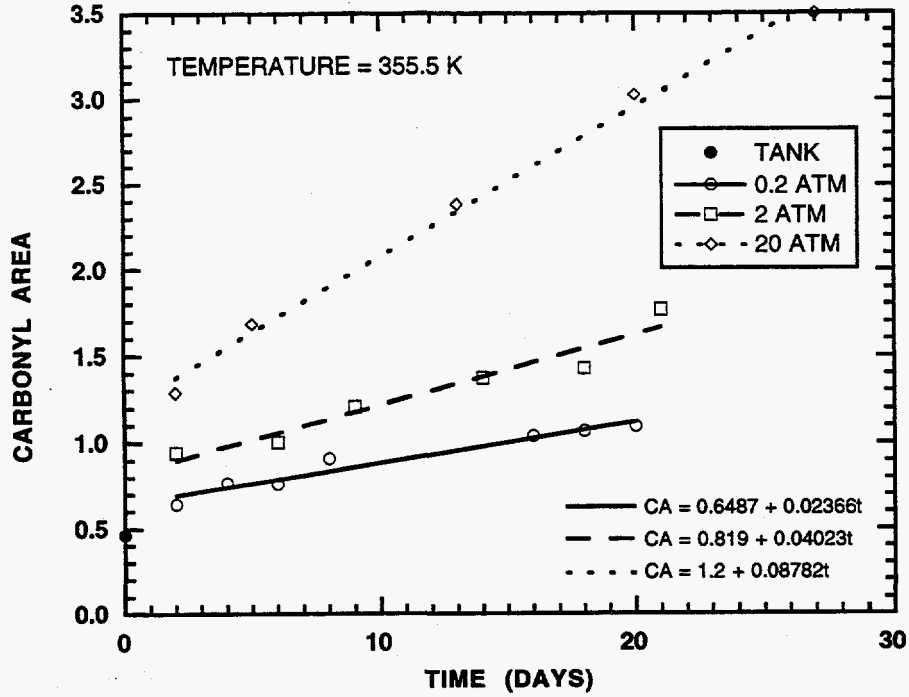


Figure 6-2. Pressure Dependence of Carbonyl Formation for Lau3 Asphalt

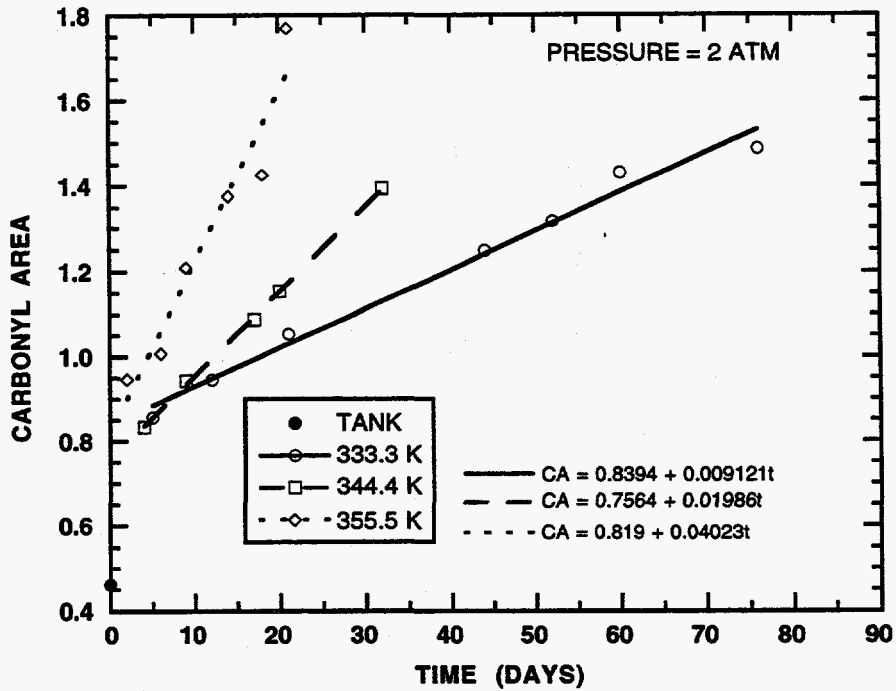


Figure 6-3. Temperature Dependence of Carbonyl Formation for Lau3 Asphalt

Table 6-2. CA Growth Rate for All Asphalts and POV Aging Conditions in the Stage 1 Experiments

Aging Condition		$r_{CA} \times 10^3$ (CA/ day)				
Pressure	Temperature	Lau1	Lau2	Lau3	Lau4	Lau5
0.2 atm	333.3 K	3.24	3.73	4.75	4.19	3.66
	344.4 K	6.85	8.91	11.41	7.87	7.78
	355.5 K	18.66	21.32	23.66	19.73	18.62
2 atm	333.3 K	6.79	6.36	9.12	8.10	6.04
	344.4 K	14.55	15.74	19.86	13.92	14.80
	355.5 K	34.50	37.92	40.23	32.47	28.63
20 atm	333.3 K	12.34	11.46	18.58	12.40	10.95
	344.4 K	25.55	31.19	32.88	29.43	26.96
	355.5 K	67.02	78.21	87.82	60.18	56.64

Table 6-3. $CA_0 - CA_{tank}$ for All Asphalts and POV Aging Conditions in the Stage 1 Experiments

Aging Condition		$CA_0 - CA_{tank}$ (CA)				
Pressure	Temperature	Lau1	Lau2	Lau3	Lau4	Lau5
0.2 atm	333.3 K	0.217	0.157	0.205	0.248	0.104
	344.4 K	0.202	0.180	0.176	0.271	0.142
	355.5 K	0.153	0.114	0.187	0.320	0.122
2 atm	333.3 K	0.278	0.334	0.377	0.413	0.248
	344.4 K	0.220	0.300	0.294	0.331	0.227
	355.5 K	0.295	0.276	0.357	0.352	0.290
20 atm	333.3 K	0.253	0.498	0.683	0.570	0.353
	344.4 K	0.438	0.548	0.920	0.616	0.376
	355.5 K	0.252	0.377	0.738	0.519	0.412

independent, and E is pressure independent.

Figure 6-4 is a plot of aging rates versus oxygen pressures for all 5 asphalts at 344.4 K. Values at all temperatures are listed in Table 6-4. The scatter in α appears random, and we conclude that α is independent of temperature. An Arrhenius plot for all 5 asphalts at 0.2 atm is shown in Figure 6-5. The activation energy, E, is calculated from the slope, and values at all pressures are given in Table 6-5. Again, the variation appears random and we conclude that E is independent of pressure. These results justify the use of Equation (6-2).

Equation (6-2) can be linearized by taking the natural logarithm of both sides

$$\ln r_{CA} = \ln A + \alpha \ln P - E/RT \quad (6-3)$$

This equation was used to perform a multi-variable regression of r_{CA} as a function of T and P. Table 6-6 shows the estimated parameters. For each of the parameters, statistical methods were employed to obtain 95% confidence limits and these are also shown in the table. The error of the estimated r_{CA} is also given. The percent errors are all under 10%.

The data in Table 6-6 show that a 95% confidence limit is roughly 15% of the value of the parameter. Unfortunately, the size of the confidence limit is such that it is difficult to conclude if the parameters are dependent on the asphalt source. Since the Arrhenius parameters describe the temperature dependence and this is the most significant factor affecting the determination of r_{CA} , it appears that the Arrhenius parameters are probably composition dependent.

Stage 2

The study was greatly expanded to determine definitively if there are significant compositional effects in asphalt kinetics. Ten asphalts were aged at the conditions listed in Table 6-1. Table 6-7 shows the rates and Table 6-8 shows the corresponding values of $CA_0 - CA_{\text{tank}}$ for all ten asphalts. Carbonyl growth with respect to aging time for three of the ten asphalts are shown in Figures 6-6 to 6-8. The data presented in Figure 6-6 are for one of the two asphalts that perhaps show some effect of oven aging on the subsequent POV aging, but only at 20 atm. We also see that the initial jump $CA_0 - CA_{\text{tank}}$ is extremely small. The data in Figure 6-7 show no

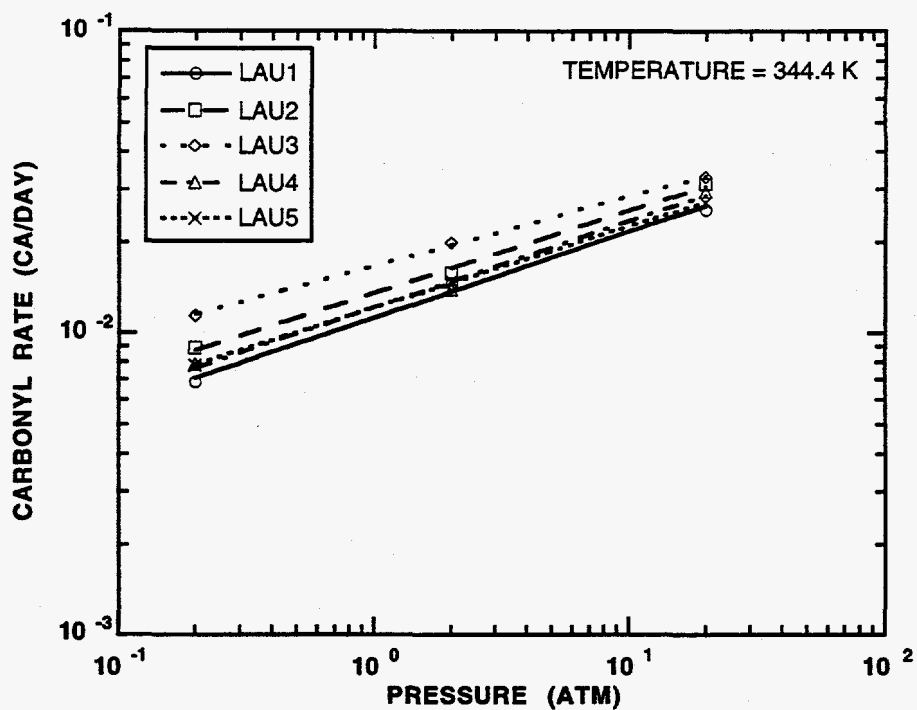


Figure 6-4. Pressure Dependence of Carbonyl Formation for All Stage 1 Asphalts

Table 6-4. α for All POV-Aged Asphalts at Different Temperatures in the Stage 1 Experiments^a

Temperature	α				
	Lau1	Lau2	Lau3	Lau4	Lau5
333.3 K	0.290	0.244	0.296	0.236	0.238
344.4 K	0.286	0.272	0.230	0.286	0.270
355.5 K	0.278	0.282	0.285	0.242	0.242
Average	0.285	0.266	0.270	0.255	0.250

^a Oxygen pressure from 0.2 to 20 atm.

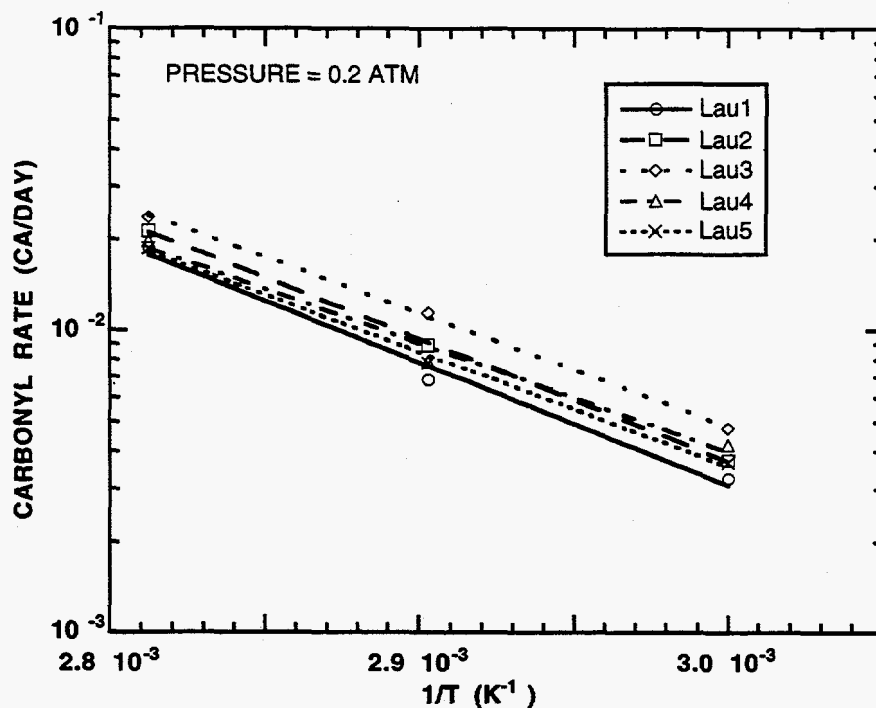


Figure 6-5. Temperature Dependence of Carbonyl Formation for All Stage 1 Asphalts

Table 6-5. E for All POV-Aged Asphalts at Different Pressures in the Stage 1 Experiments^a

Pressure	<i>E</i> (kJ/mole)				
	Lau1	Lau2	Lau3	Lau4	Lau5
0.2 atm	77.5	77.2	71.2	68.5	72.0
2 atm	72.0	79.1	65.8	61.4	68.3
20 atm	74.8	85.1	68.6	70.1	72.9
Average	74.8	80.5	68.5	66.7	71.1

^a Aging temperature from 333.3 K to 355.5 K.

Table 6-6. Kinetic Model Parameters for All POV-Aged Asphalts in the Stage 1 Experiments

Asphalt	ln(A) ln (CA / day atm ^a)	E kJ/mole	α	Average % Error ^a
Lau1	21.71±2.60	74.8±7.4	0.285±0.036	7
Lau2	23.83±1.55	80.5±4.4	0.266±0.022	4
Lau3	19.86±2.67	68.6±7.6	0.270±0.037	7
Lau4	19.86±2.89	66.7±8.3	0.255±0.040	8
Lau5	20.42±1.77	71.1±5.1	0.250±0.025	5

$$^a \% \text{Error} = 100 \sqrt{\sum \frac{1}{n} \left(\frac{\text{mea} - \text{cal}}{\text{mea}} \right)^2}$$

Table 6-7. CA Growth Rate for All POV-Aged Asphalts in the Stage 2 Experiments at All Conditions

Asphalt	$r_{\text{CA}} \times 10^3$ (CA/day)						
	C1	C2	C3	C4	C5	C6	C7
AAA-1	121.7	179.5		349.6	19.84	48.68	58.77
AAA-1 R ^a	114.5	181.9			16.29	49.12	54.90
AAD-1	133.3	223.5		403.9	22.53	43.69	60.01
AAD-1 R ^a	124.6	214.1			22.77	35.30	56.80
AAF-1	63.96	86.40		164.3	31.83	41.63	64.98
AAF-1 R ^a	65.84	88.55			32.83	37.75	61.61
AAG-1	74.66	102.0		163.3	41.41	60.17	87.57
AAG-1 R ^a	69.38	99.67			38.04	69.74	74.55
AAM-1	52.31	65.36		111.9	22.36	44.56	56.32
AAM-1 R ^a	50.66	62.15			28.30	45.26	59.33
AAB-1	68.77	132.3		222.2		58.19	80.39
AAB-1 R ^a	67.15	130.9	101.4	220.2		53.95	77.12
AAS-1	60.49			188.8			64.50
AAS-1 R ^a	58.19	105.1	86.59	197.8		46.17	64.72
TX1				229.4			85.39
TX1 R ^a	70.61	132.0	108.5	239.5		62.27	85.27
Lau4		108.0					
Lau4 R ^a	79.22	101.3	76.19	149.3		57.92	79.65
TX2		135.4					
TX2 R ^a	71.27	133.3	108.5	244.4		61.23	75.57

^a Asphalt pre-treated by Rolling Thin Film Oven Test before aging under the conditions.

Table 6-8. $CA_0 - CA_{\text{tank}}$ of All POV-Aged Asphalts in the Stage 2 Experiments at All Aging Conditions

Asphalt	$CA_0 - CA_{\text{tank}}$ (CA)						
	C1	C2	C3	C4	C5	C6	C7
AAA-1	0.103	0.068		0.024	0.250	0.109	0.082
AAA-1 R ^a	0.092	-0.037			0.320	0.119	0.129
AAD-1	0.225	0.071		0.047	0.271	0.134	0.082
AAD-1 R ^a	0.253	0.040			0.292	0.304	0.150
AAF-1	0.782	0.771		0.742	0.336	0.385	0.279
AAF-1 R ^a	0.755	0.734			0.309	0.415	0.313
AAG-1	1.771	1.686		1.713	0.572	0.473	0.415
AAG-1 R ^a	1.801	1.694			0.630	0.405	0.503
AAM-1	0.780	0.839		0.811	0.402	0.281	0.309
AAM-1 R ^a	0.782	0.829			0.297	0.284	0.273
AAB-1	0.508	0.393		0.395		0.210	0.198
AAB-1 R ^a	0.533	0.412	0.358	0.383		0.259	0.223
AAS-1	0.404			0.342			0.206
AAS-1 R ^a	0.404	0.350	0.291	0.325		0.225	0.202
TX1				0.415			0.176
TX1 R ^a	0.447	0.352	0.356	0.361		0.171	0.190
Lau4		0.593					
Lau4 R ^a	0.501	0.643	0.549	0.706		0.252	0.267
TX2		0.365					
TX2 R ^a	0.371	0.348	0.310	0.280		0.188	0.185

^a Asphalt pre-treated by Rolling Thin Film Oven Test before aging under the conditions.

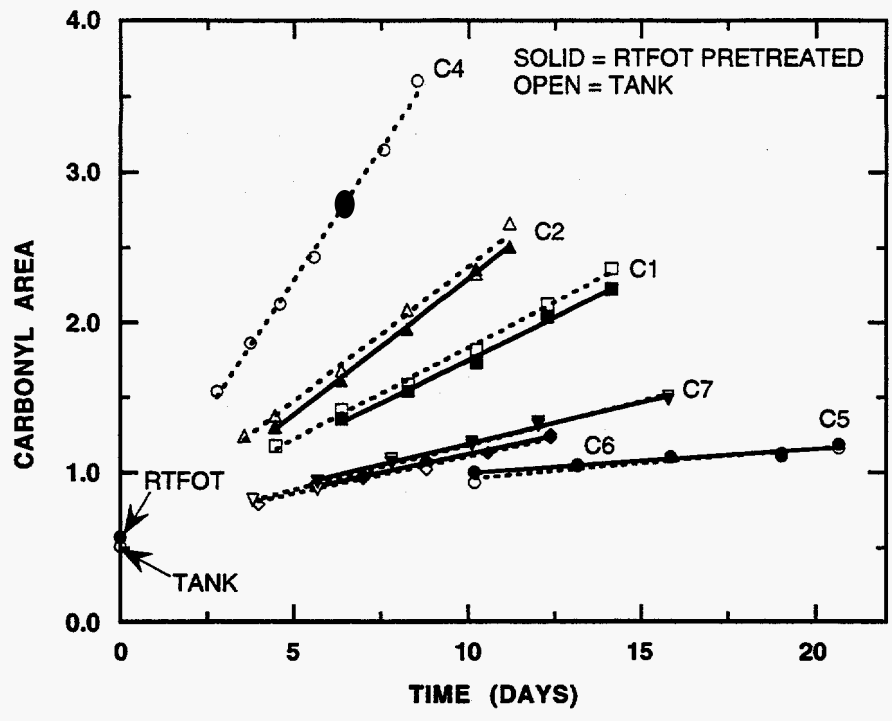


Figure 6-6. Carbonyl Formation for AAA-1 at All Stage 2 Conditions

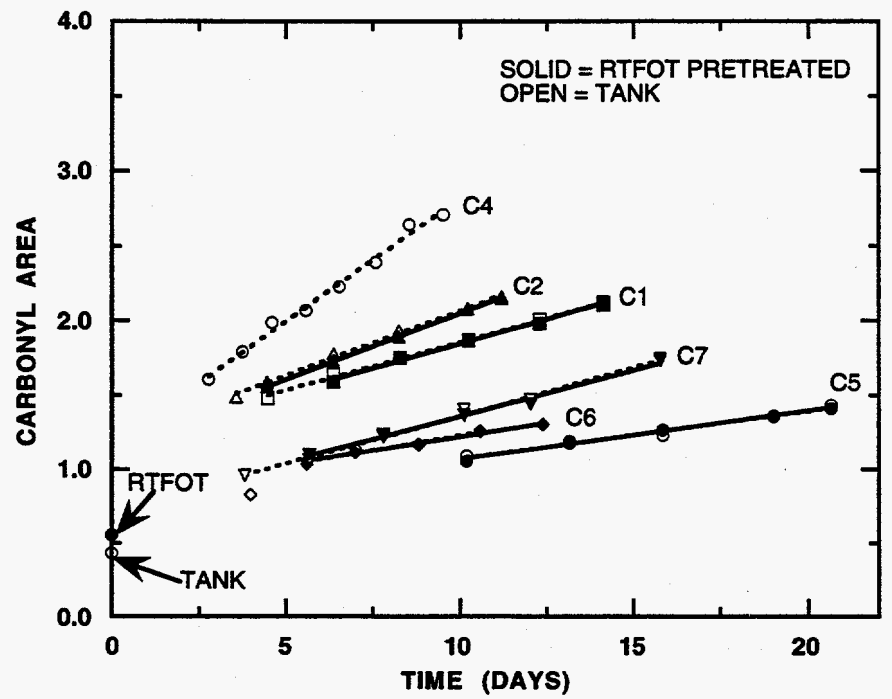


Figure 6-7. Carbonyl Formation for AAF-1 at All Stage 2 Conditions

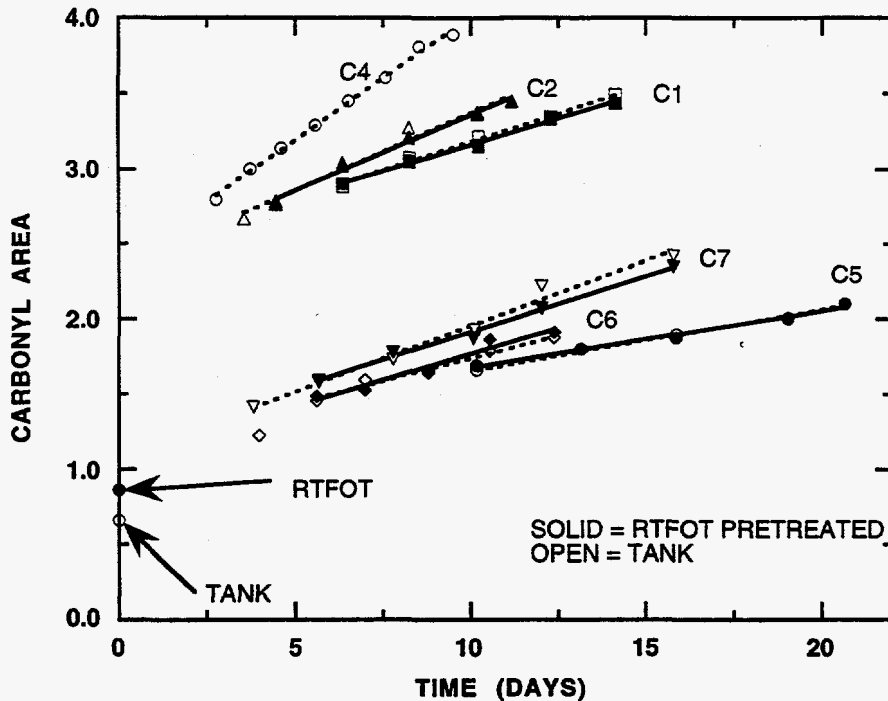


Figure 6-8. Carbonyl Formation for AAG-1 at All Stage 2 Conditions

evidence of an oven aging effect but a larger pressure effect on CA_0 is evident. Figure 6-8 also shows no oven test effect but does show a very large pressure dependent initial jump. In these runs, not all conditions were duplicated for both oven aged and virgin material. Within the scatter of the data in Table 6-8, CA_0 appears temperature independent, and all but AAA-1 and AAD-1 show a definite pressure effect. For these two $CA_0 - CA_{\text{tank}}$ is negligible.

The constants in Equation (3) determined by a multi-variable regression for the stage 2 asphalts are listed in Table 6-9. Unlike the stage 1 results, a much wider variation in reaction order, α , and activation energy, E , was obtained. The one duplicate asphalt, Lau4, yielded values very close to those previously obtained. We have in stage 1 a classic example of the statistical danger of small samples. Of the 14 asphalts tested in both phases, 7 have values of α between 0.25 and 0.29 with others ranging up to 0.61, yet all 5 of the asphalts tested by Lau and used in stage 1 lie in that narrow range. Similarly, the activation energies for the stage 1 asphalts ranged

Table 6-9. Kinetic Model Parameters of All POV-Aged Asphalts Studied in the Stage 2 Experiments

Asphalt	lnA ln (CA / day atm ^a)	E kJ/mole	α	Average % Error ^a
	33.28±10.86	AAA-1	0.604±0.099	16
	30.59±4.19	AAD-1	0.611±0.038	6
	22.06±5.92	AAF-1	0.340±0.054	9
	20.71±5.08	AAG-1	0.279±0.046	7
	19.43±4.67	AAM-1	0.260±0.042	7
	31.60±4.93	AAB-1	0.426±0.047	7
	31.98±5.58	AAS-1	0.445±0.052	6
	31.29±6.82	TX1	0.421±0.064	7
	18.64±8.51	Lau4	0.272±0.076	6
TX2	31.06±13.06	101.5±41.1	0.429±0.122	9

^a As defined in Table 6.

from about 67 to 81 kJ/mole while the range of all 14 was 64 to 109. It is interesting that there seems to be distinct groupings of low α , low E asphalts and high α , high E asphalts with no values of E between 81 and 100 and only one α between 0.29 and 0.42. The same kind of variation is seen in ln A.

In Figure 6-9, ln A + α ln 0.2 (the value of E/RT where ln r_{CA} = 0 for oxidation pressure of 0.2 atm) is plotted versus E with remarkable linearity. This indicates that at 0.2 atm oxygen pressure there exists an isokinetic temperature (Boudart, 1991) where all 14 asphalts will exhibit nearly the same rate. From the fit in Figure 6-9, this temperature is calculated to be 370.8 K. In Figures 6-10 and 6-11, Arrhenius plots for the 10 stage 2 asphalts are shown corrected to 0.2 atm and the rates do tend to converge in that region.

In Figure 6-12, we see the strong relation between E and α with only AAA-1 and AAD-1 appearing anomalous, but these 2 asphalts are alike in other respects. The confidence limits are

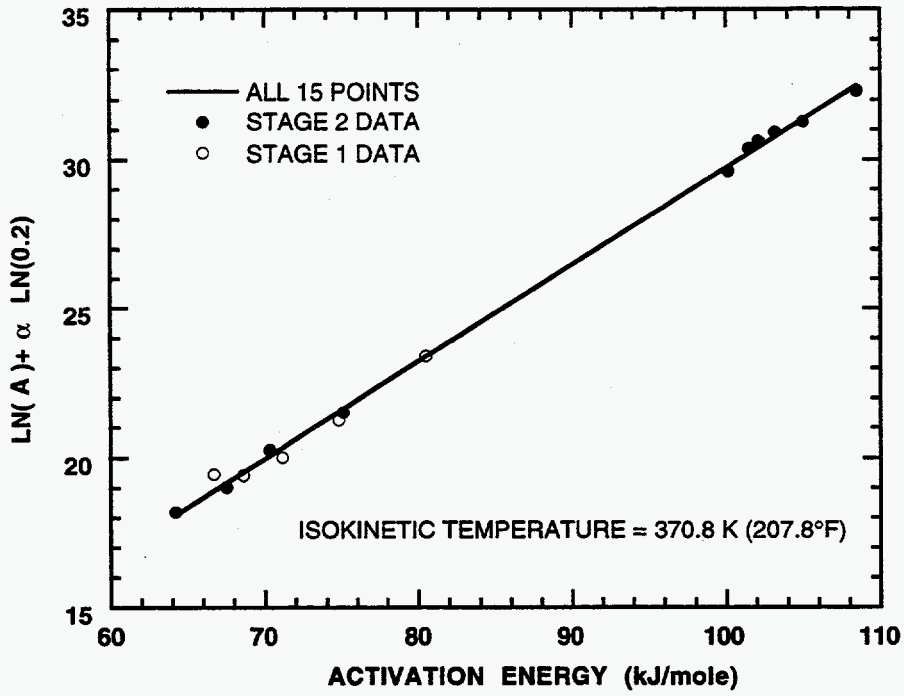


Figure 6-9. Isokinetic Diagram for All 15 Asphalts

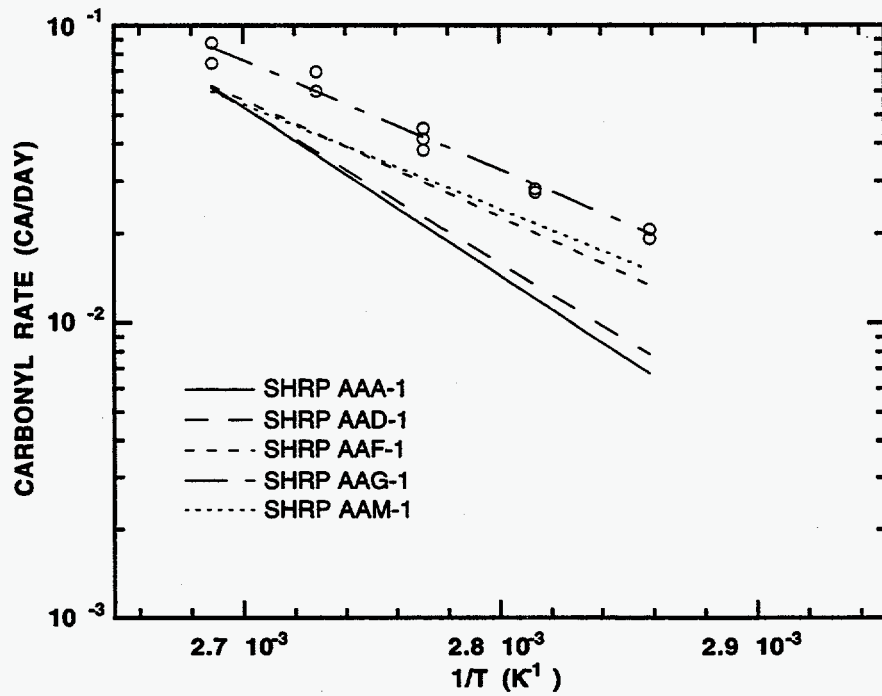


Figure 6-10. Arrhenius Plot for the First 5 Stage 2 Asphalts

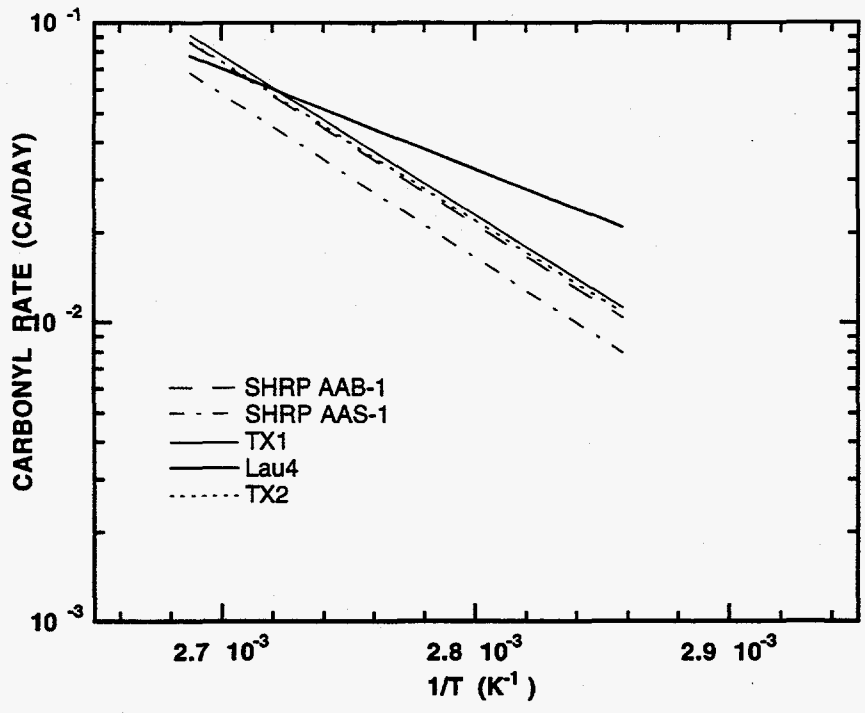


Figure 6-11. Arrhenius Plot for the Second 5 Stage 2 Asphalts

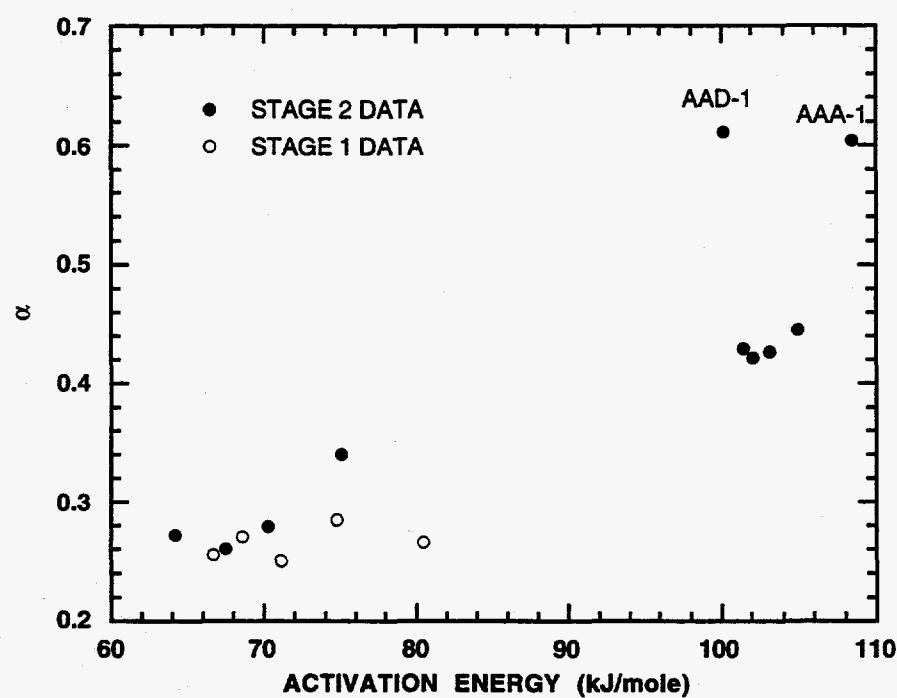


Figure 6-12. Reaction Order Versus Activation Energy for All 15 Asphalts

higher for the 2nd stage runs because of fewer experimental conditions and differences in experimental design. However, the average errors are not much greater and the good correlations in Figures 6-9 and 6-12, as well as the close agreement between the Lau4 results from each stage, give confidence in the results.

In Figures 6-9 and 6-12, we have distinguished between stage 1 and stage 2 which were run a year apart by different researchers. Both the narrow range of the stage 1 data as well as the general agreement with stage 2 results are evident.

Activation Energies and Reaction Orders

There are a few activation energies published in the literature for asphalt oxidation. Whether these activation energies were measured for oxygen consumption or carbonyl formation is immaterial, because the linear relation between the two (see Figure 6-1) results in no effect on either E or α and only on $\ln A$. Most of the published activation energies were obtained by measuring the rate of oxygen consumption at only two or three temperatures. Van Oort et al. (1956) measured oxygen uptake at about one atm at 25, 50 and 75°C. Correcting for diffusion and assuming the reaction to be first order relative to oxygen pressure they obtained a value of E of 100 kJ/mole. Blokker and Van Hoorn (1959) gave the times required for 1 cm³ of oxygen to absorb into a 200 micron film at 30 and 50°C. For the four asphalts they studied, the data yielded values of E from 55 to 79 kJ/mole. These authors also reported a value for α of 0.6 but gave no data. Dickinson and Nicholas (1949) and Dickinson et al. (1958) obtained values of E of 29 and 43 kJ/mole but concluded these values contained diffusion effects. Verhasselt and Choquet (1991) reported a value of E for one asphalt of 87 kJ/mole measured between 343 and 373 K using carbonyl growth as the measurement.

All of these values except for those recognized as being affected by diffusion fall in the range of the present study. It should be pointed out, however, that several and perhaps all of them are based on rates measured totally or in part in the initial rapid rate region and may well be different from values calculated in the constant rate region. The single value given for the reaction order of 0.6 is at the upper limit of values obtained in this work. Again, it is quite possible that it was measured in the initial rate region in which the pressure effect is quite different.

The Initial Rapid Rate Region

As shown above, the initial jump of the rapid rate region, $CA_0 - CA_{\text{tank}}$, is not a function of reaction temperature but generally increases with reaction pressure. Also, Table 6-8 and Table 6-3 show that asphalts with larger reaction orders α (e.g., AAA-1 and AAD-1) have smaller initial jumps, compared to those with lower α (e.g., AAF-1, AAG-1, AAM-1 and Lau4). This is particularly clear for the 20 atm data.

To evaluate the initial rapid rate region, it was assumed that the pressure effect could be represented by

$$CA_0 - CA_{\text{tank}} = \beta P^\gamma \quad (6-4)$$

All values of $CA_0 - CA_{\text{tank}}$ were used to fit β and γ and the results are given in Table 6-10. For asphalts AAA-1 and AAD-1 the pressure effects are negligible and were calculated to be negative, but this is probably error. Some of these values are calculated from only two data points. The constant β doesn't vary much, but γ is plotted versus α in Figure 6-13 and surprisingly the pressure effect on CA_0 varies inversely with α , the reaction order with respect to oxygen pressure in the constant rate region.

IMPLICATIONS OF THE RESULTS

The results of this work have profound significance in the development of a reliable aging test, as well as in the evaluation of asphalt binder quality.

The fact that each asphalt has a specific set of kinetic parameters gives guidance in developing a reliable aging test. Data in Table 6-9 show that asphalts from different sources may exhibit far different reaction orders and activation energies. Therefore, the relative aging rates which exist at one temperature and pressure may be reversed at another temperature and/or pressure. Any test using the information of only one aging experiment performed at a single elevated temperature and/or elevated pressure may be unreliable. Furthermore, if the aging experiment is conducted within the initial rapid rate region, the resulting relative rates also may

Table 6-10. β and γ Values of All Asphalts in the Stage 1 and Stage 2 Experiments^a

	AAA-1	AAD-1	AAF-1	AAG-1	AAM-1
β	0.1102	0.1738	0.4492	0.7717	0.4312
γ	-0.2631	-0.1047	0.1741	0.2700	0.2097
	AAB-1	AAS-1	TX1	Lau4 ^b	TX2
β	0.2755	0.2473	0.2361	0.3514	0.2300
γ	0.1383	0.1065	0.1699	0.1881	0.1305
	Lau1	Lau2	Lau3	Lau4 ^c	Lau5
β	0.2330	0.2340	0.2987	0.3481	0.1938
γ	0.1079	0.2498	0.3078	0.1536	0.2449

^a $CA_0 - CA_{\text{tank}} = \beta P^\gamma$.

^b By data of the stage 2 experiments.

^c By data of the stage 1 experiments.

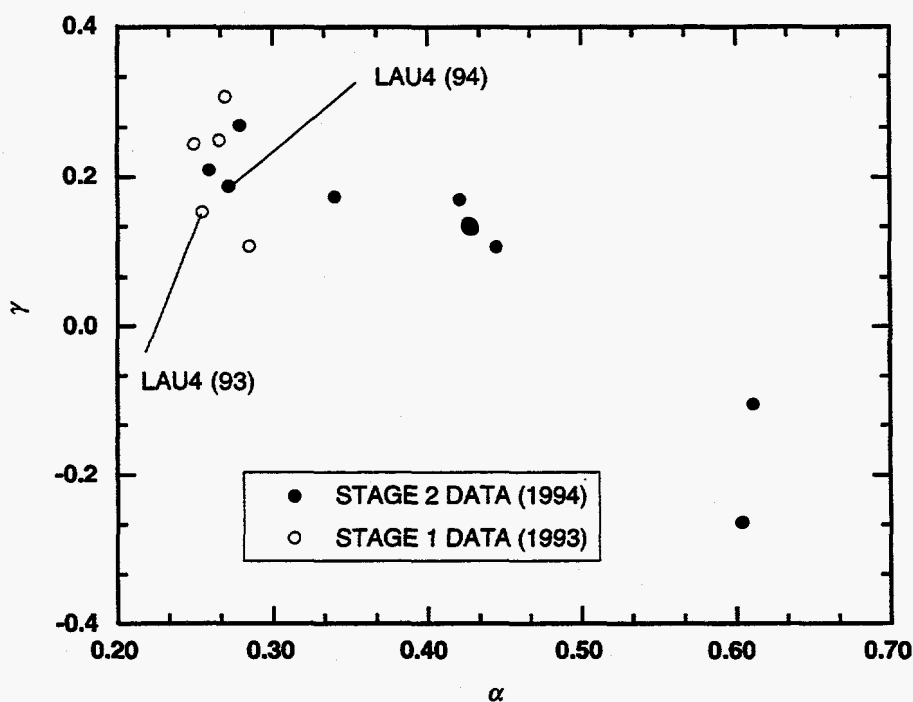


Figure 6-13. Initial Jump Pressure Dependence Versus Constant Rate Reaction Order

not represent the constant-rate-period relative rates which are relevant in the pavement. Based on this work, we conclude that a reliable aging test should be conducted by running aging experiments at multiple temperatures and/or pressures to measure the kinetic parameters. The kinetic parameters can then be used to determine the aging rates at road conditions. The optimum protocol for such a testing procedure is yet to be established.

The differences between the kinetic parameters also indicate that aging characteristics are an important part of asphalt binder quality. Since the asphalts have an isokinetic temperature near 100°C, those with higher activation energies will have a lower oxidation rate at road conditions. Also, a small initial jump is desirable. On the other hand, as shown in Figures 6-12 and 6-13, the reaction order α , the activation energy E , and the initial jump pressure dependence factor γ are closely correlated. Since the kinetic parameters should be a manifestation of the chemical compositions of the asphalts, improvements in aging quality can be realized through compositional manipulations. The compositional dependence of the activation energy, reaction order and initial jump is currently under investigation. Future results may yield techniques to manufacture asphalts with superior aging characteristics.

Finally, the isokinetic phenomenon as shown in Figure 6-9 is remarkable, and of fundamental significance. Boudart (1991) reported an isokinetic diagram for hydrocarbon cracking (C_3 - C_6). By contrast, asphalt is a very complex petroleum residue consisting of thousands of compounds of much higher carbon number and widely-varying functionalities. The existence of the isokinetic phenomenon in such a material is likely to be a valuable observation for understanding and describing the aging mechanism.

CONCLUSIONS

When asphalts are oxidized at constant oxygen pressure and constant temperature in the absence of diffusion, the carbonyl growth undergoes a period of rapid growth and then a lengthy period of constant rate. The kinetics of the constant rate region are represented by Equation (6-2) with both E and α being asphalt dependent and strongly cross correlated in that generally high values of E accompany high values of α .

The initial jump, CA_0 , is also highly asphalt dependent and is pressure dependent according to Equation (6-4), but correlates inversely with the constant rate reaction order. From these results it is apparent that an attempt to use relative asphalt aging rates at elevated temperatures and pressures and to assume they represent relative rates at road conditions could be highly misleading.

CHAPTER 7

PRELIMINARY EXPERIMENTS USING SUPERCRITICAL FRACTIONS AS ASPHALT RECYCLING AGENTS

There are currently several methods for processing the heaviest compounds in crude oil. These include visbreaking, coking, and supercritical fractionation. The supercritical fractionation processes, licensed by UOP (DeMex) and Kerr McGee (ROSE), are capable of producing an asphaltene-rich fraction or asphaltenes and a saturate-rich fraction known as deasphalted oil or DAO. Some of the commercial units are also set up to produce a third, intermediate fraction known as resins.

In previous works (Stegeman et al., 1992; Jemison et al., 1995), several asphalts and reduced crudes were fractionated in the laboratory using a combination of supercritical and room temperature separations as well as using a combination of supercritical solvents. These papers primarily focused on the analyses and the chemistry of these fractions. This chapter focuses on a preliminary experiment to investigate the potential use of supercritical fractions as recycling agents for aged asphalts.

MATERIALS

Asphalts for Supercritical Fractionation

Four asphalts were fractionated in the supercritical pilot plant at Texas A&M University (TAMU) during the first year of this project. One asphalt, an AC-20, was obtained from a local paving contractor and is given the designation YBF. Three asphalts: AAA-1, AAF-1, and ABM-1, were obtained from the Strategic Highway Research Program's (SHRP) Materials Reference Library (MRL). Three supercritical fractions (SCFs) produced at TAMU were investigated as potential recycling agents. The three TAMU SCFs are YBF F3, AAF F3, and ABM F3. SHRP AAF-1 was also aged in the air bubbling apparatus described in Chapter 2 to produce aged asphalt for the comparison of rejuvenating agents.

Industrial Supercritical Fractions

Several refiners currently utilize supercritical operations to process various heavy end feedstocks. Supercritical fractions were obtained from a few of these companies. These industrial SCFs (ISCFs) were analyzed and three were chosen for a preliminary study to determine if ISCFs are suitable as recycling agents for aged asphalt binders. The three ISCFs investigated in detail have been given the arbitrary designations ISCF A, B, and C to protect the identities of the companies supplying material. The properties of these fractions are listed in Table 7-1.

Table 7-1. Industrial Supercritical Fraction and Commercial Rejuvenating Agent Properties

Sample	Viscosity (dPa·s) ¹	Saturates (wt%)	Asphaltenes (wt%)	Aromatics (wt%) ²
ISCF A	17.6	20.4	0.3	79.3
ISCF B	58.0	30.8	0.7	68.5
ISCF C	434.0	11.4	3.4	85.2
CRA A	2.4	8.7	0.7	90.6
CRA B	1.2	12.4	0.9	86.7
CRA C	1.0	28.0	0.5	71.5

¹ 1 dPa·s = 1 poise

² determined by difference

Commercial Recycling Agents

Many commercial rejuvenating agents (CRAs) are currently available. Most of these CRAs were not developed specifically for asphalt recycling but are actually aromatic extract by-products of lube oil manufacture, and thus, are high in saturate content. Several of these commercial recycling agents were obtained and analyzed. Three were chosen for comparison in this study. These three were obtained from different companies and have been given arbitrary designations to protect the identities of the manufacturers. The properties of CRA A, B, and C are listed in Table 7-1.

EXPERIMENTAL METHODS

Supercritical Fractionation

The supercritical fractionation experiments were performed during the first year of this DOE effort. The details of these experiments are included in this chapter and in Appendix A of this second-year technical progress report only as background information. A brief description of the fractionation experiments follows.

Supercritical fractionation was performed using the four stage pilot plant scale unit at Texas A&M University. This unit is primarily a semi-batch process, with the solvent being continuously recycled and the feed introduced in batches. Detailed operation of the unit has been described previously (Stegeman et al., 1992) as have previous fractionation experiments (Stegeman et al., 1992; Jemison et al., 1995). The fractionation conducted in this study differs from the previous experiments in that all of the fractionation was performed in the supercritical extraction unit using only n-pentane as the solvent.

The four asphalts fractionated in this work were fractionated in two passes through the unit. The lightest fraction from the first pass was fed through the unit a second time yielding eight fractions that may be analyzed. The lightest fraction from the second pass is designated as fraction F1 and the heaviest fraction from the first pass is designated as fraction F8 (fraction F5 is the feed material for the second pass through the unit). The properties of the fractions produced in the supercritical unit at TAMU are listed in Table 7-2. The fractions chosen for investigation in this limited study were YBF F3, ABM F3, and AAF F3.

Aged Asphalt Production

To investigate the feasibility of using supercritical fractions as recycling agents, it was necessary to obtain an aged asphalt. SHRP AAF-1 was aged in an air bubbling apparatus as described in Chapter 2. The aged asphalt used in this study is SHRP AAF-1 aged to a final viscosity of 55,000 dPa·s (poise). This sample is referred to as AAF-AB1.

Table 7-2. Representative Texas A&M Supercritical Fraction Properties

Fraction	Viscosity (poise)	M _w	Saturates (wt %)	Asphaltenes (wt %)	Aromatics (wt %)
YBF F1	6	649	33.1	1.5	65.4
YBF F2	29.2 ± 7.3	895	22.7 ± 0.9	2.6 ± 0.4	74.8 ± 0.6
YBF F3	137.4 ± 9.0	1152	11.0	0.1	84.1 ± 0.8
YBF F4	1040	1388	7.6	2.4	90
YBF F5	43.2 ± 5.2	986 ± 19	16.2 ± 3.0	2.4 ± 0.5	81.4 ± 3.2
YBF F6	1813 ± 835	1460 ± 51	6.2 ± 1.3	2.5 ± 1.1	91.3 ± 1.5
YBF F7	5.95 × 10 ⁵ ± 3.91 × 10 ⁵	1912 ± 182	1.3 ± 0.8	7.5 ± 1.8	91.2 ± 1.8
YBF F8	--	2668 ± 96	0.3 ± 0.3	63.4 ± 5.1	36.3 ± 5.2
ABM F1	11.1 ± 1.5	495 ± 9	17.5 ± 0.6	0.0 ± 0.0	82.6 ± 0.6
ABM F2	91.1 ± 8.0	748 ± 28	12.9 ± 0.6	0.0 ± 0.0	87.1 ± 0.6
ABM F3	627.3 ± 18.7	918	7.7 ± 0.7	0.0 ± 0.1	92.3 ± 0.7
ABM F4	1610	1085	9.5 ± 2.2	0.0 ± 0.0	90.6 ± 2.2
ABM F5	115.8 ± 17.1	758 ± 4	11.5 ± 0.5	0.0 ± 0.0	88.5 ± 0.7
ABM F6	8.21 × 10 ⁴ ± 1.32 × 10 ⁴	1266 ± 36	3.4 ± 0.2	0.3 ± 0.5	96.4 ± 0.5
ABM F7	1.44 × 10 ⁷ ± 1.10 × 10 ⁷	1531 ± 44	1.7 ± 0.1	6.7 ± 2.0	91.6 ± 2.0
ABM F8	--	2232 ± 63	1.0 ± 0.4	47.7 ± 1.7	51.4 ± 1.9
AAA F1	2.0 ± 0.1	572 ± 27	31.3 ± 3.4	0.5 ± 0.6	68.3 ± 2.8
AAA F2	14.5 ± 3.2	875 ± 6	20.0 ± 1.5	0.2 ± 0.3	79.8 ± 1.4
AAA F3	99.2 ± 28.5	1237 ± 5	11.0 ± 1.3	0.4 ± 0.5	88.6 ± 0.8
AAA F4	76.1 ± 81.8	1178 ± 285	16.2 ± 6.5	0.6 ± 0.6	83.2 ± 5.9
AAA F5	10.7 ± 0.5	902 ± 5	22.7 ± 0.3	0.2 ± 0.0	77.2 ± 0.2
AAA F6	250	1701 ± 304	7.6 ± 4.6	0.6 ± 0.2	92.0 ± 4.3
AAA F7	30,000	2257 ± 233	6.2 ± 0.6	6.5 ± 1.6	87.4 ± 1.0
AAA F8	--	4867 ± 83	1.8 ± 0.8	62.0	36.8
AAF F1	2.1	661	32.6	0.8	66.6
AAF F2	11.7 ± 1.6	928	23.5 ± 0.4	0.4 ± 0.1	76.2 ± 0.4
AAF F3	67.1 ± 8.0	1111	14.3 ± 0.1	0.4 ± 0.3	85.4 ± 0.4
AAF F4	315.6	1334	10.0	1.0	89.0
AAF F5	15.9 ± 0.2	966 ± 15	24.6 ± 0.4	0.1 ± 0.1	75.4 ± 0.4
AAF F6	3,000	1417 ± 27	8.1 ± 0.1	1.1 ± 0.1	90.9 ± 0.1
AAF F7	50,000	1696 ± 17	6.2 ± 1.7	7.4 ± 0.4	86.5 ± 1.3
AAF F8	--	2495 ± 1	1.2 ± 0.6	51.5 ± 2.1	47.3 ± 2.7

Recycled Blend Comparison

Nine recycled blends were produced using AAF-AB1 as the aged asphalt. Three different CRAs, three ISCFs, and three TAMU SCFs were utilized as the rejuvenating agents. The target viscosity for the recycled blends was chosen as $\pm 20\%$ of the viscosity of unaged SHRP AAF-1 so that the recycled blends could be compared not only against each other, but also against the original parent asphalt. The initial amount of softening agent required for blending to achieve the target viscosity was determined using the dimensionless log viscosity (DLV) mixing rule developed during the first year of this DOE effort (Chaffin et al., 1995). The DLV is given by Equation (7-1).

$$DLV = \frac{\ln(\eta_m/\eta_1)}{\ln(\eta_2/\eta_1)} \quad (7-1)$$

In Equation (7-1), η_m is the blend viscosity, η_1 is the viscosity of the recycling agent and η_2 is the viscosity of the aged asphalt. Blending was performed in a manner similar to that suggested in specification ASTM D4887.

The recycled blends and the unaged SHRP AAF-1 were subjected to a slightly modified pressure aging vessel (PAV) accelerated aging test. The standard PAV test, developed under the auspices of the SHRP program, consists of pretreating the asphalt using the thin film oven test, or TFOT (ASTM D1754), and placing the pretreated asphalt directly in the PAV vessel. The test was modified for this study in that the TFOT pretreated material was stirred and a sample was taken to measure the viscosity after the TFOT pretreatment. This may significantly alter the absolute value of the data obtained after the complete PAV test but should not inhibit comparison of the samples investigated in this study. Caution is advised when dealing with the PAV test because the PAV aging test consisting of a single condition of both elevated temperature and elevated pressure. The studies described in Chapter 6 in addition to other studies (Lau et al., 1992; Davison et al., 1994; Liu et al., in press) have shown that the kinetics of aging are both temperature and pressure dependent and that the relative ranking of various asphalts may

be much different at road conditions than the rankings at the PAV conditions. This weakness of the PAV aging test has never been fully addressed in the SHRP specifications.

To investigate the effects that aging temperature and pressure may have on the ranking of the asphalts, the residues from the PAV test were then further aged in the POV using atmospheric air at temperatures of 80, 90, and 100°C.

Properties Testing

Low frequency limiting dynamic viscosities were measured at 60°C, as described in Appendix A. To obtain the viscosity for some materials it was necessary to conduct measurements at additional temperatures and use the time temperature superposition principle to obtain the 60°C low frequency limiting dynamic viscosity (Ferry, 1985).

Compositional analyses of the softening agents were performed utilizing HPLC methods, as described in Chapter 5 and Appendix A. Molecular weight distributions were measured using GPC and carbonyl measurements were performed using FTIR, as described in Appendix A.

RESULTS AND DISCUSSIONS

RTFO and PAV Test Comparison

Figure 7-1 shows the location of blend DLV data points in relation to the data points collected in the previous mixing rules study conducted by Chaffin et al. (in press) which was reported in the technical progress report for the first year of this DOE effort. The diagonal line represents the mixing rule suggested in ASTM D4887 for recycled blends. Previously, it was shown that the ASTM mixing rule is adequate for blends using low viscosity asphalts as the softening agent, but is completely unsuitable for blends using commercial recycling agents or supercritical fractions produced in the laboratory. The data presented in Figure 7-1 clearly show that the industrial supercritical fractions (ISCFs) behave like commercial recycling agents (CRAs) and supercritical fractions produced at TAMU in terms of viscosity reduction. The target viscosity was obtained for four of the

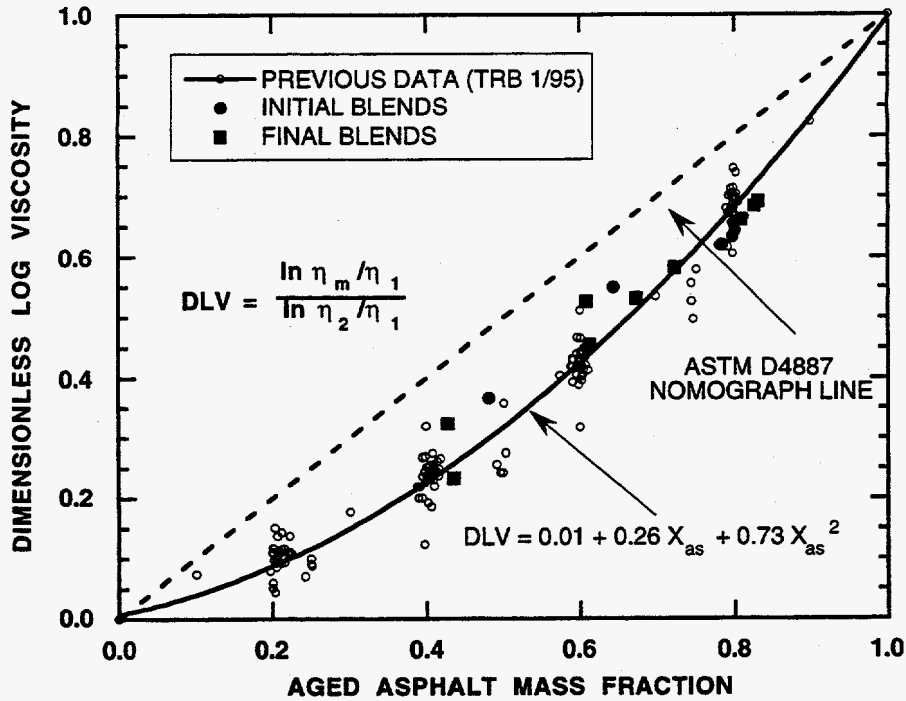


Figure 7-1. Dimensionless Log Viscosity for Blends Studied

nine recycled blends on the first blending attempt as is indicated by the * in Table 7-3. The target viscosity was obtained after the second blending attempt for four of the remaining five recycled blends. This is a marked improvement over the results that would have been obtained using the mixing rule suggested in ASTM D4887.

The aging indexes (AIs), which are calculated as the viscosity after aging divided by the unaged viscosity, for all materials after TFOT pretreatment and after the PAV aging test are also shown in Table 7-3. The recycled blend using ISCF B was very problematic from the initial blending through the end of the PAV test. In fact, blending with this agent required multiple tries to obtain the correct viscosity and a low frequency limiting dynamic viscosity could not be obtained for the TFOT treated and PAV aged materials. This is likely the result of the extremely high saturate content of ISCF B. Thus, the AIs could not be determined for this recycled blend.

Table 7-3. Composition and Viscosity Data for Asphalts Subjected to PAV Test

Sample	Composition (Asphalt/Agent) ¹	Viscosity (dPa·s) ²	TFOT AI ³	PAV AI ³
SHRP AAF-1	N/A	1890	2.80	12.42
AAF-AB1/ISCF A	72/28 *	1900	1.68	4.21
AAF-AB1/ISCF B	61/39	2140	N/A	N/A
AAF-AB1/ISCF C	43/57	2080	1.67	3.89
AAF-AB1/CRA A	81/19	1840	1.85	4.30
AAF-AB1/CRA B	83/17	1850	1.70	4.46
AAF-AB1/CRA C	83/17	1900	1.96	5.53
AAF-AB1/YBF F3	61/39 *	2000	1.50	3.00
AAF-AB1/AAF F3	67/33 *	2090	1.67	3.85
AAF-AB1/ABM F3	44/56 *	1670	1.59	2.93

¹ Approximate composition (unless denoted by *)

² 1 dPa·s = 1 poise

³ AI = viscosity after aging/unaged viscosity

* Target viscosity achieved first attempt

The remaining data shown in Table 7-3 show that all of the recycled blends have lower AIs than the parent asphalt SHRP AAF-1. Furthermore, the data show that the AIs of the recycled blends using CRAs are higher than the AIs of the blends which used supercritical fraction rejuvenating agents, either those obtained from industrial sources or those produced in the laboratory at Texas A&M. In addition, the AIs for the blends using the laboratory SCFs are the lowest of all the AIs. This is undoubtedly due to the narrower cuts that are obtained by fractionating into seven fractions rather than the two or three cuts that are produced industrially.

POV Test Comparison

The residues from the PAV aging test were then distributed into POV trays and subsequently aged at 80, 90, and 100°C using atmospheric air to determine aging kinetics. Approximate values for the carbonyl rates, activation energies, and hardening

susceptibilities (HS) were obtained. However, because the samples had been previously aged in the PAV, there was no way to determine the initial jump, CA_0 . In other words, there is no way to determine the POV time period which is equivalent to the PAV aging conditions.

The samples were aged and analyzed in much the same manner as that described in Chapter 6. After aging, carbonyl area measurements were performed on all of the samples and viscosity measurements were performed on enough samples (at least one-half of the samples) to determine HS values for each mixture. The one exception to this was the rejuvenated blend using ISCF B as the softening agent. Viscosity measurements did not yield low frequency limiting values, so the HS could not be determined. Once again, the inability to obtain limiting viscosities for the blends using ISCF B is likely due to the extremely high saturate content of ISCF B.

Figure 7-2 shows a plot of CA versus time (time = 0 arbitrarily set to be when the POV aging started) for the original asphalt AAF-1. The slopes of each of the three lines are equal to the oxidation rate (as measured by CA) at the various temperatures. Figure 7-3 shows a logarithmic plot of CA rate versus the reciprocal of the absolute temperature ($1/T$). This plot should be linear as suggested by Equation (6-3) with a slope proportional to the activation energy. Clearly, the data presented in Figure 7-3 are linear. The calculated value of the activation energy is reported in Table 7-4. Figure 7-4 is a logarithmic plot of viscosity versus carbonyl area for the PAV pre-aged AAF-1. The slope of the line produced from these data is the HS. The numerical value for the HS of the PAV pre-aged AAF-1 is reported in Table 7-4. Plots similar to those shown in Figures 7-2 and 7-3 were produced for all ten materials examined in this experiment. Plots similar to Figure 7-4 were produced for all of the materials except the blend using ISCF B as the softening agent. The activation energies and HS values for these samples are reported in Table 7-4, as are extrapolated values of the CA rate and $\ln \eta$ rate at 50°C (a reasonable value for road temperature).

The data in Table 7-4 show that the activation energies vary widely for the materials investigated in this study. Of particular importance is the fact that the activation

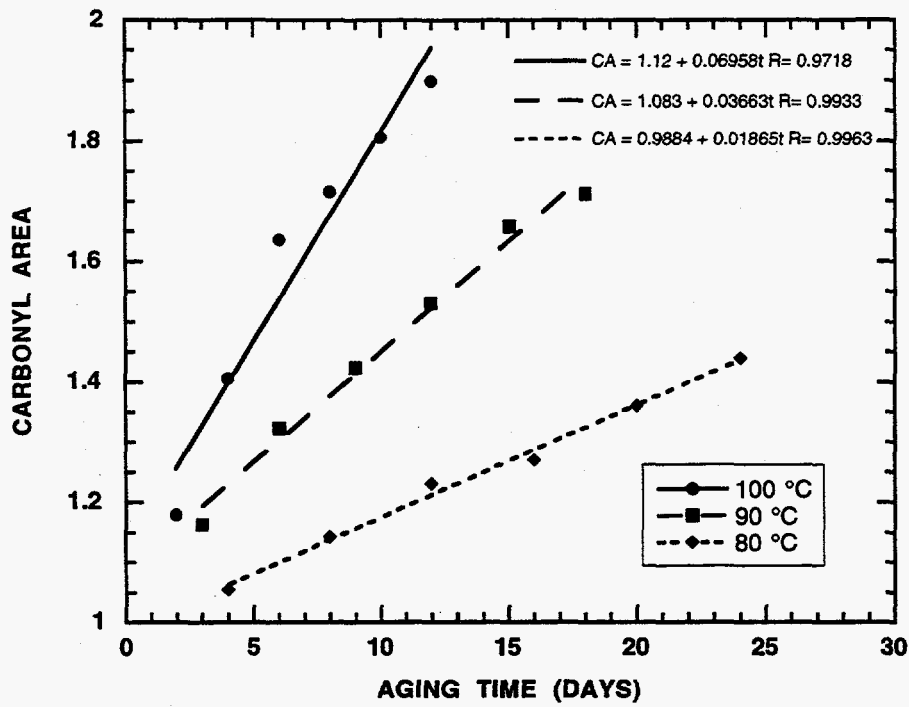


Figure 7-2. Carbonyl Formation Rates for POV Aged PAV Aged AAF-1

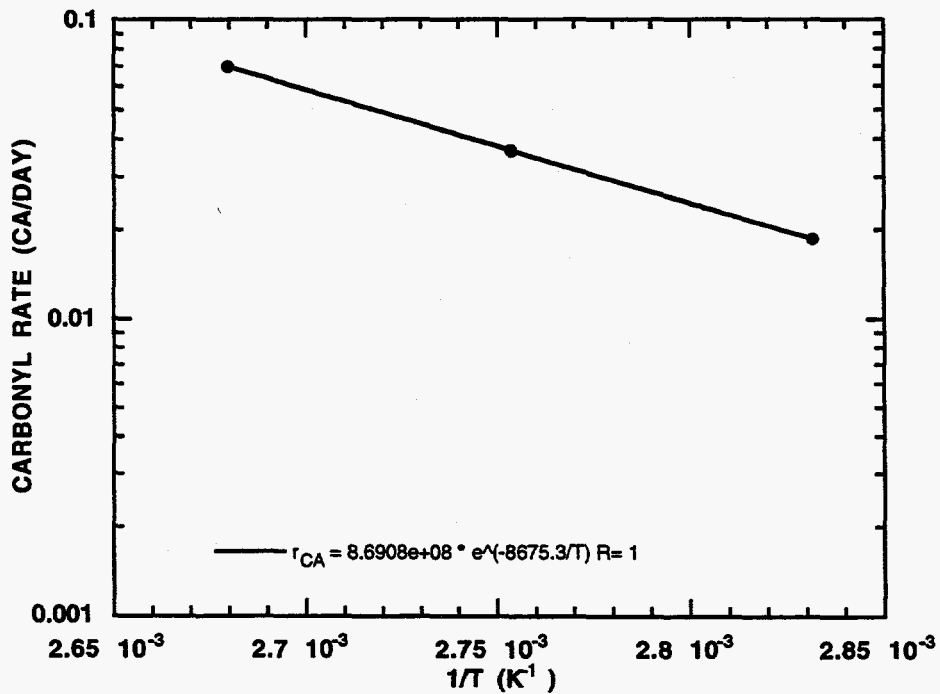


Figure 7-3. Arrhenius Plot for POV Aged PAV Aged AAF-1

Table 7-4. POV Aging Results

Agent	E (kJ/mol)	HS	50°C CA Rate ($\times 10^{-3}$ CA/day)*	50°C In η Rate ($\times 10^{-3}$)*
NONE	72.1	4.48	1.91	8.54
ISCF A	85.0	4.91	1.03	5.07
ISCF B	72.5	N/A	0.85	N/A
ISCF C	80.5	3.41	1.23	4.19
CRA A	88.9	3.49	0.89	3.11
CRA B	93.4	4.70	0.82	3.86
CRA C	83.3	5.11	1.03	5.25
YBF F3	98.3	3.20	0.54	1.73
AAF F3	74.4	3.53	1.55	5.46
ABM F3	83.1	2.22	1.11	2.45

* subject to errors associated with extrapolation

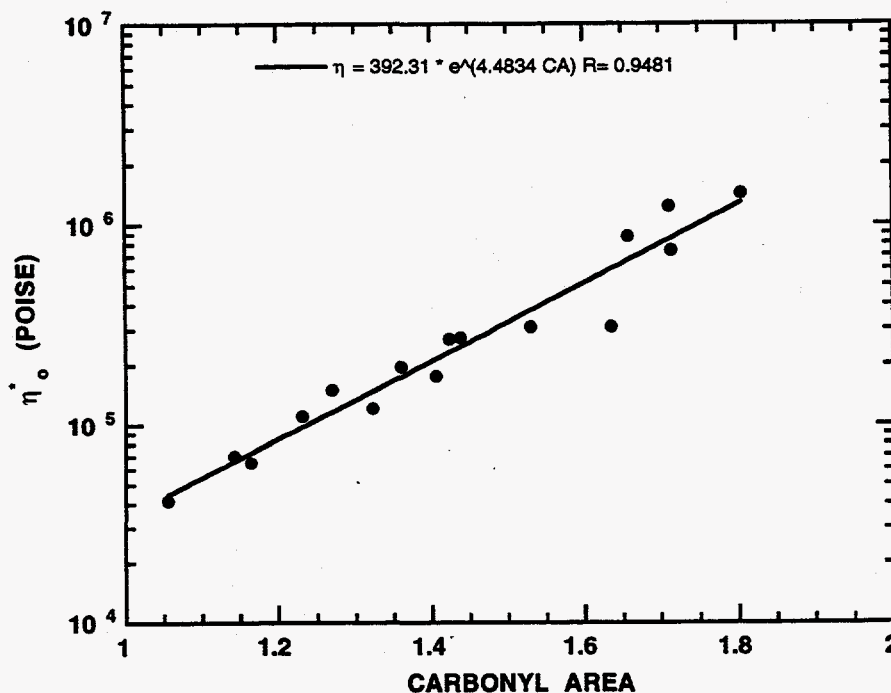


Figure 7-4. HS for POV Aged PAV Aged AAF-1

energy of the original asphalt is lower than the activation energies of all of the recycled blends. This results in CA rates (extrapolated) at 50°C higher than the recycled blends as shown in Table 7-4. The HS values are more variable with some recycled materials having higher (worse) HS values and some having lower (better) HS values than the original asphalt. Using the data in Tables 5-3, 7-1, 7-2, and 7-3, the approximate saturate content in the materials were calculated and the rankings in terms of saturate content were tabulated in Table 7-5 along with the HS rankings. The variability in HS is roughly correlated with the saturate content in the material as shown in Figure 7-5. The correlation seen in Figure 7-5 is further evidence that the saturate content should be minimized to produce superior HS values.

The combination of HS and CA rate (extrapolated) at 50°C yields the hypothetical $\ln \eta$ rate at 50°C. As was the case with the aging indexes determined from the TFOT and PAV tests, the data in Table 7-4 indicate that all of the recycled materials will harden slower than the original asphalt. This results mostly from the improvements in activation energy. The data in Table 7-4 also indicate that the hypothetical hardening rates of the

Table 7-5. Saturate Content and Hardening Susceptibility Rankings

Agent	Saturate Content Ranking (1 = lowest)	Hardening Susceptibility Ranking (1 = lowest)
NONE	6	6
ISCF A	8	8
ISCF B	10	N/A
ISCF C	3	3
CRA A	2	4
CRA B	5	7
CRA C	9	9
YBF F3	4	2
AAF F3	7	5
ABM F3	1	1

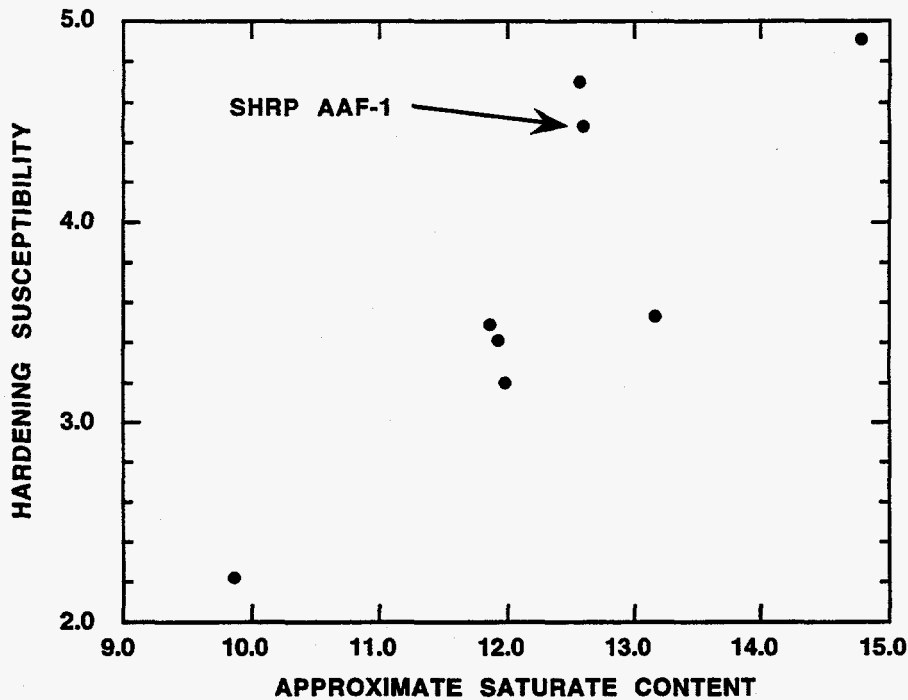


Figure 7-5. HS Versus Approximate Material Saturate Content

recycled asphalts softened with supercritical fractions are not dramatically worse than the hardening rates of the recycled asphalts using commercial recycling agents. In fact, the two best hardening rates were obtained for recycled asphalts using TAMU SCFs. Once again, this can be attributed to the narrow cuts that are obtained by fractionation into seven fractions as opposed to two or three.

The data collected on the original asphalt AAF-1 were then compared to the data collected on RTFOT pre-treated and neat AAF-1 reported in Chapter 6. Notably, the activation energy determined from PAV pre-aged AAF-1 is nearly the same as the activation for AAF-1 determined from the multi-variable regression reported in Table 6-9. The AAF-1 CA rate data determined from Figure 7-2 and the CA rates obtained from atmospheric aging conditions reported in Table 6-8 were then plotted together in Figure 7-6. Figure 7-6 clearly shows that the CA rate data for AAF-1 obtained using PAV pre-aged material, RFTOT pre-treated material, and neat asphalt are highly consistent. In

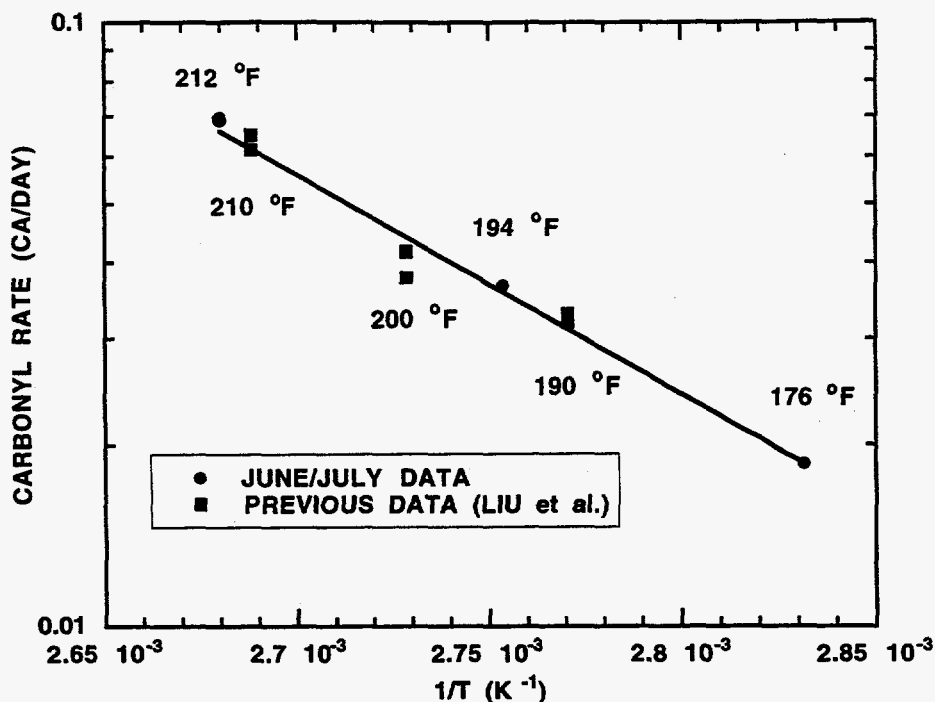


Figure 7-6. Arrhenius Plot for Atmospheric Aging of AAF-1

addition, the rate reported at 80°C effectively extends the atmospheric data 14°F beyond the data reported in Chapter 6. Because Chapter 6 describes only the oxidation kinetics of asphalts, no HS values are reported. However, it should be noted that the HS value for the AAF-1 samples investigated in Chapter 6 is nearly identical to the HS value for the PAV pre-aged AAF-1 investigated in this study. The consistency of the activation energy and the HS prove conclusively for the first time that the aging history of the material has little, if any, influence on the kinetic parameters. This means that it may be possible to extract an asphalt from a pavement sample and subject it to the POV test to determine kinetic parameters. From these kinetic parameters and the HS, it may be possible to accurately predict the future condition of the pavement. This is a pleasing, but unintended result of this experiment.

CONCLUSIONS

The initial conclusion that can be made is that recycled binders are superior to the original asphalt in terms of hardening rate. Furthermore, it can be concluded from the aging indices after thin film oven treatment and the pressure aging vessel testing that supercritical fractions from heavy end processing have the potential for use as asphalt rejuvenating agents. In fact, if narrow cuts can be produced industrially, dramatic improvements in hardening at road conditions may be possible.

CHAPTER 8

THE USE OF LIME AND AMINES IN RECYCLING ASPHALT

Lime has been used effectively as an anti-stripping agent for many years. In recent decades data have accumulated indicating that lime also slows the hardening of asphalt on the road and in the hot-mix plant (Jones, 1971) as well as in laboratory aging tests (Plancher et al., 1976; Petersen, 1982; Petersen et al., 1987). Plancher et al. (1976) slurried hydrated lime with asphalt in benzene for 24 hours and then centrifuged to remove the lime. Following oxidation there were much lower levels of carboxylic acids and somewhat lower levels of ketones than in control samples. Aging indexes (the ratio of viscosity after and before aging) were considerably reduced for the lime treated material as was the asphaltene content.

Petersen (1982) reported that merely mixing lime with asphalt resulted in a steady decrease in 225°C viscosity over 24 hours. Petersen et al. (1987) reported considerable improvement in aging index when asphalts were oxidized with hydrated lime in their Thin Film Accelerated Aging Test at 113°C. Lime loadings were 10, 20 and 30% high-calcium lime and 20% dolomitic lime. While all loadings considerably improved the aging index, there was no great difference between loadings. In general, those asphalts most sensitive to hardening were helped the most by the addition of lime. They also reported a reduction in ketone formation rate for lime-treated asphalts.

As the reduction in asphaltene content and hardening seemed to be greater than could be explained by the small reduction in oxidation products, the main effect would seem to be that the lime interfered with the association of oxidation products. This would reduce asphaltene formation and the concomitant viscosity increase. As old oxidized asphalt contains large amounts of asphaltenes, it seems plausible that lime might be particularly beneficial in asphalt recycling.

Asphalt hardening can be expressed in terms of viscosity change (1995) by where η_0^* is the low shear rate limiting dynamic viscosity, AS is asphaltenes and CA is the carbonyl area, or carbonyl content. The first term can be expressed in terms of particle suspension models such as that of Pal and Rhodes (Pal and Rhodes, 1989; Lin et al., in press, c). The lime particles can probably be treated like asphaltenes and included in this term. The first two terms can be

$$\frac{\partial \ln \eta_0^*}{\partial \text{time}} = \frac{\partial \ln \eta_0^*}{\partial \text{AS}} \cdot \frac{\partial \text{AS}}{\partial \text{CA}} \cdot \frac{\partial \text{CA}}{\partial \text{time}} \quad (8-1)$$

combined to give $\frac{\partial \ln \eta_0^*}{\partial \text{CA}}$ which is termed the hardening susceptibility, HS (Lau et al., 1992). The HS is linear for a wide range of temperatures, though it changes as a function of the viscosity temperature susceptibility. It is independent of the oxidation temperature below 100°C and it is a unique function for a given asphalt. The last term in Equation (8-1) is simply the carbonyl formation rate which is a linear, but asphalt dependent, function of the oxidation rate.

Based on the above analysis and reported literature (Plancher et al., 1976) it is expected that lime should reduce the asphaltene formation in response to carbonyl formation (AFS), the second term in Equation (8-1), and perhaps reduce the first term by disassociating existing asphaltenes. Additionally, according to the literature cited above, the last term might be slightly reduced. Another group of compounds with potential as anti-oxidants are amines. Previously, very little work has been done with these agents. The objective of the work reported in this chapter was to quantify the effect of lime and amines on the HS and carbonyl formation rate in Equation (8-1) in recycling applications.

EXPERIMENTAL DESIGN

Two SHRP asphalts, AAA-1 and AAF-1, picked for differences in HS, were mixed with different levels of CaO and Ca(OH)₂ (0, 1, 2, 5, 10 and 20 weight %) and aged in Pressure Oxygen Vessels (POV) at temperatures of 210°F (98.9°C), 200°F (93.3°C) and 190°F (87.8°C). Samples were removed periodically and η_0^* at 60°C, and carbonyl values were measured as describe in Appendix A. From these measurements, the HS was calculated. Aging indexes (viscosity of sample divided by viscosity of unaged material) were then calculated.

The same two asphalts were hardened by air bubbling to the viscosities shown in Table 8-1. These aged asphalts were then "recycled" using the recycling agents shown in Table 8-1.

Table 8-1. Materials Properties

Material	Asphalt (%)	Recycling Agent (%)	η_0^* @60°C Poise
Aged Asphalts			
AAA-1	100	----	54,300
AAF-1	100	----	85,000
Recycling Agent			
ABM-F2	----	100	91
YBF-F2	----	100	30
AAF-F3	----	100	67
Rejuvenated Blends			
AAA/ABM-F2	64	36	1,500
AAF/ABM-F2	62	38	1,600
AAF/YBF-F2	64	36	1,800
AAF/AAF-F3	68	32	1,800
AAA/YBF-F2	71	29	2,550
AAA/AAF-F3	67	33	2,900

These agents were produced from asphalts by supercritical extraction: ABM-F2 is the next to lightest fraction from SHRP ABM-1, YBF-F2 is the next to lightest fraction from a Texas asphalt and AAF F3 is the third lightest fraction from SHRP AAF-1. The lightest fraction usually is too high in saturates and thus was not used as a recycling agent. The hardened asphalts and recycling agents were blended to obtain the mixtures shown in Table 8-1. All of these rejuvenated asphalts were then blended with CaO at different levels (0, 1, 2 and 5 weight %) and aged in the POV at 80, 90 and 100°C. The blends produced using ABM-F2 as the rejuvenating agent were also mixed with 2% of three different amines and aged at the same conditions. The amines used are 2-Aminophenol, 4-(3-Phenylpropyl)-pyridine, and n-Phenyl-1-naphthylamine. These amines were chosen because they have three widely varying chemical functionalities. The

carbonyl areas were measured for all of the samples to obtain oxidation kinetics and 60°C viscosity measurements were performed on enough samples to obtain HS values.

EXPERIMENTAL METHODS

Lime-Asphalt Blending

Lime and asphalt were weighed into a sample tin to yield a combined weight of about 50g at the desired lime (CaO or Ca(OH)_2) concentration. The material was heated on a hot plate and stirred with a spatula until a uniform mixture was obtained.

Recycled Asphalt Blending

Using recently developed mixing rules (Chaffin et al., 1995), hardened asphalt and recycling agents were blended to obtain mixtures of about 2000 poise at 60°C. Blending was accomplished by heating and stirring with a mixing paddle driven by a hand-held drill. These rejuvenated asphalts were then combined with lime and amines and blended as described above.

RESULTS AND DISCUSSION

Lime Treated Asphalts

Though the objective of this research was to study the effect of lime on recycled material, it is desirable to compare this to the effect of lime on the same asphalts prior to recycling. It was expected that lime would have a greater effect on the recycled material because of the higher asphaltene content. Because of some temperature control problems, good kinetic data were not obtained. However, HS is independent of aging temperature and would be unaffected by upsets.

The HS values are tabulated in Table 8-2. Figure 8-1 is an HS plot for asphalt AAA-1 treated with Ca(OH)_2 . In view of the scatter in Figure 8-1 and the small difference in HS values between CaO and Ca(OH)_2 it was concluded that the differences, if any, were trivial and thus only CaO was used in the subsequent recycling studies. Also, the benefit above 5% was very small and so no concentrations above 5% were run.

Table 8-2. Hardening Susceptibilities of Lime-Treated Tank Asphalts

Lime Treatment (%)	AAA-1		AAF-1	
	CaO	Ca(OH) ₂	CaO	Ca(OH) ₂
0	7.5	7.6	4.9	4.3
1	5.4	5.5	4.3	4.3
2	5.7	5.2	4.0	3.9
5	7.1	5.6	3.8	3.7
10	6.2	5.5	3.7	3.6
20	5.8	5.4	3.2	3.3

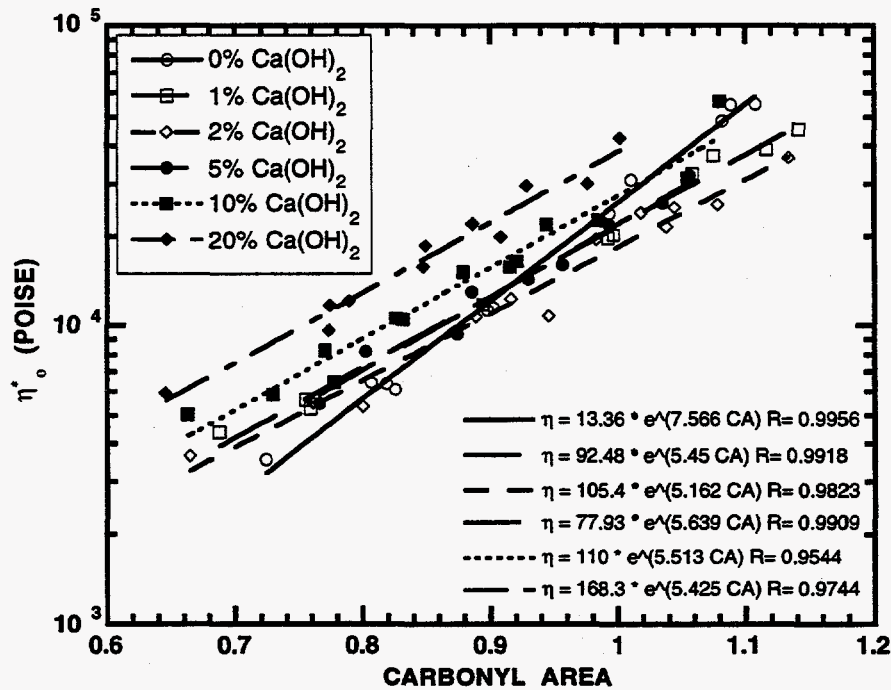


Figure 8-1. Hardening Susceptibility Plot for Ca(OH)_2 -Treated SHRP AAA-1

In retrospect, probably Ca(OH)_2 should have been chosen. It is after all cheaper, easier to handle, and perhaps better. In Table 8-3 aging indexes are computed at several times and temperatures for those asphalts that were aged in the same vessel at a given temperature. The indexes have been averaged for easy comparison and while there is essentially no difference between 5 and 10%, Ca(OH)_2 appears to be more effective at reducing hardening. The difference is still small and what is very apparent is that both CaO and Ca(OH)_2 are slowing the hardening of these asphalts.

Table 8-3. Aging Indexes of Lime-Treated Tank Asphalts

Temperature °F	Time (days)	No Lime (average of 2)	CaO		Ca(OH) ₂		
			5%	10%	5%	10%	
Asphalt AAA-1							
190	10	9	10	10	7	7	
	16	32	21	21	20	17	
200	6	8	7	7	6	5	
	12	27	22	28	14	13	
	15	57	46	47	32	44	
210	7	11	9	10	10	8	
	13	61	36	42	30	24	
Asphalt AAF-1							
190	10	13	9	10	10	10	
	16	39	26	22	21	23	
Average							
	----	29	21	22	17	17	

Lime Treated Recycled Material

The asphalt-recycling agent combinations at four levels of CaO treatment yielded 24 separate mixtures which were aged at three temperatures. Seven samples were removed for analyses over time periods ranging from 15 to 25 days. This yielded a very large amount of data

which are summarized here. Table 8-4 shows viscosity and carbonyl data and resulting hardening susceptibilities for the untreated aged materials at 90°C. It is interesting to compare the HS values for the untreated blends to those of the two asphalts. A lower HS is good in that such a material does not tend to harden in response to oxidative aging as much as one with a higher HS. Comparing values in Tables 8-2 and 8-4, it is seen that agent ABM-F2 was by far the most effective in lowering the HS for both asphalts. Agent YBF-F2 considerably improved the HS for asphalt AAA-1 but only slightly for AAF-1. Usually asphalts with higher values of HS are the most improved by proper recycling agents. This is reversed for agent AAF-F3. Perhaps the fact that the agent and asphalt were from the same material was a factor.

Amine Experiments

2-Aminophenol, 4-(3-Phenylpropyl)-pyridine, and n-Phenyl-1-naphthylamine were mixed only with the aged SHRP AAA-1 and AAF-1 rejuvenated with ABM-F2. Initial analysis of these experiments eliminated further examination. From the outset, the amine blends were problematic. First, while blending, one of the amines produced rather unpleasant fumes. The fumes were also apparent during POV aging later. Second, because the amines are miscible with the asphalt, and are of relatively low viscosity, the viscosity of the amine treated rejuvenated asphalts were quite low.

The POV aging experiments indicated that few, if any, benefits would be realized by the addition of amines to the recycled asphalts. The carbonyl formation rates, activation energies, and hardening susceptibilities were not affected greatly by any of the amine additives. In fact, the data indicate that the activation energy may have been adversely affected by the amines in several cases. The activation energies and HS values are listed in Table 8-5. The one possible beneficial additive was the 2-Aminophenol, but this additive was only beneficial in terms of activation energy, and then only for the rejuvenated AAA-1 asphalt. Figure 8-2 indicates that the seemingly improved activation energy is likely due more to scatter in the data than anything else. When the relatively small benefits of using amines are weighed with the costs of the various amines in comparison with the costs and benefits of lime as an additive, it is clear that lime should be the additive of choice for recycling asphalt, and amines should not be studied further.

Table 8-4. Aging Data for Untreated Rejuvenated Asphalts at 90°C

	Aging Time (Days)	Carbonyl Area	Viscosity (Poise)		Aging Time (Days)	Carbonyl Area	Viscosity (Poise)
#1 HS=5.3	0.0	0.8774	1500	#4 HS=4.1	0.0	0.9023	1829
	5.0139	1.1015	2281		4.9757	1.0796	3940
	7.9931	1.1529	4084		7.9444	1.2117	5900
	10.962	1.1963	5392		10.879	1.2834	8700
	13.927	1.2754	7667		14.069	1.3876	12900
	16.132	1.3519	10900		16.889	1.5350	22200
	19.069	1.3876	12200		19.948	1.6090	32200
	22.024	1.4497	18100		23.892	1.7050	47000
#2 HS=2.8	0.0	0.9683	1500	#5 HS=7.6	0.0	0.8364	2550
	5.0313	1.2250	3106		3.8750	1.0226	7530
	7.9861	1.3283	3905		7.8194	1.1669	14600
	10.924	1.4134	4919		10.879	1.1918	30100
	13.129	1.5092	6475		13.698	1.2340	48200
	16.094	1.5629	7922		16.889	1.3131	61000
	19.063	1.7062	11590		19.823	1.3519	77800
	22.042	1.7427	10600		22.792	1.4345	107000
#3 HS=3.9	0.0	0.9463	1792	#6 HS=7.0	0.0	0.7690	2900
	4.9757	1.0717	3685		3.8750	1.0472	6830
	7.9444	1.1525	5640		7.8194	1.1329	13200
	10.879	1.3166	7700		10.879	1.1995	22900
	14.069	1.3967	11800		13.968	1.2227	25200
	16.889	1.5204	21900		16.889	1.3092	44500
	19.948	1.6429	29600		19.823	1.3548	69900
	23.892	1.6722	49200		22.792	1.4066	93000

#1: AAA-1/ABM-F2

#2 : AAF-1/ABM-F2

#3: AAF-1/YBF-F2

#4: AAF-1/AAF-F3

#5: AAA-1/YBF-F2

#6: AAA-1/AAF-F3

Table 8-5. POV Aging Parameters for Amine Treated Rejuvenated Asphalts

Asphalt	Amine	Activation Energy (kJ/mole)	Hardening Susceptibility
AAA-1/ABM-F2	None	69.7	5.34
	2-Aminophenol	89.7	4.91
	Pyridine ^a	72.7	5.04
	Naphthylamine ^b	59.5	4.89
AAF-1/ABM-F2	None	80.8	2.75
	2-Aminophenol	82.5	2.96
	Pyridine ^a	77.8	2.83
	Naphthylamine ^b	67.6	2.97

^a 4-(3-Phenylpropyl)-pyridine

^b n-Phenyl-1-naphthylamine

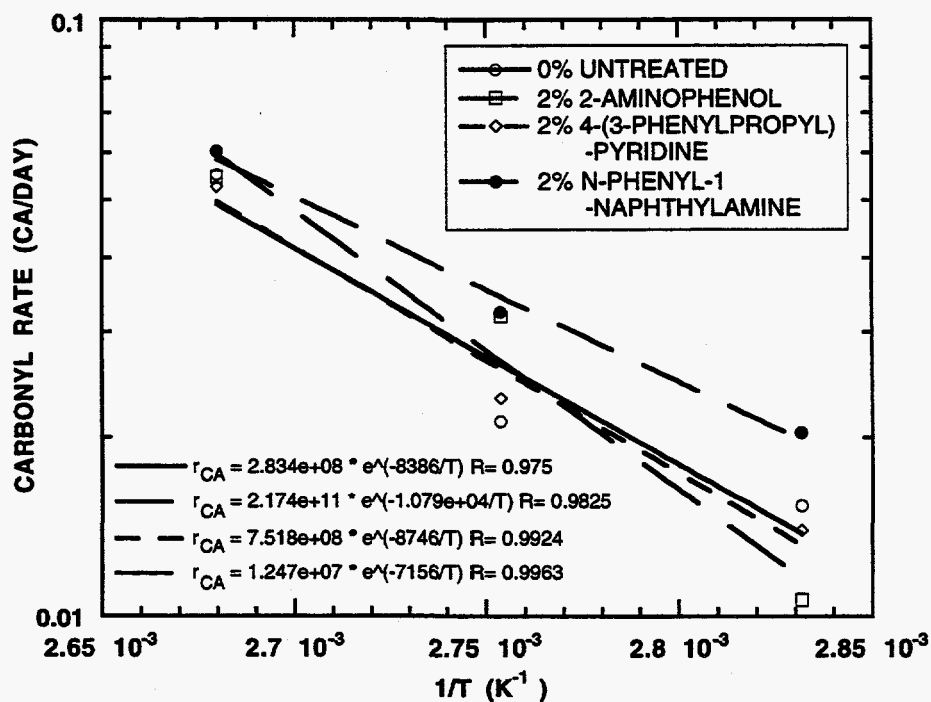


Figure 8-2. Arrhenius Plot for Amine Treated Rejuvenated AAA-1/ABM F2

Lime Additive Data Manipulation

Table 8-6 shows data for the system AAF/YBF-F2 at 90°C with lime treatment. These data and similar results for all systems were manipulated in several ways. Figure 8-3 shows carbonyl versus time for data taken from Tables 8-4 and 8-6. The slopes of these lines give the carbonyl rate data. These values for all samples and temperatures are listed in Table 8-7. Figure 8-4 shows a plot for the same mixture of $\ln \eta_0^*$ versus carbonyl. The slope of this line yields the temperature-independent hardening susceptibility, HS. HS values for all mixtures are listed in Table 8-7.

Table 8-6. Aging Data for CaO Treated AAF-1/YBF-F2 at 90°C

% CaO	Aging Time (days)	Carbonyl Area	Viscosity (Poise)
1	0.0	0.8661	1665
	4.9757	1.0290	2865
	7.9444	1.1123	3890
	10.879	1.2230	5290
	14.069	1.3232	7340
	16.889	1.4045	9220
	19.948	1.4369	11500
	23.892	1.5203	15600
2	0.0	.8767	1671
	4.9757	1.0536	3220
	7.9444	1.1378	4020
	10.879	1.1908	5460
	14.069	1.2885	7530
	16.889	1.3606	9380
	19.948	1.4148	12500
	23.892	1.4972	14400
5	0.0	.8653	1734
	4.9757	1.1100	3420
	7.9444	1.2051	4330
	10.879	1.2645	5630
	14.069	1.3238	6840
	16.889	1.4067	9760
	19.948	1.4594	12100
	23.892	1.5379	14900

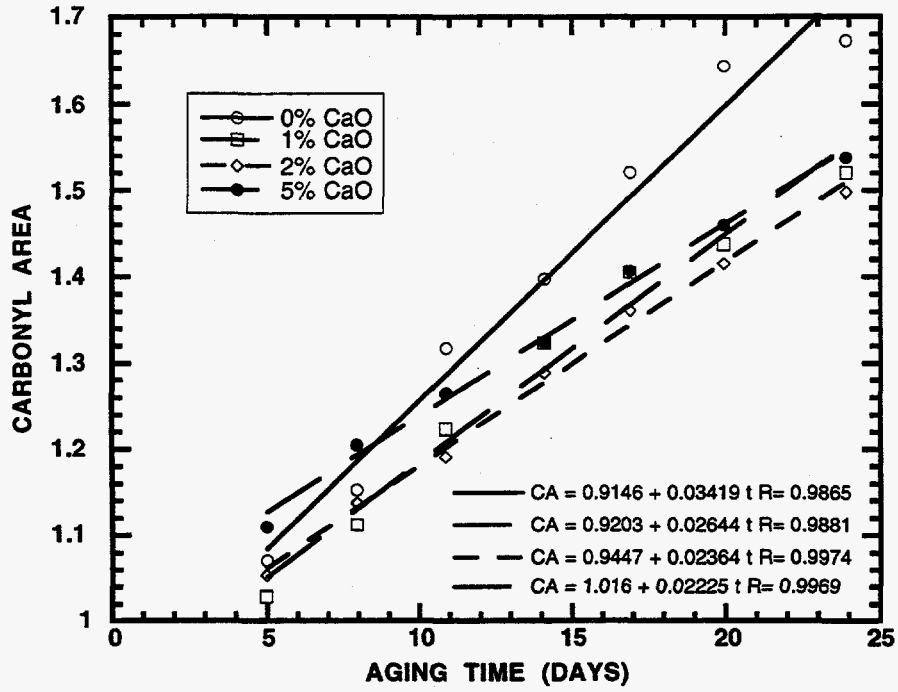


Figure 8-3. Oxidation Rates of CaO-Treated AAF-1/YBF-F2

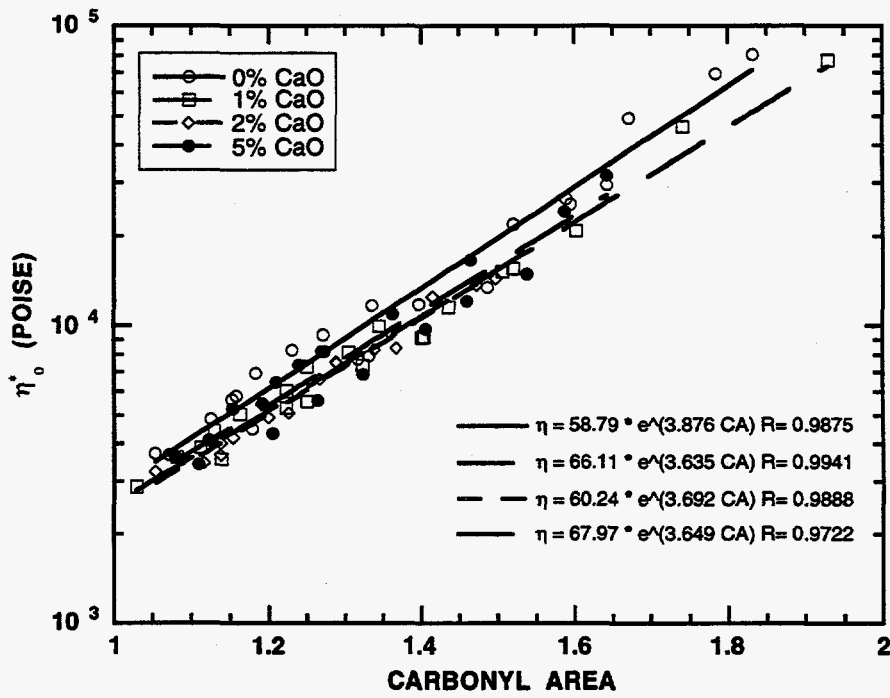


Figure 8-4. Hardening Susceptibility Plot for CaO-Treated AAF-1/ YBF-F2

Table 8-7. The Effect of CaO on Oxidative Aging Parameters of Asphalt Blends

Mixture	CaO (%)	CA Formation Rates (CA/day)			Activation Energy (kJ/mol)	Hardening Susceptibility
		80°C	90°C	100°C		
AAA/ABM-F2	0	0.0153	0.0213	0.0551	69.7	5.3
	1	0.0119	0.0233	0.0538	82.4	3.8
	2	0.0113	0.0255	0.0611	92.1	3.4
	5	0.0110	0.0239	0.0521	85.1	3.0
AAF/ABM-F2	0	0.0158	0.0313	0.0690	80.8	2.8
	1	0.0144	0.0346	0.0611	79.3	2.5
	2	0.0117	0.0346	0.0636	92.9	2.3
	5	0.0117	0.0314	0.0581	87.7	2.3
AAF/YBF-F2	0	0.0144	0.0342	0.0586	77.1	3.9
	1	0.0145	0.0264	0.0643	81.3	3.6
	2	0.0119	0.0236	0.0504	79.0	3.7
	5	0.0100	0.0223	0.0497	88.0	3.7
AAF/AAF-F3	0	0.0129	0.0326	0.0732	79.9	4.1
	1	0.0123	0.0213	0.0680	93.4	4.1
	2	0.0126	0.0255	0.0592	80.5	3.9
	5	0.0112	0.0256	0.0555	87.6	3.3
AAA/YBF-F2	0	0.0097	0.0202	0.0369	73.5	7.6
	1	0.0119	0.0184	0.0305	51.7	7.1
	2	0.0105	0.0180	0.0336	63.7	6.0
	5	0.0086	0.0183	0.0314	71.2	6.2
AAA/AAF-F3	0	0.0090	0.0188	0.0353	74.7	7.0
	1	0.0100	0.0193	0.0281	56.6	6.9
	2	0.0101	0.0200	0.0394	74.5	6.1
	5	0.0087	0.0196	0.0367	78.7	6.2

In Figure 8-5, carbonyl formation rate data for blend AAF/YBF-F2 are plotted versus reciprocal absolute temperature according to the Arrhenius equation which was defined in Chapter 6. When analyzing data taken at only one aging pressure, the relation given in Equation 6-3 becomes

$$\ln(\text{rate}) = \ln A - \frac{E}{RT} \quad (8-2)$$

where A is the frequency factor and E the activation energy. The activation energies for all of the rejuvenated asphalt systems, with and without lime treatment, are given in Table 8-7.

Results for the oxidation rates are ambiguous, with differences often well within the scatter of the data. In general it appears that the rates decrease for all the blends with the addition of lime except for AAA/ABM-F2 and AAA/AAF-F3. For the former blend, four of the nine lime-treated rates (three values at each of three temperatures) are above their respective control values while the corresponding number is seven of the nine for the latter blend. For

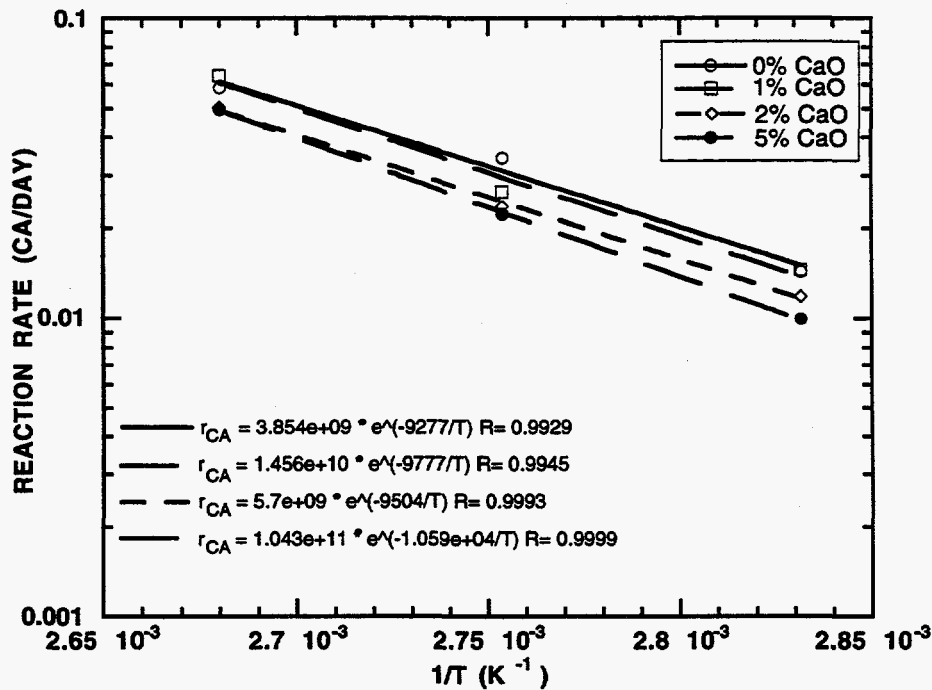


Figure 8-5. Arrhenius Plot for CaO-Treated AAF-1/YBF-F2

AAF/AAF-F3 all nine values are below their controls. One would expect the 5% mixtures to be the most affected. All be the most affected. All of these values are below controls except two of three for AAA/AAF-F3. Thus, it appears that at those temperatures, lime may, but does not necessarily, improve oxidation rates.

Overall the HS was improved for all blends with the addition of lime, although the improvement was small for AAF/YBF-F2. For this system and AAA/AAF-F3 no additional improvement is indicated above 2% lime. The greatest improvement was for the AAA/ABM-F2 blend and the poorest improvement was AAF/YBF-F2. With agents ABM-F2 and YBF-F2, asphalt AAA benefited the most, probably because it started with a higher HS; on the other hand AAF/AAF-F3 improved more percentage wise, than AAA/AAF-F3. It could be that it is desirable to derive a recycling agent from the original asphalt that is to be softened. Agent ABM-F2 was the most effective when used alone and with lime. For asphalt AAA-1 about half of the large improvement in HS, relative to the whole asphalt, occurred from the addition of the agent and the rest from 5% lime.

The differences in HS in Table 8-7 may not appear large but as the relation with viscosity is exponential, the effect on the hardening rate is considerable

$$\frac{d \ln \eta_0^*}{d (\text{time})} = (\text{rate})(\text{HS}) \quad (8-3)$$

Thus at a given temperature

$$\ln \eta_0^* = \ln \eta_{0,\text{unaged}}^* + (\text{rate})(\text{HS})(\text{time}) \quad (8-4)$$

$$\frac{\eta_0^*}{\eta_{0,\text{unaged}}^*} = \exp[(\text{rate})(\text{HS})(\text{time})] \quad (8-5)$$

The left hand side of this equation is the aging index.

Theoretically Equation (8-5) should agree with measured aging indexes. However, because HS and rate are curve fits and the aging indexes are point functions, and because of the exponential form of Equation (8-5), the deviations are often considerable. Also, because asphalts exhibit faster aging rates initially, the initial carbonyl value and viscosity will usually be below the constant rate lines. This "initial jump" phenomenon is less severe for recycled material as the old asphalt has already passed this region. Even so, because of the presence of the recycling agent, it does occur. This generally causes values of aging indexes calculated by Equation (8-5) to be low. However, Equation (8-5) can be used to calculate the percent reduction in hardening that can be expected from a reduction in oxidation rate or HS.

Of course, the relative improvement that occurs in aging index also depends on the aging time and temperature. That is, if one asphalt has a lower HS-rate product than a second asphalt, then its relative reduction in aging index increases as hardening proceeds. This nonlinearity can be eliminated by solving for the time it takes to reach a given degree of hardening. Thus

$$\text{time} = \frac{1}{\text{HS-rate}} \ln \left(\frac{\eta_{0,\text{aged}}^*}{\eta_{0,\text{unaged}}^*} \right) \quad (8-6)$$

or if one wishes to compare the relative time it takes for asphalts 1 and 2 to reach a critical viscosity, assuming η_0^* is the same for each the result is

$$\frac{\text{time 1}}{\text{time 2}} = \frac{(\text{HS-rate})_2}{(\text{HS-rate})_1} \quad (8-7)$$

This still ignores the effect of the initial jump, but before this is considered, a more serious problem must be addressed. Even if hardening is reduced at elevated temperatures, will this be true at road conditions? Recent kinetic studies (Liu et al., in press) indicate that data at high temperatures can be misleading because of differences in the activation energy in Equation (8-5). A high value of E means that an asphalt that ages relatively fast at high temperature, might age relatively slowly at road conditions.

While Equation (8-5) can be used to estimate oxidation rates at lower temperatures, the precision will not be good. The values of E are slopes based on rates which were themselves

obtained from slopes. Furthermore, the exponential nature of Equation (8-5) means that small errors in E will cause large errors in calculated rates. There are, however, sufficient data to determine trends.

We will arbitrarily calculate the time it takes each asphalt to reach 100,000 poise at 50°C, assumed to be a good average effective pavement temperature. From plots such as Figure 8-4, we can determine the CA value corresponding to this viscosity. For instance, for untreated AAF/YBF-F2 the critical carbonyl value is 1.919. From plots at three temperatures, as in Figure 8-6, the carbonyl intercepts CA₀ are determined. These are relatively temperature independent and average values are used. For AAF/YBF-F2, this value is 0.978. Next, Figure 8-5 is extrapolated to 323°K and the rate determined. Again, for untreated AAF/YBF-F2 this value is 0.001313. The time to reach the critical carbonyl can now be calculated by

$$\text{time} = \frac{\text{CA critical} - \text{CA}_0}{\text{rate}} \tag{8-8}$$

and for untreated AAF/YBF-F2 the time to reach 100,000 poise at 50°C is 717 days.

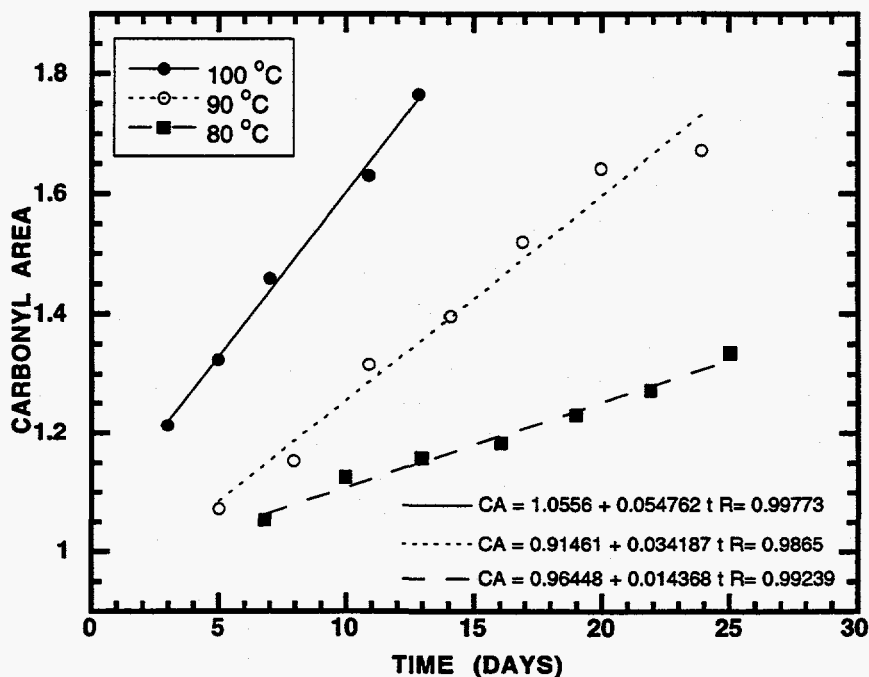


Figure 8-6. Carbonyl Formation Rates for AAF-1/YBF-F2 at Three Temperatures

Table 8-8 shows the critical carbonyl, the 50°C rate and critical time for all of the rejuvenated asphalt blends examined in this work. The critical times definitely trend upward with lime content and several exceptions such as AAF/YBF-F2 at 1% and AAA/AAF-F3 at 1% correspond to obviously low values of E. Liu et al. (in press) determined activation energies for 14 asphalts and none was less than 64 kJ/mole. This emphasizes that in addition to good HS and measured rates, if an asphalt has a high E or improving E with treatment, then low temperature results will be relatively better than its high temperature performance. In general, E trends up with lime content except for AAA/AAF-F3, although even here, the improvement in HS gives a plus for lime treatment. High aging times were obtained with agent ABM-F2 with both asphalts. Its blends were particularly responsive to lime. Blends of AAA-1 with other agents gave much lower times because of very low times for the untreated material. The overall percent gain in time with 5% lime addition was about the same for both asphalts with agents AAF-F3 and YBF-F2.

CONCLUSIONS

The preliminary data on the use of amines as additives indicate that the cost of amine additives can not be justified by improved asphalt performance and that additional experiments are unwarranted at this time. The data indicate that as far as oxidative hardening is concerned and for the limited sample of asphalts and blends studied in this work, lime addition during recycling has a uniformly beneficial effect. For the materials tested with lime, the hardening susceptibility was uniformly improved, and for most maltenes, the oxidation rate was reduced. Using the Arrhenius equation to extrapolate to road temperatures, it appeared that the improvement might be even greater than indicated by higher temperature measurements. For the agents used in this study, recycling alone improved the HS relative to the original material.

Table 8-8. Calculation of Critical Time at 50°C

Mixture	CaO (%)	Critical CA	CA _o	Rate x 10 ³ , @50°C (CA/day)	Critical Time (days)
AAA/ABM-F2	0	1.766	0.958	1.521	531
	1	2.005	0.927	0.852	1265
	2	2.098	0.900	0.613	1954
	5	2.159	0.908	0.747	1676
AAF/ABM-F2	0	2.483	1.071	1.197	1180
	1	2.609	1.028	1.228	1287
	2	2.706	1.042	0.660	2520
	5	2.690	1.053	0.778	2106
AAF/YBF-F2	0	1.919	0.978	1.313	717
	1	2.014	0.947	1.056	1011
	2	2.008	0.994	0.962	1055
	5	1.999	0.987	0.611	1656
AAF/AAF-F3	0	1.873	0.975	1.316	682
	1	1.851	0.929	0.583	1580
	2	1.931	0.944	1.025	963
	5	2.008	0.945	0.700	1518
AAA/YBF-F2	0	1.369	0.993	0.961	391
	1	1.409	0.970	2.284	192
	2	1.441	0.959	1.369	352
	5	1.430	0.947	0.929	520
AAA/AAF-F3	0	1.418	0.998	0.863	487
	1	1.359	0.978	1.737	220
	2	1.347	0.861	0.952	510
	5	1.344	0.879	0.741	627

CHAPTER 9

DEVELOPMENT OF A MICRODUCTILITY TEST

The ductility of an asphalt binder is defined as the distance to which it will elongate before breaking when two ends of a specified geometry are pulled apart at a defined speed and temperature. It is a physical test that can be used to help characterize the performance properties of a binder. Although the significance of ductility for unaged asphalts is highly debatable, changes in ductility over a binder's service life appear to correlate with overall roadway performance (Hveem et al., 1963).

Several methods are currently being used to test the ductility of a binder. The most widely used ductility method is the method specified in ASTM D113. The drawback to the current methods is that they require large sample sizes. For example, ASTM D113 requires a 1.0 cm thick "dog bone" briquette that is over 7.0 cm long. The total sample mass is close to 10 g. This method is particularly unsuitable when small amounts of material are available, as is the case with laboratory aged samples or binder recovered from pavement samples. To measure the ductility of a small amount of these materials, a micro-ductility test method was developed in the 1960s by Hveem et al. (1963). The apparatus and method developed by Hveem et al. and a modified version of their method are described below.

EXPERIMENTAL METHODS

Original Method

The apparatus and procedure used for the microductility experiment was developed in November, 1962 by California's Division of Highways. This test method (Calif. 349-A) is designed to measure ductility of a small sample (0.05 g) of bituminous material at 77 +/- 1F. Test specimens are liquified on a hot plate, thoroughly stirred, and then placed inside a two part brass mold of cylindrical geometry. This mold is allowed to cool to ambient conditions for 15 minutes. The mold forms a 0.069 inch diameter cylinder of asphalt binder and grips it at both

ends. The mold is placed into a ductility machine designed to pull the mold halves apart along their axis. After the machine and mold have been immersed in a water bath for 10 minutes, the mold is placed into a holder. One end of the holder is attached to a motor. The motor is then activated and pulls the sample apart at a constant rate of 0.5 cm/min. As the test progresses, the original cylinder of asphalt binder stretches into a very thin thread and eventually breaks. The separation distance of the two mold halves is measured in millimeters and reported as the ductility. In addition to being able to measure the ductility using a small sample size, approximately 60-75% of the specimen can be recovered at the conclusion of the test, if necessary.

The biggest limitation of the equipment used by the Calif. 349-A method is the inability to measure the force required to generate the constant strain rate. Such force information could be used to create a stress-strain curve for the sample. Another limitation is the small size of the asphalt cylinder formed inside the mold. Aged binders will often fail before the molds separate a significant distance.

Modifications

As described above, one limitation of the original method is the small size of the asphalt cylinder. To minimize this problem, molds with larger diameter holes were fabricated. The largest of the hole sizes is approximately twice that of the original mold. This only increases the sample mass required by a factor of four, so the apparatus is still capable of measuring the ductility of a material using much less than 1 g of sample. An additional benefit of using a larger hole size is the ability to perform the test at lower temperatures, where ductility is generally greatly reduced.

RESULTS AND DISCUSSION

Two asphalts, SHRP AAB-1 and AAD-1, were subjected to original and modified microductility testing. SHRP AAD-1 was used to study the temperature dependence of the ductility, while SHRP AAB-1 was used extensively to study the ductility as a function of both temperature and hole size.

Figure 9-1 shows the ductility of SHRP asphalt AAD-1 over a temperature range of 31 to 52°F. The strong dependence on temperature is shown, as well as a curious drop in ductility around 34°F. This transition may best be described as a ductile to brittle transformation. Below 34°F, the binder failed almost immediately, forming no thread and breaking cleanly. In fact, an audible "snap" often accompanied failure in this region. SHRP asphalt AAB-1 was tested using two mold sizes, and it exhibited a similar transition at approximately 43°F. Figure 9-2 records the results of both hole sizes, and shows the transition temperature for SHRP AAB-1. Although these experiments are still in their preliminary stages, it is hypothesized that this transition temperature might be fairly independent of the specimen size and geometry although the actual numerical value of the ductility at temperatures higher than the transition temperature clearly is a function of hole size.

CONCLUSIONS

Current experiments are further investigating this transition temperature phenomena. Other SHRP asphalts are being tested, and laboratory aged samples will be compared to their tank counterparts. These experiments will continue to consist of ductility measurements over a range of temperatures. This aspect of the test is crucial. Single temperature measurements of ductility do not reflect the temperature dependence, nor do they reveal any ductile to brittle transition. Hopefully, the information provided by micro-ductility experiments will help complete the physical characterization of asphalt binders. The very small sample requirement (0.05 - 0.10 g) of the test provides a feasible means to evaluate laboratory aged materials, and may aid in the prediction of long-term binder performance.

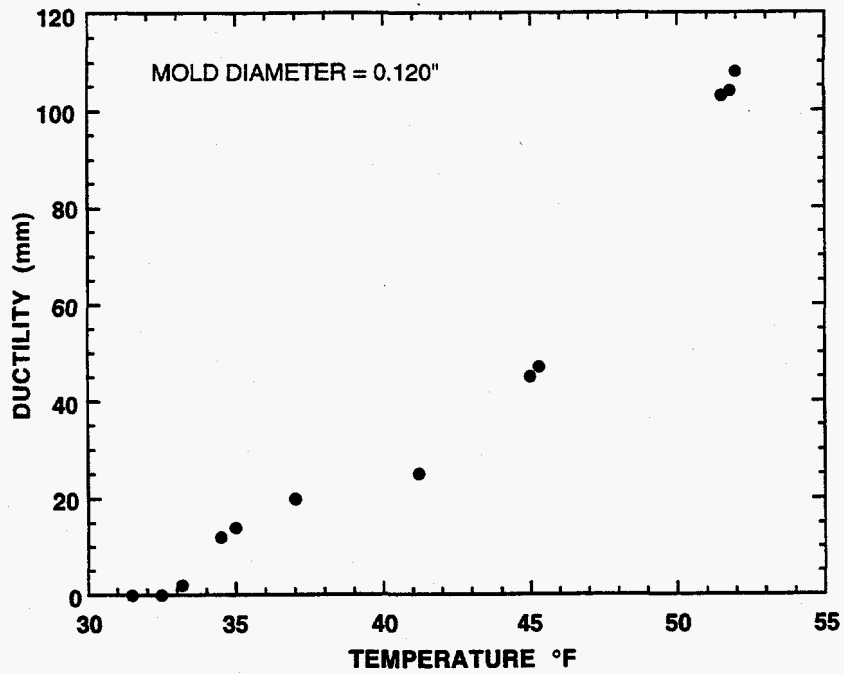


Figure 9-1. Temperature Dependence of Microductility for AAD-1

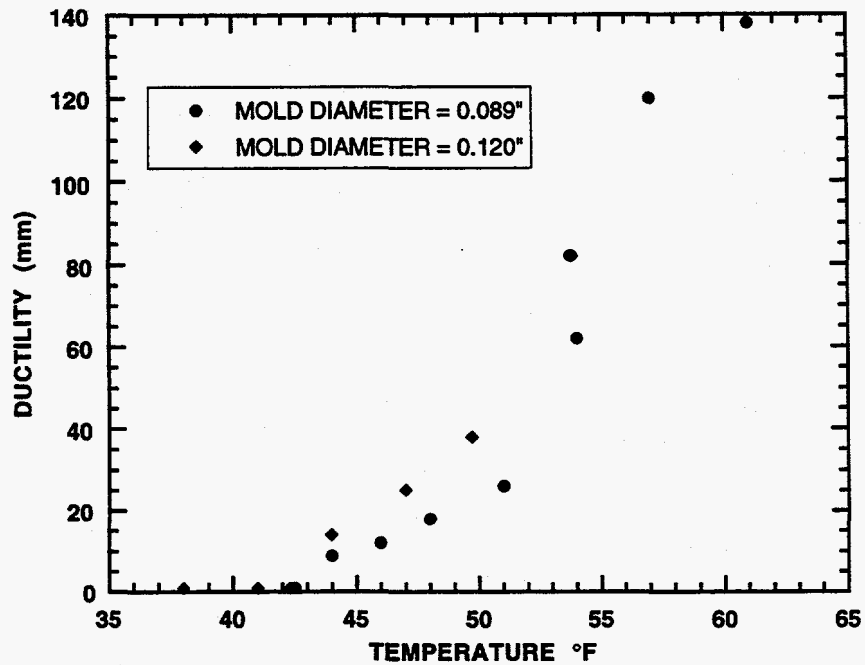


Figure 9-2. Temperature and Hole Size Dependence of Microductility for AAB-1

CHAPTER 10

ECONOMIC SUMMARY

This chapter provides economic analyses for using superior asphalt binder in original construction and for using recycling agents with reclaimed asphalt pavement (RAP) to construct overlays. Both of these applications envision the use of a supercritical refinery process to produce an optimal material, either asphalt binder or rejuvenating agent, at added cost (relative to conventional asphalt binder).

Three types of evaluations are considered in this chapter. The first addresses the incentive for the refiner (as producer) to construct a ROSE unit for producing the recycling agent and/or superior asphalt binder. The second type of evaluation addresses the incentive for departments of transportation (as users) to construct pavements using supercritically-refined asphalt binder. The third addresses the incentive for departments of transportation to recycle pavements using a supercritically-refined rejuvenating agent to mix with reclaimed asphalt pavement (RAP) to produce a viable pavement material.

In considering the two pavement options, the essence of the economic argument is this. By using the superior binder or the rejuvenating agent, the road either will have extended life (and therefore require less materials over the lifetime of the pavement, resulting in less cost, reduced energy usage, and reduced waste) or it will cost less initially (and probably have an extended life as well). With sufficient reduced cost (either capital cost or maintenance cost) there will be a strong economic incentive for implementation. The key, of course, is to have reduced cost that is sufficient to drive implementation. In the case of superior asphalt binder, the savings is achieved by producing extended life of the pavement while in the case of the recycled pavement, the savings is immediate due to the reduced cost of the material used in the recycling (i.e., by using the RAP) and perhaps savings also will be achieved through extended life of the pavement.

THE ROSE REFINING PROCESS

This analysis is for a single residual oil supercritical extraction (ROSE) refinery process with a capacity of handling 30,000 bbl/day of feed to produce 10,000 bbl/day of superior asphalt or recycling agent (actually, the conversion to superior asphalt should be considerably greater than that for producing recycling agent – more than 10,000 bbl of superior asphalt should be produced for 30,000 bbl of feed – but a single value of 10,000 bbl/day for both processes is assumed). The cost for such a plant is summarized in Table 10-1 and is based upon data taken from *Hydrocarbon Processing* (1992) and Peters and Timmerhaus (1991). The data in Table 10-1 show that the annualized cost of producing the recycling agent (RA) is \$3.40/bbl of RA.

Table 10-1. Estimated Cost to Produce Recycling Agent Using a Supercritical Fractionation Unit.

Basis: 30,000 Bbl/day of feed (10,000 Bbl/day of recycling agent)

Item	Cost
Installed Cost	\$30 × 10 ⁶
Utilities ^a (\$/yr)	3.5 × 10 ⁶
Labor & supervision (\$/yr)	1.5 × 10 ⁶
Maintenance & supplies (\$/yr)	1.8 × 10 ⁶
Other (\$/yr)	1.5 × 10 ⁶
Depreciation (10-yr)	3.0 × 10 ⁶
Total Annual Operating Cost	11.3 × 10 ⁶
Cost/Bbl of feed	\$1.14
Cost/Bbl of recycling agent	\$3.40

^a 10⁵ Btu/Bbl of feed, 330 operating days/yr, \$3.5/10⁶ Btu

Using the numbers in Table 10-1 and an assumed sales price for the superior asphalt/rejuvenating agent of \$6.25/bbl of RA over and above the feed cost/bbl, an economic analysis using the OIT spreadsheet is obtained (Appendix B).

As a result of these calculations, it is seen that a sales price of \$6.25/bbl above the feed cost is sufficient to provide an internal rate of return (IRR) of 26% for the ROSE process, with a discounted payback period of 4.4 years. This is a superior asphalt binder (or rejuvenating agent) cost of approximately \$135/ton. This cost of the supercritically-refined material is passed on to the next sections for calculating the cost of the superior asphalt pavement or for the cost of the

recycled pavements.

SUPERIOR ASPHALT PAVEMENT

This section compares the relative cost and benefit of a superior asphalt pavement compared to a conventional asphalt binder pavement. It is assumed that a new overlay is placed which is 4 inches thick, 30 feet wide (2 lanes), contains 5 wt% binder and 95 wt% aggregate and has a density approximately twice that of water. With these assumptions, there are 3,270 tons of pavement per mile. At 5% binder in the mix, this is 164 tons of asphalt binder/mile.

Capital Cost

The in-place cost of a conventional pavement is approximately \$30/ton of pavement (0.95 t of aggregate at \$5/t of aggregate, 0.05 t of binder at \$100/t of binder, and \$20/t of mix for placement) which is approximately \$98,100/mile of pavement.

The in-place cost of a superior asphalt pavement, assuming the same costs except \$135/t of superior binder (see the above section on the ROSE refining process analysis), is approximately \$6,000/t of pavement more or \$103,823/mile of pavement.

Maintenance

For both the conventional and superior asphalt pavement, a baseline maintenance cost was approximated as one-fourth of the original capital cost (including construction) distributed over the life of the pavement. For the conventional pavement (having an average service life of 12 years), this is \$2,040/mile/year. For the superior-asphalt pavement, assuming a service life of 15 years for example, this is \$1,730/mile/year. This level of maintenance cost for the conventional binder is supported by the actual amount, approximately \$1,000/lane-mile/year (for conventional pavement), budgeted for pavement maintenance by Texas DOT.

Several superior-asphalt pavement performance levels were considered in the analysis. Each level represented a different pavement life (15, 18, and 24 years) and was compared to an average life of 12 years for a conventional pavement. To compare the two pavements at each performance level over the same time period, the cost to replace the conventional pavement was

prorated over its expected life (12 years), multiplied by the additional number of years needed to meet the projected life of the superior pavement, and then this total additional expense was distributed over the entire performance period as additional maintenance cost. For example, with the cost of the conventional pavement at \$98,100/mile, the added "maintenance" cost to bring the 12 year conventional pavement to 15 years would be

$$\frac{\$98,100}{12 \text{ mi yr}} \times \frac{2 \text{ yr}}{15 \text{ yr}} = \frac{\$1,090}{\text{mi yr}}$$

and this is added to the usual baseline maintenance cost in the preceding paragraph to obtain the total.

Energy Use

The energy use entered for each pavement is the amount of binder used, converted to energy equivalents. For the conventional material, this is

$$\frac{163.5 \text{ tons of asphalt}}{\text{mile}} \times \frac{2000 \text{ lbm}}{\text{ton}} \times \frac{20,000 \text{ Btu}}{\text{lbm}} \times \frac{1}{12 \text{ yr}} = 545 \times 10^6 \frac{\text{Btu}}{\text{mi yr}}$$

For the superior asphalt binder, this amount is proportionately less because of the extended lifetime of the pavement.

Waste

The amount of waste for the conventional pavement is simply 3,270 tons/mile over 12 years or 273 tons/mi/yr. For the superior pavement, this amount is reduced proportionately due to the extended lifetime of the pavement.

Table 10-2 summarizes the economic results obtained for three hypothetical lifetimes of the pavement constructed with superior asphalt: 15 years, 18 years, and 24 years.

Table 10-2. Superior Asphalt (SA) Pavement versus Conventional Asphalt Pavement Comparison

SA Pvmnt Life (years)	Cap Cost (\$10 ³ /mi)		Maint Cost (\$/mi/yr)		Energy Use (10 ⁶ Btu/mi/yr)		Waste (tons/mi/yr)		IRR (%)	Payback Period (yr)
	Conv	SA	Conv	SA	Conv	SA	Conv	SA		
15	98	104	3,678	1,730	545	436	273	218	36.5	3.3
18	98	104	4,770	1,440	545	363	273	182	63.0	1.8
24	98	104	6,130	1,081	545	272	273	137	95.5	1.2

RECYCLED ASPHALT PAVEMENT

This section compares the relative cost and benefit of a recycled asphalt pavement compared to a conventional asphalt binder pavement. It is assumed that an overlay is placed which is 4 inches thick, 30 feet wide, contains 5 wt% binder and 95 wt% aggregate and has a density approximately twice that of water. With these assumptions, there are 3,270 tons of pavement per mile. At 5% binder in the mix, this is 164 tons of asphalt binder/mile.

Capital Cost

The in-place cost of a conventional pavement is approximately \$30/ton of pavement (0.95 t of aggregate at \$5/t of aggregate, 0.05 t of binder at \$100/t of binder, \$20/t of mix for placement) which is approximately \$100,000/mile of pavement.

The in-place cost of a recycled asphalt pavement, assuming the same costs except for \$135/t for the rejuvenating agent (RA) instead of \$100/t for conventional asphalt (see the above section on the ROSE refining process analysis) and that one ton of the recycled pavement consists of 2/3 ton RAP and 1/3 ton RA/fresh aggregate mixture (0.017 ton RA and 0.316 ton fresh aggregate), is approximately \$8,200/mile of pavement less than the conventional pavement or approximately \$89,900/mile of pavement.

Maintenance

For both the conventional and the recycled asphalt pavement, a baseline maintenance cost was approximated as one-fourth of the original capital cost (including construction) of the conventional pavement distributed over the life of the pavement. Note that it is assumed that the recycled pavement will not cost less for maintenance than the conventional pavement, even though its capital cost is less. This gives a baseline maintenance cost for each pavement of \$24,960/mile to be distributed over the pavement life.

Several recycled-asphalt pavement performance levels were considered in the analysis. Each level represented a different pavement life (12, 15, and 18 years) and was compared to an average life of 12 years for a conventional pavement. (Note: we anticipate that with the proper design of the rejuvenating agent and its use in the right proportions, a recycled pavement life

greater than 12 years can be achieved). To compare the two pavements at each performance level over the same time period, the cost to replace the conventional pavement was prorated over its expected life (12 years), multiplied by the additional number of years needed to meet the projected life of the superior pavement, and then this total additional expense was distributed over the entire performance period as additional maintenance cost (see the previous section).

Energy Use

The energy use entered for each pavement is the amount of binder used, converted to energy equivalents. For the conventional material, this is 545 million Btu/mi/yr (see the previous section). For the recycled asphalt binder, this amount is proportionately less because of any extended lifetime of the pavement and also because only 1/3 as much fresh hydrocarbon (RA) is used to construct the pavement. For example, for a recycled pavement with an extended life of 18 years,

$$\frac{163.5 \text{ tons of asphalt}}{\text{mile}} \times \frac{1}{3} \times \frac{2000 \text{ lbm}}{\text{ton}} \times \frac{20,000 \text{ Btu}}{\text{lbm}} \times \frac{1}{18 \text{ yr}} = 121 \times 10^6 \frac{\text{Btu}}{\text{mi yr}}$$

To this amount, an energy cost to produce the RA which is approximately 3 million Btu/mi/yr can be added.

Waste

The amount of waste for the conventional pavement is, as above, 273 tons/mi/yr. For the recycled pavement, this amount is reduced proportionately due to the extended lifetime of the pavement and due to the use of RAP which provides 2/3 of the material which would otherwise be waste. Thus, for an 18 year recycled pavement, the amount of waste would be 61 tons/mi/yr.

Table 10-3 summarizes these results obtained for three hypothetical lifetimes of the pavement constructed with recycled asphalt: 12 years, 15 years, and 18 years. The Department of Energy Office of Industrial Technologies (DOE-OIT) spreadsheet could not be used because, with benefit achieved with reduced cost, the rate of return is infinite.

Table 10-3. Recycled Asphalt Pavement versus Conventional Asphalt Pavement Comparison

RA Pvmnt Life (years)	Cap Cost (\$10 ³)		Maint Cost (\$/mi)		Energy Use (10 ⁶ Btu/mi/yr)		Waste (tons/mi/yr)		IRR (%)	Payback PB Period (yr)
	Conv	RAP	Conv	RAP	Conv	RAP	Conv	RAP		
12	98.1	89.9	2,040	2,040	545	185	273	91	∞	0
15	98.1	89.9	3,680	1,635	545	148	273	73	∞	0
18	98.1	89.9	4,770	1,360	545	124	273	61	∞	0

OTHER SUPPORTING CALCULATIONS

Basis: 2 million miles of highway having an average life of 12 years, of which 1/3 of the total amount repaired in a year will be recycled. Also, an average replacement depth of 4 in (1/3 ft) is assumed.

Baseline Energy Consumption

Amount of Pavement Material Repaired, per year.

$$\frac{2 \times 10^6 \text{ mi}}{12 \text{ yr}} \left| \frac{(30 \text{ ft})(0.333 \text{ ft})(5280 \text{ ft})}{\text{mi}} \right| \left| \frac{(2)(62) \text{ lbm}}{3 \text{ ft}} \right| \frac{\text{ton of mix}}{2000 \text{ lbm}} = \frac{545 \times 10^6 \text{ tons of pavement}}{\text{yr}}$$

Amount of Binder in the Pavement Repaired, per year. The pavement is approximately 5 wt% binder.

$$\frac{545 \times 10^6 \text{ tons pvmnt}}{\text{yr}} \left| \frac{0.05 \text{ tons asphalt binder}}{\text{ton pavement}} \right| = \frac{2.73 \times 10^7 \text{ tons asphalt binder}}{\text{yr}}$$

Energy Cost per year Without Recycling. Without recycling, hydrocarbons would be used in the highways which possess energy in the amount of 1.1×10^{15} Btu/yr. This is the energy

cost per year of the competing technology:

$$\frac{2.73 \times 10^7 \text{ tons of binder}}{\text{yr}} \left| \frac{2000 \text{ lbm}}{\text{ton}} \right| \frac{20,000 \text{ Btu}}{\text{lbm}} = 1.1 \times 10^{15} \frac{\text{Btu}}{\text{yr}}$$

Market Penetration

Miles/year of Pavement Recycled. The amount of pavement recycled, per year is:

$$\frac{1}{3} \frac{545 \times 10^6 \text{ tons of pavement}}{\text{yr}} = \frac{182 \times 10^6 \text{ tons of pavement}}{\text{yr}}$$

Miles of pavement recycled per year:

$$\frac{1}{3} \frac{2 \times 10^6 \text{ mi}}{12 \text{ yr}} = 55,500 \frac{\text{mi}}{\text{yr}}$$

Energy Efficiency Improvement

Binder Saved by Recycling. If 1/3 of the repaired pavement is recycled, then the amount of binder which will not be replaced is

$$\frac{1}{3} \frac{2.73 \times 10^7 \text{ tons of binder}}{\text{yr}} = \frac{9.13 \times 10^6 \text{ tons of binder recycled}}{\text{yr}}$$

Energy Savings Associated with the Recycled Binder.

$$\frac{9.13 \times 10^6 \text{ tons of binder recycled}}{\text{yr}} \left| \frac{2000 \text{ lbm}}{\text{ton}} \right| \frac{20,000 \text{ Btu}}{\text{lbm}} = 365 \times 10^{12} \frac{\text{Btu}}{\text{yr}}$$

Energy Cost of the Recycling Agent (Excluding Processing Cost.) If the recycled binder is 25% recycle agent (3 tons of binder per ton of recycle agent), then

$$\frac{9.13 \times 10^6 \text{ tons of binder recycled}}{\text{yr}} \left| \frac{\text{ton or recycle agent}}{3 \text{ tons of binder}} \right| \frac{2000 \text{ lbm}}{\text{ton}} \left| \frac{20,000 \text{ Btu}}{\text{lbm}} \right| = 122 \times 10^{12} \frac{\text{Btu}}{\text{yr}}$$

Energy Cost of Processing the Recycle Agent. For a basis of one recycle agent plant having a capacity of 30,000 Bbl/day of feed to produce 10,000 Bbl/day of recycling agent, the utilities requirement would be approximately 10^5 Btu/Bbl of feed or 3×10^5 Btu/Bbl of recycle agent. The recycle agent required, per year is:

$$\frac{9.13 \times 10^6 \text{ tons of binder}}{\text{yr}} \left| \frac{\text{ton of RA}}{3 \text{ tons of binder}} \right| \frac{\text{Bbl}}{5.62 \text{ ft}^3} \left| \frac{\text{ft}^3}{62 \text{ lbm}} \right| \frac{2000 \text{ lbm}}{\text{ton}} = \frac{17.5 \times 10^6 \text{ Bbl RA}}{\text{yr}}$$

Hence, the energy cost of processing the recycle agent is

$$\frac{17.5 \times 10^6 \text{ Bbl RA}}{\text{yr}} \left| \frac{3 \times 10^5 \text{ Btu}}{\text{Bbl RA}} \right| = 5.2 \times 10^{12} \text{ Btu/yr}$$

Energy Efficiency Improvement.

$$\frac{365 - 122 - 5}{365} \times 100\% = 65\%$$

Energy Savings Result

$$(1.1)(0.65)(0.33) = 0.24 \text{ quads}$$

Alternate calculation:

$$0.365 - 0.122 - 0.005 = 0.24 \text{ quads}$$

Capital Investment

Bbl of Recycle Agent Required per Mile of Pavement.

$$\frac{1 \text{ Bbl of recycling agent}}{3 \text{ Bbl asphalt binder}} \left| \frac{1 \text{ Bbl}}{42 \text{ gal}} \right| \frac{7.48 \text{ gal}}{\text{ft}^3} \left| \frac{\text{ft}^3}{62 \text{ lbm}} \right| \frac{5 \text{ lbm}}{100 \text{ lbm pavement}} \left| \frac{182 \times 10^6 \text{ tons of pavement}}{\text{yr}} \right| \frac{\text{yr}}{55,500 \text{ mi}} \left| \frac{2000 \text{ lbm}}{\text{ton of pavement}} \right| = 317 \frac{\text{Bbl of RA}}{\text{mi}}$$

Size or Capacity of a Typical RA Production Unit. At 30,000 Bbl of feed/day (10,000 Bbl/day of recycling agent produced) and a lifetime of 10 years, one recycling agent processing plant can provide RA for 1.04×10^5 miles of pavement:

$$\frac{10,000 \text{ Bbl of RA}}{\text{da}} \left| \frac{\text{mi}}{317 \text{ Bbl}} \right| \frac{330 \text{ da}}{\text{yr}} \left| \frac{10 \text{ yr}}{1} \right| = 1.04 \times 10^5 \text{ mi}$$

Installed Cost/Bbl of Recycle Agent. For an installed cost of $\$30 \times 10^6$, the cost per Bbl of RA produced over the life of the plant is

$$\frac{\$30 \times 10^6}{10 \text{ yr}} \left| \frac{\text{da}}{10,000 \text{ Bbl RA}} \right| \frac{\text{yr}}{330 \text{ da}} = \frac{\$0.91}{\text{Bbl of RA}}$$

Installed Cost/mile.

$$\frac{\$0.91}{\text{Bbl RA}} \left| \frac{317 \text{ Bbl RA}}{\text{mi}} \right| = \frac{\$290}{\text{mi}}$$

REFERENCES

- Ali, M.A. and W.A. Nofal, "Application of High Performance Liquid Chromatography for Hydrocarbon Group Type Analysis of Crude Oils," *Fuel Sci. Technol. Int.*, **12**, 21-33 (1994).
- Altgelt, K.H. and O.L. Harle, "The Effect of Asphaltenes on Asphalt Viscosity," *Ind. Eng. Chem. Prod. Res. and Dev. (now Ind. Eng. Chem. Res.)*, **14**, 240-246 (1975).
- Anderson, D.I., D.E. Peterson, and M. Wiley, *Characteristics of Asphalts as Related to the Performance of Flexible Pavements*, Utah Department of Transportation Final Report UDOT-MR-76-6 (1976).
- Beg, S.A., F. Mahmud, and D.K. Al-Harbi, "Hydrocarbon Group Analysis of Arabian Crude Oils TBP-Fractions," *Fuel Sci. Technol. Int.*, **8**, 125-134 (1990).
- Bishara, S.W. and E. Wilkins, "Rapid Method for the Chemical Analysis of Asphalt Cement: Quantitative Determination of the Naphthene Aromatic and Polar Aromatic Fractions Using High Performance Liquid Chromatography," *Transp. Res. Rec.*, **1228**, 183-190 (1989).
- Blokker, P.C., and H. van Hoorn, "Durability of Bitumen in Theory and Practice," *5th World Petroleum Congress*, 417-429 (1959).
- Boduszynski, M.M., J.F. McKay, and D.R. Latham, "Asphaltenes, Where are You?," *Proc. Assoc. Asphalt Paving Technol.*, **49**, 123-143 (1980).
- Boudart, M., *Kinetics of Chemical Process*, Butterworth-Heinemann, Stoneham (1991).
- Branthaver, J.F., M. Nazir, J.C. Petersen, and S.M. Dorrence, "The Effect of Metalloporphyrins on Asphalt Oxidation. I. The Effect of Synthetic Chelates," *Liq. Fuels Technol. (now Fuel Sci. Technol. Int.)*, **1**, 355-369 (1983).
- Branthaver, J.F., M. Nazir, J.C. Petersen, S.M. Dorrence, and M.J. Ryan, "The Effect of Metalloporphyrins on Asphalt Oxidation. II. The Effect of Vanadyl Chelates Found in Petroleum," *Liq. Fuels Technol. (now Fuel Sci. Technol. Int.)*, **2**, 67-89 (1984).
- Burr, B.L., R.R. Davison, C.J. Glover, and J.A. Bullin, "Solvent Removal from Asphalt," *Transp. Res. Rec.*, **1269**, 1-8 (1990).
- Burr, B.L., R.R. Davison, C.J. Glover, and J.A. Bullin, "Softening of Asphalts in Dilute Solutions at Primary Distillation Conditions," *Transp. Res. Rec.*, **1436**, 47-53 (1994).

- Burr, B.L., R.R. Davison, H.B. Jemison, C.J. Glover, and J.A. Bullin, "Asphalt Hardening in Extraction Solvents," *Transp. Res. Rec.*, **1342**, 50-57 (1991).
- Carbognani, L. and A. Izquierdo, "Preparative Compound Class Separation of Heavy Oil Vacuum Residua by High Performance Liquid Chromatography," *Fuel Sci. Technol. Int.*, **8**, 1-15 (1990).
- Chaffin, J.M., R.R. Davison, C.J. Glover, and J.A. Bullin, "Viscosity Mixing Rules for Asphalt Recycling," *Transp. Res. Rec.*, **1507**, 78-85 (1995).
- Corbett, L.W., "Composition of Asphalt Based on Generic Fractionation, Using Solvent Deasphalting, Elution-Adsorption Chromatography, and Densimetric Characterization," *Anal. Chem.*, **41**, 576-579 (1969).
- Corbett, L.W., "Dumbbell Mix for Better Asphalt," *Hydrocarbon Process.*, **58**, 173-177 (1979).
- Dark, W.A., "Crude Oil Hydrocarbon Group Separation Quantitation," *J. Liq. Chromatogr.*, **5**, 1645-1652 (1982).
- Dark, W.A., "Shale Oil Separation by High Performance Liquid Chromatography," *J. Liq. Chromatogr.*, **6**, 325-342 (1983).
- Dark, W.A. and W.H. McFadden, "The Role of HPLC and LC-MS in the Separation and Characterization of Coal Liquefaction Products," *J. Chromatogr. Sci.*, **16**, 289-293 (1978).
- Dark, W.A. and R.R. McGough, "Use of Liquid Chromatography in The Characterization of Asphalts," *J. Chromatogr. Sci.*, **16**, 610-615 (1978).
- Davison, R. R., J. A. Bullin, C. J. Glover, J. R. Stegeman, H. B. Jemison, B. L. Burr, A. L. G. Kyle, and C. A. Cipione, *Design and Manufacture of Superior Asphalt Binders*, Texas Department of Transportation Final Report No. 1155 (1991).
- Davison, R. R., J. A. Bullin, C. J. Glover, H. B. Jemison, C. K. Lau, K. M. Lunsford, and P. L. Bartnicki, *Design and Use of Superior Asphalt Binders*, Texas Department of Transportation Final Report No. 1249 (1992).
- Davison, R.R., J.A. Bullin, C.J. Glover, J.M. Chaffin, G.D. Peterson, K.M. Lunsford, M.S. Lin, M. Liu, M., A. Ferry, *Verification of an Asphalt Aging Test and Development of Superior Recycling Agents and Asphalts*, Texas State Department of Highways and Public Transportation Final Report No. 1314-1F (1994).

- Davison, R.R., C.J. Glover, B.L. Burr, and J.A. Bullin, "SEC of Asphalts," in *Handbook of Size Exclusion Chromatography*, Ed. Chi-San Wu, Marcel-Dekker, Inc., New York, NY, 211-247 (1995).
- Dickinson, E.J., and J.H. Nicholas, "The Reaction of Oxygen with Tar Oils," *Road Research Technical Paper No 16*, 1 (1949).
- Dickinson, E.J., J.H. Nicholas, and S. Boas-Traube, "Physical Factors Affecting the Absorption of Oxygen by Thin Film of Bitumen Road Binders," *J. Appl. Chem.*, **8**, 673-687 (1958).
- Eilers, H.J., "The Colloidal Structure of Asphalt," *J. Phys. Colloid Chem.*, **53**, 1195-1211 (1948).
- Epps, J.A., D.N. Little, R.J. Holmgreen, and R.L. Terrel, *Guidelines for Recycling Pavement Materials*. NCHRP-224 (1980).
- Ferry, J., *Viscoelastic Properties of Polymers*, John Wiley and Sons, 4th ed., New York, NY (1985).
- Gayla, L.C. and J.C. Suatoni, "Rapid SARA Separations by High Performance Liquid Chromatography," *J. Liq. Chromatogr.*, **3**, 229-242 (1980).
- Girdler, R.B., "Constitution of Asphaltene and Related Studies," *Proc. Assoc. Asphalt Paving Technol.*, **34**, 45-79 (1965).
- Goodrich, J.L., J.E. Goodrich, and W.J. Kari, "Asphalt Composition Tests: Their Application and Relation to Field Performance," *Transp. Res. Rec.*, **1096**, National Research Council, Washinton, D.C., 164-167 (1986).
- Handbook of Chemistry and Physics*, Editors R.C. Weast, M.J. Astle, and W.H. Beyer, **68** (1987).
- Heukelom, W. and P.W.O. Wijga, "Viscosity of Dispersions as Governed by Concentration and Rate of Shear," *Proc. Assoc. Asphalt Paving Technol.*, **40**, 418-437 (1971).
- Hveem, F.N., Zube, E., and Skog, J., "Proposed New Tests and Specifications for Paving Grade Asphalts," *Proc. Assoc. Asphalt Paving Technol.*, **32**, 271-327 (1963).
- Hydrocarbon Processing*, **71**:11, 159 (Nov. 1992).
- Jemison, H.B., B.L. Burr, R.R. Davison, J.A. Bullin, and C.J. Glover, "Application and Use of the ATR, FT-IR Method to Asphalt Aging Studies," *Fuel Sci. Technol. Int.*, **10**, 795-808 (1992).

- Jemison, H.B., R.R. Davison, C.J. Glover, and J.A. Bullin, "Fractionation of Asphalt Materials by Using Supercritical Cyclohexane and Pentane," *Fuel Sci. Technol. Int.*, **13**, 605-638 (1995).
- Jones, G.M., *The Effect of Hydrated Lime on Asphalt in Bituminous Pavements*, Paper prepared for presentation at the National Lime Association Meeting, Colorado Springs, CO, May 22, 1971.
- Lau, C.K., K.M. Lunsford, C.J. Glover, R.R. Davison, J.A. and Bullin, "Reaction Rates and Hardening Susceptibilities as Determined from POV Aging of Asphalts," *Transp. Res. Rec.*, **1342**, 50-57 (1992).
- Lee, D.Y. and R.J. Huang, "Weathering of Asphalts as Characterized by Infrared Multiple Internal Reflectance Spectra," *Appl. Spectrosc.*, **27**, 435-440 (1973).
- Lin, M.S., *The Formation of Asphaltenes and Its Impact on the Chemical and Physical Properties of Asphalts*, Ph.D. Dissertation, Texas A&M University, College Station, Texas (1995).
- Lin, M.S., C.J. Glover, R.R. Davison, and J.A. Bullin, "The Effect of Asphaltenes on Asphalt Recycling and Aging," *Transp. Res. Rec.*, **1507**, 86-95 (1995).
- Lin, M.S., J.M. Chaffin, M. Liu, C.J. Glover, R.R. Davison, and J.A. Bullin, "The Effect of Asphalt Composition on the Formation of Asphaltenes and Their Contribution to Asphalt Viscosity," *Fuel Sci. Technol. Int.*, **14**(1&2), 139-162 (1996).
- Lin, M.S., K.M. Lunsford, C.J. Glover, R.R. Davison, and J.A. Bullin, "The Effects of Asphaltenes on the Chemical and Physical Characteristics of Asphalts," In *Asphaltenes: Fundamentals and Applications*, Ed. E. Y. Sheu, Plenum Press, in press.
- Liu, M., K.M. Lunsford, R.R. Davison, C.J. Glover, and J.A. Bullin, "The Kinetics of Carbonyl Formation in Asphalt," *AIChE J.*, in press.
- Lundanes, E. and Tyge Greibrokk, "Quantitation of High Boiling Fractions of North Sea Oil After Class Separation and Gel Permeation Chromatography," *J. Liq. Chromatogr.*, **8**, 1035-1051 (1985).
- Manheimer, J., "The Effects of Paraffins on Asphalt," *Proceeding of The First World Petroleum Congress*, Vol 2, 553-556 (1933).
- Martin, K.L., R.R. Davison, C.J. Glover, and J.A. Bullin, "Asphalt Aging in Texas Roads and Test Sections," *Transp. Res. Rec.*, **1269**, 9-19 (1990).

- Mortazavi, M. and J.S. Moulthrop, *The SHRP Materials Reference Library*, SHRP-A-646 (1993).
- Pal R. and E. Rhodes, "Viscosity/Concentration Relationship for Emulsions," *J. Rheol.*, **33**, 1021-1045 (1989).
- Pearson, C.D., G.S. Huff, and S.G. Gharfeh, "Technique for the Determination of Asphaltenes in Crude Oil Residues," *Anal. Chem.*, **58**, 3266-3269 (1986).
- Peters, M.S. and K.D. Timmerhaus, *Plant Design and Economics for Chemical Engineers*, 4th edition, McGraw-Hill, Inc., New York, 210 (1991).
- Petersen, J.C., *Relationships Between Asphalt Chemical Composition and Performance-Related Properties*, Prepared for presentation at the annual meeting of the Asphalt Emulsion Manufacturers Association, Las Vegas, Nevada, March 16-19, 1982.
- Petersen, J.C., H. Plancher, and P.M. Harnsberger, "Lime Treatment of Asphalt to Reduce Age Hardening and Improve Flow Properties," *Proc. Assoc. Asphalt Paving Technol.*, **56**, 632-653 (1987).
- Petersen, J.C., J.F. Branthaver, R.E. Robertson, P.M. Harnsberger, J.J. Duvall, and E.K. Ensley, "Effects of Physicochemical Factors on Asphalt Oxidation Kinetics," *Transp. Res. Rec.*, **1391**, 1-10 (1993).
- Peterson, G.D., R.R. Davison, C.J. Glover, and J.A. Bullin, "The Effect of Composition on Asphalt Recycling Agent Performance," *Transp. Res. Rec.*, **1436**, 38-46 (1994).
- Plancher, H., E.L. Green, and J.C. Petersen, "Reduction of Oxidative Hardening of Asphalts by Treatment with Hydrated Lime - A Mechanistic Study," *Proc. Assoc. Asphalt Paving Technol.*, **45**, 1-19 (1976).
- Que, G., W. Liang, Y. Chen, C. Liu, and Y. Zhang, "Relationships Between Chemical Composition and Performance of Paving Asphalt," *Proceeding of the International Symposium: Chemistry of Bitumens*, Rome, Italy, **2**, 517-527 (1991).
- Rostler, F.S. and H.W. Sternberg, "Compounding Rubber and Petroleum Products," *Ind. Eng. Chem.*, **41**, 598-608 (1949).
- Rostler, F.S., and R.M. White, *Influence of Chemical Composition of Asphalt on Performance, Particularly Durability*, ASTM STP 277, Symposium on Road and Paving Materials, 64-88 (1959).

- Savastano, C.A., "The Solvent Extraction Approach to Petroleum Demetallization," *Fuel Sci. Technol. Int.*, **9**, 855-871 (1991).
- Sheu, E.Y., M.M. De Tar, and D.A. Storm, "Rheological Properties of Vacuum Residue Fractions in Organic Solvents," *Fuel*, **70**, 1151-1156 (1991).
- Stegeman, J.R., R.R. Davison, C.J. Glover, and J.A. Bullin, "Supercritical Fractionation and Reblending to Produce Improved Asphalts," in *Proceedings of the International Symposium: Chemistry of Bitumens*, Rome, Italy, **1**, 336-381 (1991).
- Stegeman, J.R., A.L. Kyle, B.L. Burr, H.B. Jemison, R.R. Davison, C.J. Glover, and J.A. Bullin, "Compositional and Physical Properties of Asphalt Fractions Obtained by Supercritical Extraction," *Fuel Sci. Technol. Int.*, **10**, 767-794 (1992).
- Suatoni, J.C., H.R. Garber, and B.E. Davis, "Hydrocarbon Group Types in Gasoline-Range Materials by High Performance Liquid Chromatography," *J. Chromatogr. Sci.*, **13**, 367-371 (1975).
- Suatoni, J.C. and R.E. Swab, "Rapid Hydrocarbon Group-Type Analysis by High Performance Liquid Chromatography," *J. Chromatogr. Sci.*, **13**, 361-366 (1975).
- Suatoni, J.C. and H.R. Garber, "Hydrocarbon Group-Type Analysis of Petroleum Fractions [b.p. 190°-360°C] by High Performance Liquid Chromatography," *J. Chromatogr. Sci.*, **14**, 546-548 (1976).
- Suatoni, J.C. and R.E. Swab, "Preparative Hydrocarbon Compound Type Analysis by High Performance Liquid Chromatography," *J. Chromatogr. Sci.*, **14**, 535-537 (1976).
- Thenoux, G., C.A. Bell, and J.E. Wilson, "Evaluation of Asphalt Physical and Fractional Properties and Their Interrelationship," Paper No.870531 presented at the Transportation Research Board 67th Annual Meeting, Washington D.C., January 11-14 (1988).
- Traxler, R. N., "Relation Between Hardening and Composition of Asphalt," *American Chemical Society Division of Petroleum Chemistry*, **5**, A71-A77 (1960).
- Traxler, R.N., "Relation Between Asphalt Composition and Hardening by Volatilization and Oxidation," *Proc. Assoc. Asphalt Paving Technol.*, **36**, 359-377 (1961).
- Van Oort, W.P., "Durability of Asphalt, Its Aging in the Dark," *Ind. Eng. Chem.*, **48**, 1196-1201 (1956).

Verhasselt, A.F., and F.S. Choquet, "A New Approach to Studying the Kinetics of Bitumen Aging," *Proceedings of the International Symposium Chemistry of Bitumens*, Rome, Italy, 2, 686 (1991).

White, R.M., W.R. Mitten, and J.B. Skog, "Fractional Components of Asphalts - Compatibility and Interchangeability of Fractions Produced from Different Asphalts," *Proc. Assoc. Asphalt Paving Technol.*, 39, 492-531 (1970).

ABBREVIATIONS

AB	air-bubbling
AI	aging index
ASTM	American Society for Testing and Materials
ATR	attenuated total reflectance
n-C ₇	n-heptane
CRA	commercial rejuvenating agent
DAO	deasphalted oil
DLV	dimensionless log viscosity
DMA	dynamic mechanical analysis
DOE-OIT	Department of Energy Office of Industrial Technologies
EtOH	ethanol
FTIR	Fourier transform infrared spectroscopy
GPC	gel permeation chromatography
HPLC	high performance liquid chromatography
IRR	internal rate of return
ISCF	industrial supercritical fraction
MeOH	methanol
MRL	materials reference library
NA	naphthene aromatic
PA	polar aromatic
PAV	pressure aging vessel
PB	payback
POV	pressure oxygen vessel
PTFE	poly tetrafluoroethylene
RA	rejuvenating agent
RAP	recycled asphalt pavement
RI	refractive index
ROSE	residual oil supercritical extraction
RTFOT	rolling thin film oven test
SA	superior asphalt
SCF	supercritical fraction
SHRP	Strategic Highways Research Program
TAMU	Texas A&M University
TCE	trichloroethylene
TFOT	thin film oven test
THF	tetrahydrofuran
VTS	viscosity temperature susceptibility

NOTATION

A	frequency factor for oxidation
%AS	weight percentage of asphaltenes
AFS	asphaltene formation susceptibility
A_{vis}	frequency factor of viscosity dependence on temperature
CA	infrared carbonyl peak area
CA_0	carbonyl peak area zero-time intercept
CA_{tank}	infrared carbonyl peak area of virgin asphalt
E	activation energy of oxidation
E_{vis}	activation energy of viscosity dependence on temperature
$HS_{60^\circ C}$	hardening susceptibility at 60°C
HS_T	hardening susceptibility at temperature T
HS_{T_0}	hardening susceptibility at reference temperature T_0
R	universal gas constant
RF_s	response factor of saturates
T	absolute temperature
α	the reaction order with respect to oxygen pressure
$\eta_{0, 60^\circ C}^*$	60°C low frequency limiting viscosity

APPENDIX A

EXPERIMENTAL METHODS

SUPERCRITICAL FRACTIONATION

The supercritical fractionation unit has been described in Study 1155 (Davison, 1991) and Study 1249 (Davison, 1992). A brief description of the process, operating conditions, and apparatus modifications follow.

Process Description

The following description is taken primarily from the TxDOT Study 1249 (Davison et al, 1992) report with appropriate modifications. The unit operates at a constant pressure above the critical pressure of the solvent. The SC fractionation unit separates heavy petroleum products into up to four fractions according to solubility in SC solvents. The temperatures of the separators determine the density of the solvent and, consequently, the solvent power in each vessel. Components of the feed precipitate when no longer soluble in the solvent. The lightest, most-soluble materials are removed by decompression during solvent recovery.

Figures A-1 and A-2 illustrate schematically the SC unit. The solvent is pumped to the operating pressure in S1-S3 by MP1. Several hours are required to bring the temperatures to the desired steady-state values. The steady-state operating temperature in S4 determines the steady state pressure for S4. Once steady-state conditions are achieved, MP2 is activated, introducing feed material into the circulating solvent stream. The temperature in each separator determines the solubility in the SC solvent. The insoluble material is transferred from the separator to its corresponding collector periodically to avoid potential plugging problems while the soluble material travels to the next separator. Finally, the overhead mixture from S3 passes through the control valve, where the pressure is reduced to significantly subcritical value. At these gaseous conditions, none of the asphaltic material is soluble and complete separation of the solvent is achieved. The solvent then

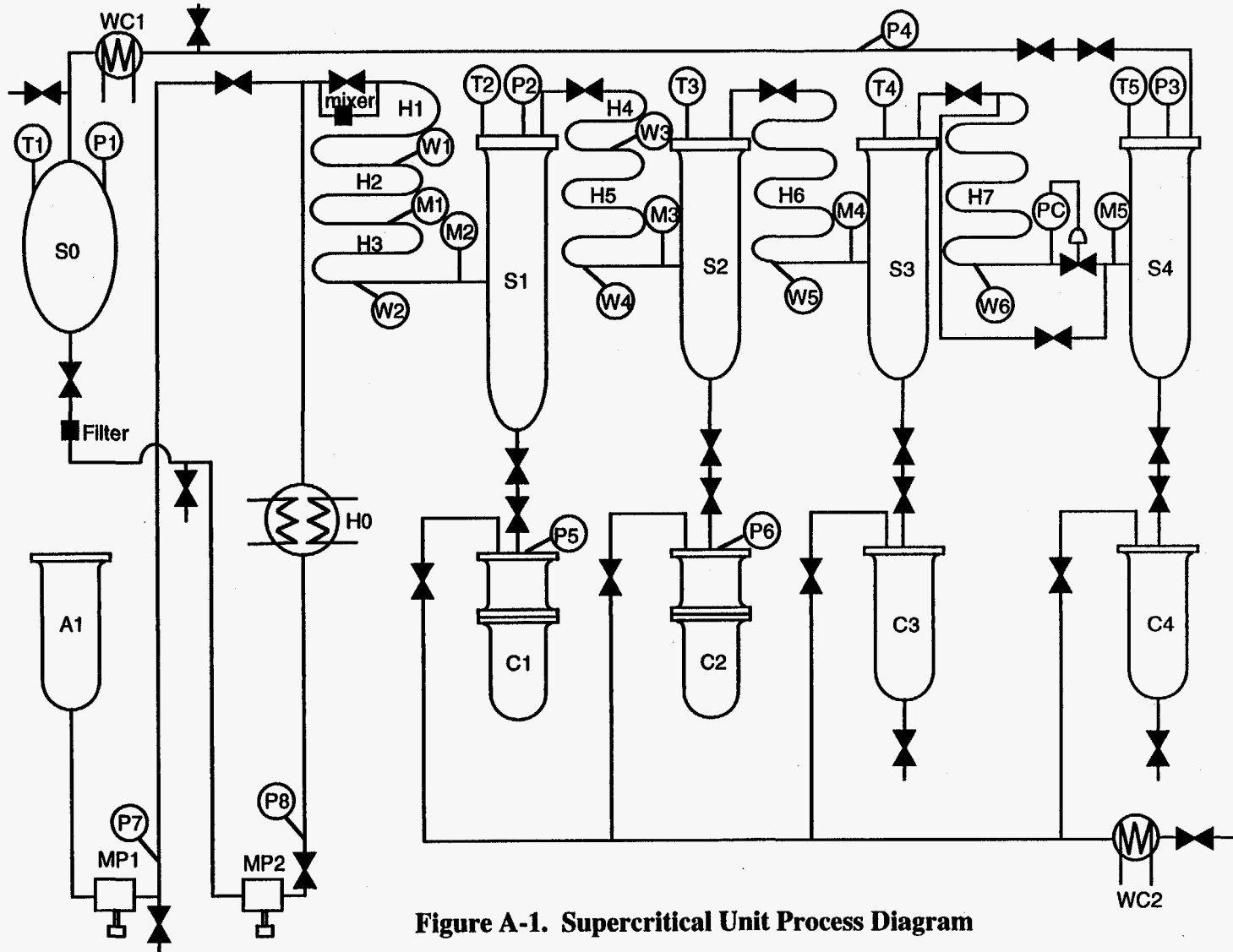


Figure A-1. Supercritical Unit Process Diagram









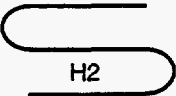

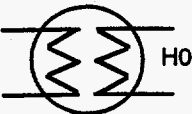

S0	Solvent Tank	S1-S4	Separators
C1-C4	Collectors	A1	Asphalt Tank
	In-line Filter/mixer		Valve
	Control Valve		Thermocouple
	Tubing Wall Temperature Thermocouple		Temperature Monitor and Controller
	Pressure Controller		Pressure Gauge
	Heating Tape Heater		Metering Pump
	Dual Purpose Heater/Cooler		Water Cooled Condenser

Figure A-2. Legend for Supercritical Extraction Unit Diagram

passes overhead, is condensed in WC1 and flows back into the solvent reservoir. For this DOE effort, n-pentane is the solvent used for supercritical fractionation.

The four asphalts fractionated during the first year of this DOE effort were fractionated in two passes through the unit. The lightest fraction from the first pass was fed through the unit a second time yielding eight fractions that may be analyzed. The lightest fraction from the second pass is designated as fraction F1 and the heaviest fraction from the first pass is designated as fraction F8 (fraction F5 is the feed material for the second pass through the unit).

AGED ASPHALT PRODUCTION

During the first year of this DOE effort, a new apparatus was developed for aging a large quantity of asphalt by bubbling air through a well mixed asphalt sample at moderate temperature. The apparatus consists of a variable speed 1/4 horsepower motor which drives a 2" diameter mixing shaft placed in a half full gallon can of asphalt. Another, less powerful mixer (1/15th horsepower) is also available for use. The can is wrapped with a heating tape connected to a variable transformer and a thermocouple actuated on/off controller.

Building air passes through a surge tank, filter, and a copper coil placed in a mineral oil temperature bath before being fed to the asphalt. The air is introduced to the asphalt through a 5" diameter sparging ring made from 1/4" stainless steel tubing with 14 nearly uniformly spaced 1/16" holes. The inlet air temperature is controlled by adjusting both the temperature of the oil bath and the air flow rate. The operating temperature of the air-bubbled reaction vessel must be high enough for the oxidation to proceed at an appreciable rate, but not so high as to drastically alter the reaction mechanism or reaction products. To produce pavement-like materials, the reaction temperature is targeted at 93.3°C (200°F), initially. However, as the asphalt ages, the temperature begins to rise due to increased viscous dissipation. This is not critical but the temperature should not be allowed to exceed 110°C (230°F).

PRESSURE OXYGEN VESSEL (POV)

The original unit is described by Lau (1992) and Davison et al. (1992). In order to improve on aging simulation capacity, four additional units were constructed and a central control panel was installed as shown in Figure A-3. Later, to eliminate temperature gradient problems with the initial design, the vessels were placed in glycol/water baths.

Figure A-4 shows a schematic of one of the POVs. The vessels are located behind a steel wall in an explosion proof hood. Each vessel is contained in an aluminum barrel filled to the bottom of the top flange with a mixture of triethylene glycol and water. The vessel is monitored and controlled from a panel outside the explosion proof hood. The control panel houses a compound pressure gauge to monitor the pressure, a variable transformer to control the amount of electrical power to the heating elements in the water/triethylene glycol bath, a temperature controller which controls the temperature of the bath, and a recorder to monitor the temperature within the POV. A stirrer is employed in the bath to insure that the temperature distribution in the bath is uniform. A vacuum pump is used to evacuate the vessels before charging with oxygen or to remove oxygen depleted air once per day. Three valves per vessel, as labeled in Figure A-3, are used for venting to atmospheric pressure, evacuating to low pressure to remove the gas inside the vessel, and charging with oxygen. The oxygen feed valve isolates the POVs from the oxygen cylinder when closed.

Asphalt samples are prepared in aluminum trays. The dimensions of the tray are 7.0 cm (2.75 in) by 3.5 cm (1.38 in). Typical film thicknesses of less than 1 mm (0.039 in) are used to minimize potential diffusion problems at low pressure; however, diffusion studies may be performed with thicker films. After preparing the asphalt samples, loading the sample rack, and allowing the temperature in the POV to reach equilibrium, the operator places the rack inside the POV and bolts the cover flange to the top. The vent valves, oxygen feed valves, and vacuum valves are closed. A vacuum pump evacuates the air in the vessel to a pressure of 0.03 atm absolute. The vessels are slowly pressurized to the desired level by manipulating the oxygen cylinder regulator and oxygen feed valves for pure oxygen aging, or by slowly opening the atmospheric venting valve for aging with air (note 0.2 atm

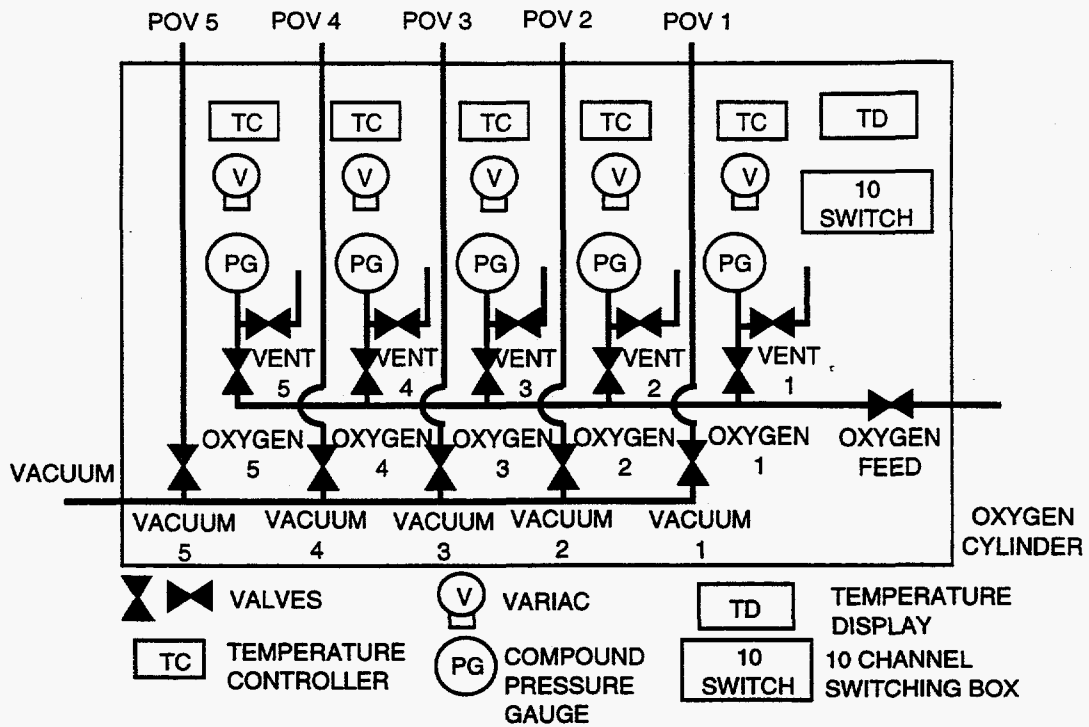


Figure A-3. Pressure Oxygen Vessel Control Panel

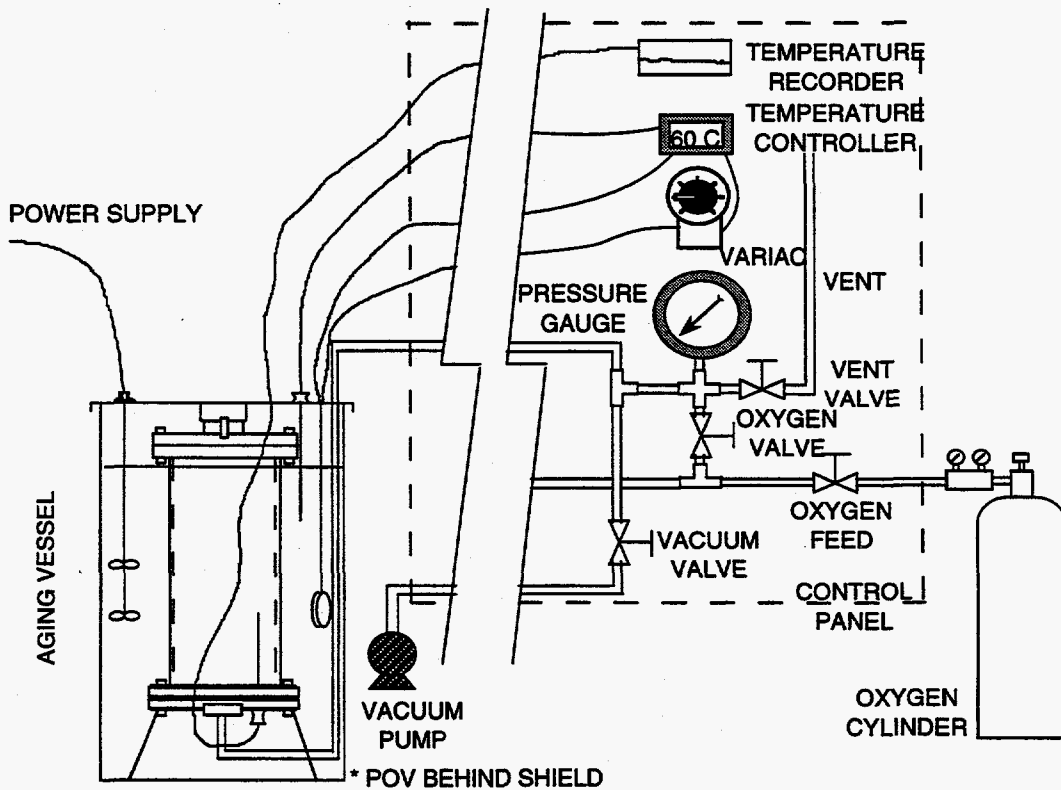


Figure A-4. Pressure Oxygen Vessel and Control Panel

oxygen is equivalent to atmospheric air aging). Once the desired oxygen pressure is reached, the cylinder, regulators, and feed valves are closed.

During the experiment, samples are periodically removed. To obtain samples, the pressure in the vessel is decreased by slowly venting off the oxygen to the atmosphere until the pressure gauge reads zero. The operator removes the top insulation, unbolts the cover flange, and collects the samples. Samples to be aged further are loaded back into the vessel, and the process is repeated. The aged samples are saved for chemical and physical analysis.

CORBETT ANALYSIS

A description of the traditional Corbett (1969) analysis can be found in the standard method ASTM D4124. However, detailed descriptions of the traditional Corbett analysis and the modifications used in this DOE effort can be found in Chapter 2. In addition, a brief description may be found in Chapter 5.

CORBETT ANALYSIS USING N-HEXANE PRECIPITATION AND HIGH PERFORMANCE LIQUID CHROMATOGRAPHY (HPLC)

As described by Pearson et al. (1986) asphalt or a similar sample is weighed to 0.2 ± 0.01 gram in a scintillation vial and mixed with 20 mL of n-hexane. The asphalt/n-hexane solution are then sonicated for 5 minutes to insure good mixing and set overnight. The asphaltenes are removed by filtering the solution through a dried preweighed $0.45 \mu\text{m}$ PTFE membrane syringe filter. After filtering, the filter is further dried in an oven at 100°C (212°F) for an hour and the filtered solution is analyzed using HPLC. The weight difference between the filter before and after filtering is the weight of the asphaltene and the asphaltene content is equal to the weight of asphaltene divided by the weight of the asphalt sample.

A detailed investigation into the use of HPLC for analyzing the saturate content of asphalt and related petroleum materials can be found in Chapter 5. The total aromatic content, the sum of the naphthene aromatic and polar aromatic contents, is determined by difference.

FOURIER TRANSFORM INFRARED SPECTROSCOPY (FTIR)

A Mattson Galaxy series 5020 Spectrometer at 4 cm^{-1} resolution and 64 scans is used to measure the infrared absorbance spectra of asphalt samples. In particular, the Attenuated Total Reflectance, ATR, method with a Zinc Selenide prism is used (Jemison et al., 1992). To quantify the changes in the spectra, the carbonyl content is defined as the integrated absorbance from 1820 to 1650 cm^{-1} with respect to the baseline at the absorbance of 1820 cm^{-1} . This area is called the Carbonyl Area or CA. The range of wave numbers includes the following carbonyl compounds: esters, ketones, aldehydes, and carboxylic acids. The primary absorbance peak for the oxidized asphalt is located at 1700 cm^{-1} and corresponds to ketone formation.

At low aging pressures of 2 and 0.2 atm oxygen and for thick ($\approx 1\text{mm}$) films, oxygen diffusion may be significant. To partially eliminate this diffusion problem, only the exposed surface, ES, of the film is analyzed for kinetic data. For analysis, a quarter of the material in the aluminum tray is removed and the ES placed on the prism face. For samples that have been aged in thinner films, diffusion is probably not significant, so it is possible to measure the spectra of a stirred sample. To insure good contact at the sample/prism interface, the sample is compressed. Heating of the sample is avoided, if possible.

For measuring the spectrum of asphaltenes, the material is dissolved in THF and the solution deposited on the ATR prism drop by drop allowing the THF to evaporate. When the film on the prism is sufficiently thick it is further dried with a heat gun.

DYNAMIC MECHANICAL ANALYSIS (DMA)

The rheological properties of neat and aged asphalt are measured using a Carri-Med 500 Controlled Stress Rheometer. The primary property of interest is the low frequency limiting complex viscosity, η_0^* . This limiting value of the viscosity is obtained at the point where the viscosity of the material becomes independent of frequency or shear rate (Lau et al., 1992). For the more viscous materials (most of the materials), a 2.5 cm (1 in) parallel plate geometry with a 0.5 mm (0.02 in) gap is used at temperatures above 60°C and a 1.5 cm parallel plate is used at

temperatures below 40°C. For low viscosity materials several sizes of cone-and-plate geometry may be used. For materials for which the limiting viscosity can not be obtained at the measurement temperature of interest, additional measurements are performed at elevated temperature. The data are then manipulated according to the time-temperature superposition principle, as described by Ferry (1985) and η_0^* can be calculated.

GEL PERMEATION CHROMATOGRAPHY (GPC)

A WATERS 600E multisolvent delivery system is utilized for gel permeation chromatography (GPC) analyses. Injection is accomplished with a WATERS 700 WISP autoinjector. A WATERS 410 differential refractometer (RI) is utilized for sample detection. Data acquisition and processing are performed using Baseline 810 software.

For GPC analyses, helium-sparged HPLC grade tetrahydrofuran (THF) is used as the mobile phase at a flow rate of 1 mL/min. Three columns of decreasing pore size of 1000, 100, and 50 Å are utilized in series to accomplish separation. The 1000 and 100 Å columns are 7.8 mm ID × 300 mm long and are packed with 7 μm ultrastyrigel particles. The 50 Å column is 7.8 mm ID × 600 mm long and is packed with 5 μm PLGel particles. Samples are prepared by dissolving 0.2 ± 0.01 g of sample in 10 mL of THF. The samples are then filtered through 0.45 μm PTFE membrane syringe filters and 100 μL aliquots are injected onto the columns. Samples are analyzed within 2 days of preparation to reduce potential solvent aging (Burr et al., 1991). Molecular weight distributions are then determined from calibration with polystyrene standards at a concentration of 0.025 g/mL. This is possible because the retention times for the asphalt samples are in the range of the PS standards. The columns and detector are operated isothermally at 313.2 K.

MICRODUCTILITY MEASUREMENTS

A detailed description of the microductility measurements can be found in Chapter 9.

APPENDIX B

DOE - OIT SPREADSHEETS

**Economic Analysis for a
ROSE Supercritical Unit for Producing
Superior Asphalt or Recycling Agent**

OIT Project Benefit Analysis Worksheet Version 2.1

Project Name:

Dvlopmnt of Superior Asphalt Recycling Agents

Filename:

saf95_4.xls

Analyst:

Charles Glover

This system of spreadsheets was developed to aid in the financial, market, and benefit analysis of OIT projects. The user is asked for a number of inputs relating to both the new and existing technologies for a certain project, such as: capital costs, annual costs, energy use, waste reduction, equipment lifetime, discount rate and market information. The system will calculate the following project statistics: initial capital investment, total annual costs, project financial information, market penetration information, net energy savings and net waste reduction. The spreadsheets are designed in such a way that the user can change information in the cells with green text only. The cells with red text contain formulas and are locked.

Industrial Partner: Texas Department of Transportation

ROSE unit for producing recycling agent/superior asphalt. The installed cost of a ROSE unit is \$30 million for a 10,000 bbl/day recycling agent produced. At 330 operating days/yr, this is \$9.09/bbl of RA (capital investment). The annualized cost of producing the recycling agent is \$2.36/bbl of RA (excluding energy costs) less an assumed sales price of \$6.25/bbl. The energy savings is a loss due to the energy cost of processing the RA. This is calculated according to 100,000 Btu/bbl of feed and 330 operating days/yr for the 30,000 bbl/day of feed unit which produces 10,000 bbl/day of RA. The energy cost is entered in the energy savings worksheet. These assumptions give an internal rate of return of 26% and a discounted payback period of 4.4 years. The energy use for this process is 990,000 million Btu/yr (100,000 Btu/Bbl of feed, 30,000 Bbl of feed/day, and 330 operating days/yr).

4/2/96

Sheet A

Capital Investment Worksheet

Development of Superior Asphalt Recycling Agents

	Conventional Unit	New Unit	Incremental Capital Costs	Incremental Savings	Net Cost Increment
1 First Cost of Equipment	\$ -	\$ -	\$ -	\$ -	\$ -
2 Site Preparation and Engineering	\$ -	\$ -	\$ -	\$ -	\$ -
3 Installation	\$ -	\$ -	\$ -	\$ -	\$ -
4 Contingency Allowance	\$ -	\$ -	\$ -	\$ -	\$ -
5 Construction Indirect Costs	\$ -	\$ -	\$ -	\$ -	\$ -
6 Interest During Construction	\$ -	\$ -	\$ -	\$ -	\$ -
7 Start-up Expenses	\$ -	\$ -	\$ -	\$ -	\$ -
8 Working Capital	\$ -	\$ -	\$ -	\$ -	\$ -
9 Other:	\$ -	\$ 30,000,000	\$ 30,000,000	\$ -	\$ 30,000,000
10 TOTAL: Initial Capital Investment	\$ -	\$ 30,000,000	\$ 30,000,000	\$ -	\$ 30,000,000

Costs should be entered in 1994 dollars.

Equipment Cost Index			
1986	797.6	1991	930.6
1987	813.6	1992	943.1
1988	852.0	1993	964.2
1989	895.1	1994	993.4
1990	915.1	1995	1015.3

Source: Marshall & Swift Equipment Cost Index
 Chemical Engineering Magazine; McGraw-Hill, Inc. New York, NY.
 (1995 index is estimated.)

Sheet B

Annual (non-energy) Cost Worksheet

Development of Superior Asphalt Recycling Agents

	Annual Cost Component	Conventional Unit	New Unit	Incremental Annual Costs	Incremental Savings	Net Cost Increment
1	Payroll plus Labor Indirects			\$ -	\$ -	\$ -
2	Operating Supplies		\$ -	\$ -	\$ -	\$ -
3	Maintenance Supplies	\$ -	\$ -	\$ -	\$ -	\$ -
4	Transportation	\$ -	\$ -	\$ -	\$ -	\$ -
5	Pollution Control and Waste Disposal			\$ -	\$ -	\$ -
6	Other Costs/Credits	\$ -	\$ (12,837,000)	\$ -	\$ 12,837,000	\$ (12,837,000)
7	TOTAL: Annual (non-energy) Costs	\$ -	\$ (12,837,000)	\$ -	\$ 12,837,000	\$ (12,837,000)

Costs should be entered in 1994 dollars.

Sheet C

Energy Savings Worksheet

	Annual Unit Energy Use (Million Btu/year)		Net Energy Saved
	Conventional Technology	New Technology	
1	Distillate Oil	990,000	(990,000)
2	Residual Oil	-	-
3	Natural Gas	-	-
4	Propane	-	-
5	Gasoline	-	-
6	Coking Coal	-	-
7	Steam Coal	-	-
8	Electricity	-	-
9	Other	-	-
10	Use by Others	-	-
11	TOTAL	990,000	(990,000)

Express end-use electricity use as primary equivalent (10,500 Btu/kWh)

Energy Savings: Only net savings were provided for the analysis.

Development of Superior Asphalt Recycling Agents

	1994 Fuel Prices (\$ per million Btu)		Default 1994 Fuel Prices* (\$ per million Btu)	
12	Distillate Oil	4.12	Distillate Oil	4.12
13	Residual Oil	2.35	Residual Oil	2.35
14	Natural Gas	2.96	Natural Gas	2.96
15	Propane	5.66	Propane	5.66
16	Gasoline	5.89	Gasoline	5.89
17	Coking Coal	1.53	Coking Coal	1.53
18	Steam Coal	1.36	Steam Coal	1.36
19	Electricity	4.50	Electricity	4.50
20	Other	2.00	Other	2.00

* Source: Energy Information Administration, Monthly Energy Review, April 1995; Energetics, Inc. estimates.

Sheet D

Waste Reduction Worksheet

	Annual Unit Waste Production (Tons/Year)		Net Waste Reduction
	Conventional Technology	New Technology	
<u>Non-combustion Related</u>			
1	Non-hazardous (RCRA)	-	-
2	Toxic (TRI)	-	-
3	Hazardous (non-TRI)	-	-
4	CFCs	-	-
5	VOCs	-	-
6	SHH	-	-
7	Other 2	-	-
8	Other 3	-	-
9	Other 4	-	-
<u>Combustion Related</u>			
10	Particulates	-	5 (5)
11	VOCs	-	1 (1)
12	Sulfur Dioxides	-	79 (79)
13	Nitrogen Oxides	-	69 (69)
14	Carbon Dioxide	-	79,695 (79,695)
15	TOTAL	-	79,849.4 (79,849.4)

SHH = Solid, hydrocarbon/organic, regulated under hazardous.

Development of Superior Asphalt Recycling Agents

Combustion Emission Rates (lbs/million Btu)						
	Particulates	VOCs	SOx	NOx	CO2	
16	Distillate Oil	0.010	0.002	0.160	0.140	161.000
17	Residual Oil	0.080	0.009	1.700	0.370	161.000
18	Natural Gas	0.003	0.006	0.000	0.140	113.000
19	Propane	0.003	0.006	0.000	0.140	113.000
20	Gasoline	0.000	0.090	0.000	0.140	162.000
21	Coking Coal	0.720	0.005	2.500	0.950	208.000
22	Steam Coal	0.720	0.005	2.500	0.950	208.000
23	Electricity	0.400	0.004	1.450	0.550	134.000
24	Other 1					

Electricity use expressed as primary equivalent (10,500 Btu/kWh)

Sheet E

Financial Worksheet**Unit Technology Inputs**

1	Discount rate:	10%
2	Equipment lifetime (yrs.):	10
3	Initial capital investment:	\$30,000,000
4	Annual costs:	(\$12,837,000)

Development of Superior Asphalt Recycling Agents

User's Unit Summary Financial Results

5	Annual energy income:	-\$4,078,800
6	Annual net income:	\$8,758,200
7	Total Life Cycle Cost:	\$30,000,000
8	Total Life Cycle Benefit:	\$53,815,348
9	Net Present Value:	\$23,815,348
10	Benefit-Cost Ratio:	1.79
11	Internal Rate of Return:	26.39%
12	Rate of Return:	29.19%
13	Uniform Capital Recovery Factor:	0.1627
14	Levelized Cost of Energy (per mil. Btu):	\$8.03
15	Annual Production Cost Savings:	\$3,875,838
16	Discounted Payback Period:	4.42

Express cost inputs as 1994\$

Sheet F

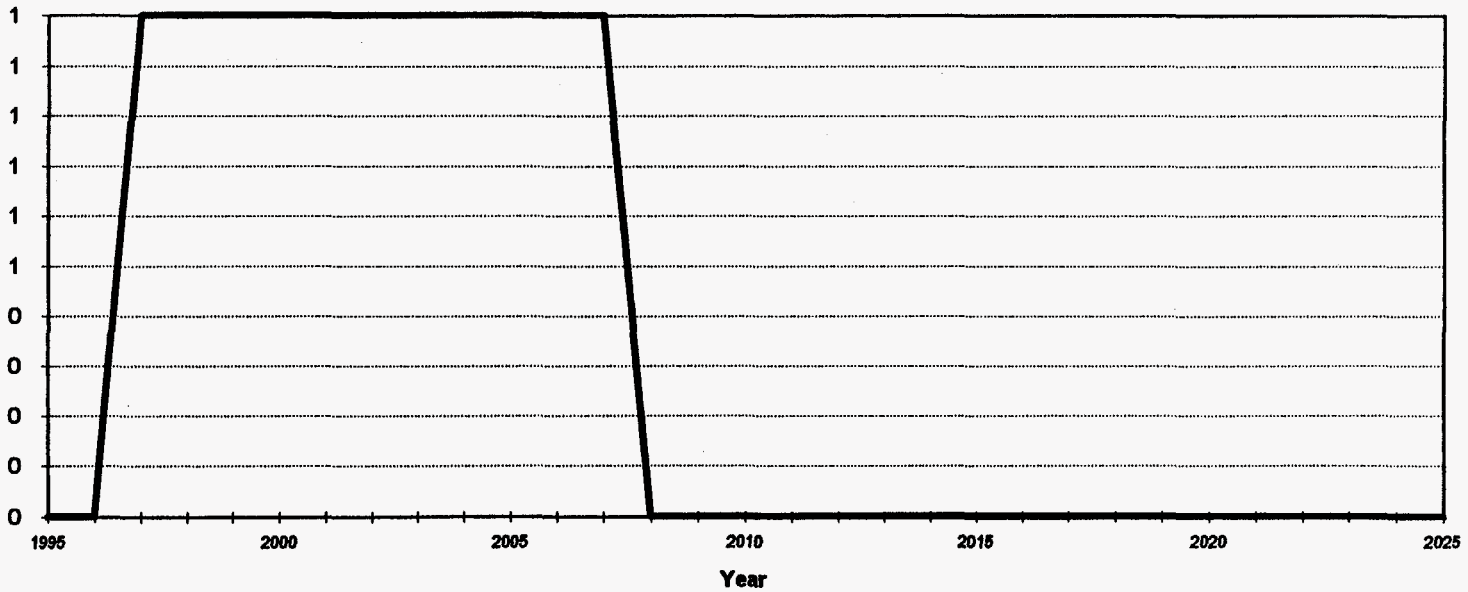
Market Penetration Worksheet

Development of Superior Asphalt Recycling Agents

Inputs		
1	Hurdle rate IRR (%):	25%
2	Year of introduction:	1997
3	Number of units at introduction:	1
4	Total potential market (# units):	1
5	Maximum market penetration (fraction):	1.00
6	Number of years at market saturation:	10

Market Penetration		
25	Internal Rate of Return:	26%
28	Market share at introduction:	100%

Number of Units in Operation



150

Sheet G

Market Penetration Results

Development of Superior Asphalt Recycling Agents

	Year	Units in Operation	Energy Savings million Btu/year	Waste Reduction tons/year	Prod. Cost Savings (\$/Year)
1	1995	-	-	-	-
2	1996	-	-	-	-
3	1997	1	-990,000	-79,849	3,875,838
4	1998	1	-990,000	-79,849	3,875,838
5	1999	1	-990,000	-79,849	3,875,838
6	2000	1	-990,000	-79,849	3,875,838
7	2001	1	-990,000	-79,849	3,875,838
8	2002	1	-990,000	-79,849	3,875,838
9	2003	1	-990,000	-79,849	3,875,838
10	2004	1	-990,000	-79,849	3,875,838
11	2005	1	-990,000	-79,849	3,875,838
12	2006	1	-990,000	-79,849	3,875,838
13	2007	1	-990,000	-79,849	3,875,838
14	2008	0	0	0	0
15	2009	0	0	0	0
16	2010	0	0	0	0
17	2011	0	0	0	0
18	2012	0	0	0	0
19	2013	0	0	0	0
20	2014	0	0	0	0
21	2015	0	0	0	0
22	2016	0	0	0	0
23	2017	0	0	0	0
24	2018	0	0	0	0
25	2019	0	0	0	0
26	2020	0	0	0	0
27	2021	0	0	0	0
28	2022	0	0	0	0
29	2023	0	0	0	0
30	2024	0	0	0	0
31	2025	0	0	0	0

	Year	Number of Units in Operation	Energy Savings by Fuel Type (million Btus)					
			Distillate Oil	Residual Oil	Natural Gas	Propane	Gasoline	Coking Coal
1	1990	-	-	-	-	-	-	-
2	1995	-	-	-	-	-	-	-
3	2000	1	(990,000)	-	-	-	-	-
4	2005	1	(990,000)	-	-	-	-	-
5	2010	-	-	-	-	-	-	-
6	2015	-	-	-	-	-	-	-
7	2020	-	-	-	-	-	-	-
8	2025	-	-	-	-	-	-	-

	Year	Number of Units in Operation	Steam Coal	Electricity	Other	Total Energy Savings	
						million Btus	1994 \$
9	1990	-	-	-	-	-	-
10	1995	-	-	-	-	-	-
11	2000	1	-	-	-	(990,000)	(4,078,800)
12	2005	1	-	-	-	(990,000)	(4,078,800)
13	2010	-	-	-	-	-	-
14	2015	-	-	-	-	-	-
15	2020	-	-	-	-	-	-
16	2025	-	-	-	-	-	-

Year	Number of Units In Operation	Waste Reduction by Waste Type (tons) ***** Non-Combustion Related *****								
		Non-hazardous (RCRA)	Toxic (TRI)	Hazardous (non-TRI)	CFCs	VOCs	SHH	Other 2	Other 3	Other 4
1 1990	-	-	-	-	-	-	-	-	-	-
2 1995	-	-	-	-	-	-	-	-	-	-
3 2000	1	-	-	-	-	-	-	-	-	-
4 2005	1	-	-	-	-	-	-	-	-	-
5 2010	-	-	-	-	-	-	-	-	-	-
6 2015	-	-	-	-	-	-	-	-	-	-
7 2020	-	-	-	-	-	-	-	-	-	-
8 2025	-	-	-	-	-	-	-	-	-	-

Year	Number of Units In Operation	Waste Reduction by Waste Type (tons) ***** Combustion Related *****					TOTAL WASTE REDUCTION (tons)
		Particulates	VOCs	Sulfur Dioxides	Nitrogen Oxides	Carbon Dioxide	
9 1990	-	-	-	-	-	-	-
10 1995	-	-	-	-	-	-	-
11 2000	1	(5)	(1)	(79)	(69)	(79,695)	(79,849)
12 2005	1	(5)	(1)	(79)	(69)	(79,695)	(79,849)
13 2010	-	-	-	-	-	-	-
14 2015	-	-	-	-	-	-	-
15 2020	-	-	-	-	-	-	-
16 2025	-	-	-	-	-	-	-

**Economic Comparison of a
Conventional Asphalt, 12-Year Pavement
with a
Superior Asphalt, 15-Year Pavement**

OIT Project Benefit Analysis Worksheet Version 2.1

Project Name:

Dvlopmnt of Superior Asphalt Recycling Agents

Filename:

saf95_1.xls

Analyst:

Charles Glover

This system of spreadsheets was developed to aid in the financial, market, and benefit analysis of OIT projects. The user is asked for a number of inputs relating to both the new and existing technologies for a certain project, such as: capital costs, annual costs, energy use, waste reduction, equipment lifetime, discount rate and market information. The system will calculate the following project statistics: initial capital investment, total annual costs, project financial information, market penetration information, net energy savings and net waste reduction. The spreadsheets are designed in such a way that the user can change information in the cells with green text only. The cells with red text contain formulas and are locked.

Industrial Partner: Texas Department of Transportation

Comparison between a) a conventional pavement placement (having an assumed life of 12 years) with b) a superior asphalt pavement placement (with an assumed life of 15 years). Also, it is assumed that the baseline annual maintenance cost in both cases equals the (total capital cost)/(yrs service)/4. In addition to this baseline cost, the conventional pavement has added cost of replacement (2 years capital cost prorated over the 15 years). Under these assumptions, the internal rate of return is 36.5% and the discounted payback period is 3.3 years.

4/2/96

Sheet A

Capital Investment Worksheet

Development of Superior Asphalt Recycling Agents

	Conventional Unit	New Unit	Incremental Capital Costs	Incremental Savings	Net Cost Increment
1 First Cost of Equipment	\$ 31,883	\$ 37,606	\$ 5,723	\$ -	\$ 5,723
2 Site Preparation and Engineering	\$ -	\$ -	\$ -	\$ -	\$ -
3 Installation	\$ 66,217	\$ 66,217	\$ -	\$ -	\$ -
4 Contingency Allowance	\$ -	\$ -	\$ -	\$ -	\$ -
5 Construction Indirect Costs	\$ -	\$ -	\$ -	\$ -	\$ -
6 Interest During Construction	\$ -	\$ -	\$ -	\$ -	\$ -
7 Start-up Expenses	\$ -	\$ -	\$ -	\$ -	\$ -
8 Working Capital	\$ -	\$ -	\$ -	\$ -	\$ -
9 Other:	\$ -	\$ -	\$ -	\$ -	\$ -
10 TOTAL: Initial Capital Investment	\$ 98,100	\$ 103,823	\$ 5,723	\$ -	\$ 5,723

Costs should be entered in 1994 dollars.

Equipment Cost Index			
1986	797.6	1991	930.6
1987	813.6	1992	943.1
1988	852.0	1993	964.2
1989	895.1	1994	993.4
1990	915.1	1995	1015.3

Source: Marshall & Swift Equipment Cost Index
 Chemical Engineering Magazine; McGraw-Hill, Inc. New York, NY.
 (1995 index is estimated.)

Sheet B

Annual (non-energy) Cost Worksheet

Dvlopmt of Superior Asphalt Recycling Agents

	Annual Cost Component	Conventional Unit	New Unit	Incremental Annual Costs	Incremental Savings	Net Cost Increment
1	Payroll plus Labor Indirects			\$ -	\$ -	\$ -
2	Operating Supplies		\$ -	\$ -	\$ -	\$ -
3	Maintenance Supplies	\$ -	\$ -	\$ -	\$ -	\$ -
4	Transportation	\$ -	\$ -	\$ -	\$ -	\$ -
5	Pollution Control and Waste Disposal			\$ -	\$ -	\$ -
6	Other Costs/Credits	\$ 3,678	\$ 1,730	\$ -	\$ 1,948	\$ (1,948)
7	TOTAL: Annual (non-energy) Costs	\$ 3,678	\$ 1,730	\$ -	\$ 1,948	\$ (1,948)

Costs should be entered in 1994 dollars.

Sheet C

Energy Savings Worksheet

	Annual Unit Energy Use (Million Btu/year)		Net Energy Saved
	Conventional Technology	New Technology	
	1 Distillate Oil	-	
2 Residual Oil	-	-	-
3 Natural Gas	-	-	-
4 Propane	-	-	-
5 Gasoline	-	-	-
6 Coking Coal	545	436	109
7 Steam Coal	-	-	-
8 Electricity	-	-	-
9 Other	-	-	-
10 Use by Others	-	-	-
11 TOTAL	545	436	109

Express end-use electricity use as primary equivalent (10,500 Btu/kWh)

Energy Savings: Only net savings were provided for the analysis.

Development of Superior Asphalt Recycling Agents

1994 Fuel Prices (\$ per million Btu)		Default 1994 Fuel Prices* (\$ per million Btu)	
12 Distillate Oil	4.12	Distillate Oil	4.12
13 Residual Oil	2.35	Residual Oil	2.35
14 Natural Gas	2.96	Natural Gas	2.96
15 Propane	5.66	Propane	5.66
16 Gasoline	5.89	Gasoline	5.89
17 Coking Coal	1.53	Coking Coal	1.53
18 Steam Coal	1.36	Steam Coal	1.36
19 Electricity	4.50	Electricity	4.50
20 Other	2.00	Other	2.00

* Source: Energy Information Administration,
Monthly Energy Review, April 1995; Energetics, Inc.
estimates.

Sheet D

Waste Reduction Worksheet

	Annual Unit Waste Production (Tons/Year)		Net Waste Reduction	
	Conventional Technology	New Technology		
<u>Non-combustion Related</u>				
1	Non-hazardous (RCRA)	273	218	55
2	Toxic (TRI)	-	-	-
3	Hazardous (non-TRI)	-	-	-
4	CFCs	-	-	-
5	VOCs	-	-	-
6	SHH	-	-	-
7	Other 2	-	-	-
8	Other 3	-	-	-
9	Other 4	-	-	-
<u>Combustion Related</u>				
10	Particulates	0	0	0
11	VOCs	0	0	0
12	Sulfur Dioxides	1	1	0
13	Nitrogen Oxides	0	0	0
14	Carbon Dioxide	57	45	11
15	TOTAL	330.8	264.3	66.6

SHH = Solid, hydrocarbon/organic, regulated under hazardous.

Development of Superior Asphalt Recycling Agents

Combustion Emission Rates (lbs/million Btu)						
	Particulates	VOCs	SOx	NOx	CO2	
16	Distillate Oil	0.010	0.002	0.160	0.140	161.000
17	Residual Oil	0.080	0.009	1.700	0.370	161.000
18	Natural Gas	0.003	0.006	0.000	0.140	113.000
19	Propane	0.003	0.006	0.000	0.140	113.000
20	Gasoline	0.000	0.090	0.000	0.140	162.000
21	Coking Coal	0.720	0.005	2.500	0.950	208.000
22	Steam Coal	0.720	0.005	2.500	0.950	208.000
23	Electricity	0.400	0.004	1.450	0.550	134.000
24	Other 1					

Electricity use expressed as primary equivalent (10,500 Btu/kWh)

Sheet E

Financial Worksheet**Unit Technology Inputs**

1	Discount rate:	10%
2	Equipment lifetime (yrs.):	14
3	Initial capital investment:	\$5,723
4	Annual costs:	(\$1,948)

Dvlopmt of Superior Asphalt Recycling Agents

User's Unit Summary Financial Results

5	Annual energy income:	\$167
6	Annual net income:	\$2,115
7	Total Life Cycle Cost:	\$5,723
8	Total Life Cycle Benefit:	\$15,579
9	Net Present Value:	\$9,856
10	Benefit-Cost Ratio:	2.72
11	Internal Rate of Return:	36.48%
12	Rate of Return:	36.95%
13	Uniform Capital Recovery Factor:	0.1357
14	Levelized Cost of Energy (per mil. Btu):	-\$10.74
15	Annual Production Cost Savings:	\$1,338
16	Discounted Payback Period:	3.33

Express cost inputs as 1994\$

Sheet F

Market Penetration Worksheet

Development of Superior Asphalt Recycling Agents

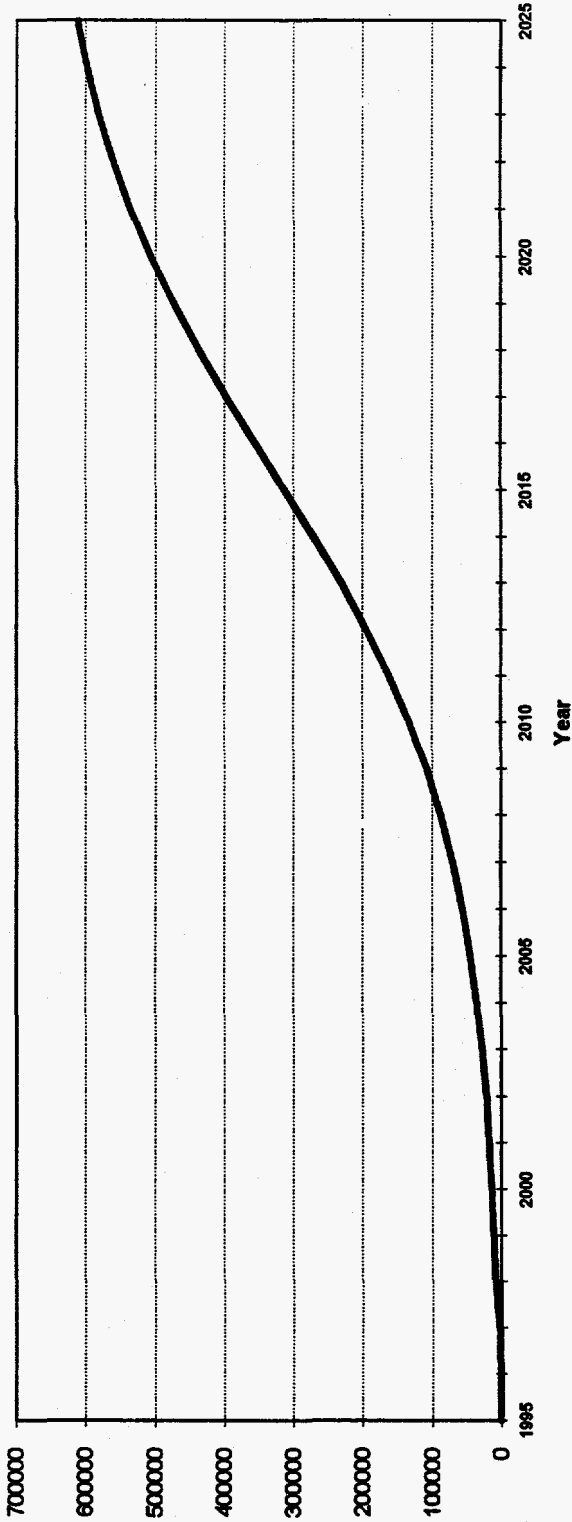
Inputs	
Hurdle rate IRR (%):	25%
Year of introduction:	1997
Number of units at introduction:	2000
Total potential market (# units):	2,000,000.00
Maximum market penetration (fraction):	0.33
Number of years at market saturation:	10

- 1
- 2
- 3
- 4
- 5
- 6

Market Penetration	
Internal Rate of Return:	38%
Market share at introduction:	0%

- 25
- 26

Number of Units in Operation



Sheet G

Market Penetration Results

Development of Superior Asphalt Recycling Agents

	Year	Units in Operation	Energy Savings <i>million Btu/year</i>	Waste Reduction <i>tons/year</i>	Prod. Cost Savings <i>(\$/Year)</i>
1	1995	-	-	-	-
2	1996	-	-	-	-
3	1997	2000	218,000	133,127	2,675,789
4	1998	7725	842,025	514,203	10,335,234
5	1999	9929	1,082,261	660,909	13,283,953
6	2000	12749	1,389,641	848,619	17,056,815
7	2001	16351	1,782,259	1,088,380	21,875,911
8	2002	20937	2,282,133	1,393,641	28,011,494
9	2003	26757	2,916,513	1,781,041	35,798,040
10	2004	34109	3,717,881	2,270,416	45,634,239
11	2005	43344	4,724,496	2,885,130	57,989,693
12	2006	54862	5,979,958	3,651,809	73,399,561
13	2007	69102	7,532,118	4,599,674	92,451,176
14	2008	86514	9,430,026	5,758,678	115,746,593
15	2009	107523	11,720,007	7,157,111	143,854,416
16	2010	132468	14,439,012	8,817,539	177,228,191
17	2011	161526	17,608,334	10,751,742	216,104,725
18	2012	194634	21,215,106	12,955,528	260,399,732
19	2013	231414	25,224,126	15,403,734	309,607,486
20	2014	271146	29,554,914	18,048,437	362,764,705
21	2015	312791	34,094,219	20,820,475	418,481,316
22	2016	355080	38,703,720	23,635,381	475,059,531
23	2017	396665	43,236,485	26,403,426	530,695,868
24	2018	436286	47,555,174	29,040,740	583,704,581
25	2019	472916	51,547,844	31,478,962	632,711,651
26	2020	505850	55,137,650	33,671,165	676,773,864
27	2021	534725	58,285,025	35,593,188	715,405,564
28	2022	559490	60,984,410	37,241,634	748,538,518
29	2023	580332	63,256,188	38,628,951	776,422,912
30	2024	597594	65,137,746	39,777,971	799,517,645
31	2025	611703	66,675,627	40,717,116	818,393,996

Total Energy Savings

Year	Number of Units in Operation	Energy Savings by Fuel Type (million Btus)					
		Distillate Oil	Residual Oil	Natural Gas	Propane	Gasoline	Coking Coal
1990	-	-	-	-	-	-	-
1995	-	-	-	-	-	-	-
2000	12,749	-	-	-	-	-	1,389,641
2005	43,344	-	-	-	-	-	4,724,496
2010	132,468	-	-	-	-	-	14,439,012
2015	312,791	-	-	-	-	-	34,094,219
2020	505,850	-	-	-	-	-	55,137,650
2025	611,703	-	-	-	-	-	66,675,627

Year	Number of Units in Operation	Steam Coal	Electricity	Other	Total Energy Savings	
					million Btus	1994 \$
1990	-	-	-	-	-	-
1995	-	-	-	-	-	-
2000	12,749	-	-	-	1,389,641	2,126,151
2005	43,344	-	-	-	4,724,496	7,228,479
2010	132,468	-	-	-	14,439,012	22,091,688
2015	312,791	-	-	-	34,094,219	52,164,155
2020	505,850	-	-	-	55,137,650	84,360,605
2025	611,703	-	-	-	66,675,627	102,013,709

Total Waste Reduction

Dvlopmt of Superior Asphalt Recycling Agents

Year	Number of Units In Operation	Waste Reduction by Waste Type (tons)								
		***** Non-Combustion Related *****								
		Non-hazardous (RCRA)	Toxic (TRI)	Hazardous (non-TRI)	CFCs	VOCs	SHH	Other 2	Other 3	Other 4
1 1990	-	-	-	-	-	-	-	-	-	-
2 1995	-	-	-	-	-	-	-	-	-	-
3 2000	12,749	701,195	-	-	-	-	-	-	-	-
4 2005	43,344	2,383,920	-	-	-	-	-	-	-	-
5 2010	132,468	7,285,740	-	-	-	-	-	-	-	-
6 2015	312,791	17,203,505	-	-	-	-	-	-	-	-
7 2020	505,850	27,821,750	-	-	-	-	-	-	-	-
8 2025	611,703	33,843,665	-	-	-	-	-	-	-	-

Year	Number of Units In Operation	Waste Reduction by Waste Type (tons)					TOTAL WASTE REDUCTION (tons)
		***** Combustion Related *****					
		Particulates	VOCs	Sulfur Dioxides	Nitrogen Oxides	Carbon Dioxide	
9 1990	-	-	-	-	-	-	-
10 1995	-	-	-	-	-	-	-
11 2000	12,749	500	3	1,737	660	144,523	848,619
12 2005	43,344	1,701	12	5,906	2,244	491,348	2,885,130
13 2010	132,468	5,198	36	18,049	6,859	1,501,657	8,817,539
14 2015	312,791	12,274	85	42,618	16,195	3,545,799	20,820,475
15 2020	505,850	19,850	138	68,922	26,190	5,734,316	33,671,165
16 2025	611,703	24,003	167	83,345	31,671	6,934,265	40,717,116

**Economic Comparison of a
Conventional Asphalt, 12-Year Pavement
with a
Superior Asphalt, 18-Year Pavement**

OIT Project Benefit Analysis Worksheet Version 2.1

Project Name:

Dvlopmnt of Superior Asphalt Recycling Agents

Filename:

saf95_a.xls

Analyst:

Charles Glover

This system of spreadsheets was developed to aid in the financial, market, and benefit analysis of OIT projects. The user is asked for a number of inputs relating to both the new and existing technologies for a certain project, such as: capital costs, annual costs, energy use, waste reduction, equipment lifetime, discount rate and market information. The system will calculate the following project statistics: initial capital investment, total annual costs, project financial information, market penetration information, net energy savings and net waste reduction. The spreadsheets are designed in such a way that the user can change information in the cells with green text only. The cells with red text contain formulas and are locked.

Industrial Partner: Texas Department of Transportation

Comparison between a) a conventional pavement placement (having an assumed life of 12 years) with b) a superior asphalt pavement placement (with an assumed life of 18 years). Also, it is assumed that the baseline annual maintenance cost in both cases equals the (total capital cost)/(yrs service)/4. In addition to this baseline cost, the conventional pavement has added cost of replacement (6 years capital cost prorated over the 18 years). Under these assumptions, the internal rate of return is 63% and the discounted payback period is 1.8 years.

4/2/96

Sheet A

Capital Investment Worksheet

Dvlopmt of Superior Asphalt Recycling Agents

	Conventional Unit	New Unit	Incremental Capital Costs	Incremental Savings	Net Cost Increment
1 First Cost of Equipment	\$ 31,883	\$ 37,606	\$ 5,723	\$ -	\$ 5,723
2 Site Preparation and Engineering	\$ -	\$ -	\$ -	\$ -	\$ -
3 Installation	\$ 66,217	\$ 66,217	\$ -	\$ -	\$ -
4 Contingency Allowance	\$ -	\$ -	\$ -	\$ -	\$ -
5 Construction Indirect Costs	\$ -	\$ -	\$ -	\$ -	\$ -
6 Interest During Construction	\$ -	\$ -	\$ -	\$ -	\$ -
7 Start-up Expenses	\$ -	\$ -	\$ -	\$ -	\$ -
8 Working Capital	\$ -	\$ -	\$ -	\$ -	\$ -
9 Other:	\$ -	\$ -	\$ -	\$ -	\$ -
10 TOTAL: Initial Capital Investment	\$ 98,100	\$ 103,823	\$ 5,723	\$ -	\$ 5,723

Costs should be entered in 1994 dollars.

Equipment Cost Index			
1986	797.6	1991	930.6
1987	813.6	1992	943.1
1988	852.0	1993	964.2
1989	895.1	1994	993.4
1990	915.1	1995	1015.3

Source: Marshall & Swift Equipment Cost Index
 Chemical Engineering Magazine; McGraw-Hill, Inc. New York, NY.
 (1995 index is estimated.)

Sheet B

Annual (non-energy) Cost Worksheet

Development of Superior Asphalt Recycling Agents

	Annual Cost Component	Conventional Unit	New Unit	Incremental Annual Costs	Incremental Savings	Net Cost Increment
1	Payroll plus Labor Indirects			\$ -	\$ -	\$ -
2	Operating Supplies		\$ -	\$ -	\$ -	\$ -
3	Maintenance Supplies	\$ -	\$ -	\$ -	\$ -	\$ -
4	Transportation	\$ -	\$ -	\$ -	\$ -	\$ -
5	Pollution Control and Waste Disposal			\$ -	\$ -	\$ -
6	Other Costs/Credits	\$ 4,770	\$ 1,440	\$ -	\$ 3,330	\$ (3,330)
7	TOTAL: Annual (non-energy) Costs	\$ 4,770	\$ 1,440	\$ -	\$ 3,330	\$ (3,330)

Costs should be entered in 1994 dollars.

Sheet C

Energy Savings Worksheet

Dvlopmt of Superior Asphalt Recycling Agents

169

	Annual Unit Energy Use (Million Btu/year)		Net Energy Saved
	Conventional Technology	New Technology	
	1 Distillate Oil	-	
2 Residual Oil	-	-	-
3 Natural Gas	-	-	-
4 Propane	-	-	-
5 Gasoline	-	-	-
6 Coking Coal	545	363	182
7 Steam Coal	-	-	-
8 Electricity	-	-	-
9 Other	-	-	-
10 Use by Others	-	-	-
11 TOTAL	545	363	182

	1994 Fuel Prices (\$ per million Btu)		Default 1994 Fuel Prices* (\$ per million Btu)	
	12 Distillate Oil	4.12	Distillate Oil	4.12
13 Residual Oil	2.35	Residual Oil	2.35	
14 Natural Gas	2.96	Natural Gas	2.96	
15 Propane	5.66	Propane	5.66	
16 Gasoline	5.89	Gasoline	5.89	
17 Coking Coal	1.53	Coking Coal	1.53	
18 Steam Coal	1.36	Steam Coal	1.36	
19 Electricity	4.50	Electricity	4.50	
20 Other	2.00	Other	2.00	

Express end-use electricity use as primary equivalent (10,500 Btu/kWh)

Energy Savings: Only net savings were provided for the analysis.

* Source: Energy Information Administration, Monthly Energy Review, April 1995; Energetics, Inc. estimates.

Sheet D

Waste Reduction Worksheet

	Annual Unit Waste Production (Tons/Year)		Net Waste Reduction
	Conventional Technology	New Technology	
<u>Non-combustion Related</u>			
1 Non-hazardous (RCRA)	273	182	91
2 Toxic (TRI)	-	-	-
3 Hazardous (non-TRI)	-	-	-
4 CFCs	-	-	-
5 VOCs	-	-	-
6 SHH	-	-	-
7 Other 2	-	-	-
8 Other 3	-	-	-
9 Other 4	-	-	-
<u>Combustion Related</u>			
10 Particulates	0	0	0
11 VOCs	0	0	0
12 Sulfur Dioxides	1	0	0
13 Nitrogen Oxides	0	0	0
14 Carbon Dioxide	57	38	19
15 TOTAL	330.8	220.5	110.3

SHH = Solid, hydrocarbon/organic, regulated under hazardous.

Development of Superior Asphalt Recycling Agents

Combustion Emission Rates (lbs/million Btu)					
	Particulates	VOCs	SOx	NOx	CO2
16 Distillate Oil	0.010	0.002	0.160	0.140	161.000
17 Residual Oil	0.080	0.009	1.700	0.370	161.000
18 Natural Gas	0.003	0.006	0.000	0.140	113.000
19 Propane	0.003	0.006	0.000	0.140	113.000
20 Gasoline	0.000	0.090	0.000	0.140	162.000
21 Coking Coal	0.720	0.005	2.500	0.950	208.000
22 Steam Coal	0.720	0.005	2.500	0.950	208.000
23 Electricity	0.400	0.004	1.450	0.550	134.000
24 Other 1					

Electricity use expressed as primary equivalent (10,500 Btu/kWh)

Sheet E

Financial Worksheet**Unit Technology Inputs**

1	Discount rate:	10%
2	Equipment lifetime (yrs.):	18
3	Initial capital investment:	\$5,723
4	Annual costs:	(\$3,330)

Dvlopmt of Superior Asphalt Recycling Agents

User's Unit Summary Financial Results

5	Annual energy income:	\$278
6	Annual net income:	\$3,608
7	Total Life Cycle Cost:	\$5,723
8	Total Life Cycle Benefit:	\$29,594
9	Net Present Value:	\$23,871
10	Benefit-Cost Ratio:	5.17
11	Internal Rate of Return:	63.04%
12	Rate of Return:	63.05%
13	Uniform Capital Recovery Factor:	0.1219
14	Levelized Cost of Energy (per mil. Btu):	-\$14.46
15	Annual Production Cost Savings:	\$2,911
16	Discounted Payback Period:	1.84

Express cost inputs as 1994\$

Sheet F

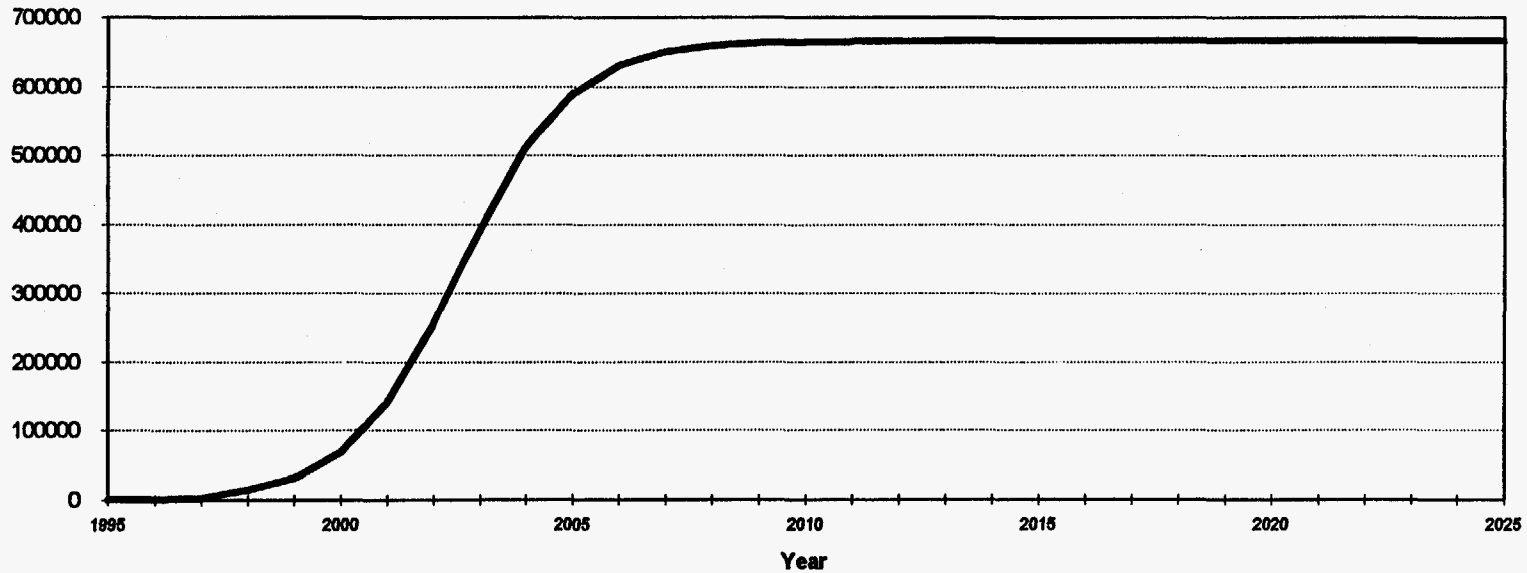
Market Penetration Worksheet

Development of Superior Asphalt Recycling Agents

Inputs		
1	Hurdle rate IRR (%):	25%
2	Year of introduction:	1997
3	Number of units at introduction:	2000
4	Total potential market (# units):	2,000,000.00
5	Maximum market penetration (fraction):	0.33
6	Number of years at market saturation:	10

Market Penetration		
25	Internal Rate of Return:	63%
26	Market share at introduction:	0%

Number of Units in Operation



Sheet G

Market Penetration Results

Dvlopmt of Superior Asphalt Recycling Agents

	Year	Units in Operation	Energy Savings million Btu/year	Waste Reduction tons/year	Prod. Cost Savings (\$/Year)
1	1995	-	-	-	-
2	1996	-	-	-	-
3	1997	2000	364,000	220,616	5,821,307
4	1998	13790	2,509,780	1,521,146	40,137,910
5	1999	31184	5,675,488	3,439,842	90,765,814
6	2000	68224	12,416,768	7,525,648	198,576,413
7	2001	139587	25,404,834	15,397,552	406,289,368
8	2002	253892	46,208,344	28,006,300	738,991,597
9	2003	392082	71,358,924	43,249,752	1,141,214,782
10	2004	512035	93,190,370	56,481,518	1,490,356,382
11	2005	589683	107,322,306	65,046,708	1,716,362,792
12	2006	630859	114,816,338	69,588,747	1,836,211,854
13	2007	650406	118,373,892	71,744,936	1,893,106,395
14	2008	659198	119,974,036	72,714,764	1,918,696,859
15	2009	663055	120,676,010	73,140,221	1,929,923,249
16	2010	664729	120,980,678	73,324,877	1,934,795,683
17	2011	665452	121,112,264	73,404,629	1,936,900,085
18	2012	665764	121,169,048	73,439,045	1,937,808,209
19	2013	665899	121,193,618	73,453,937	1,938,201,147
20	2014	665956	121,203,992	73,460,225	1,938,367,055
21	2015	665981	121,208,542	73,462,982	1,938,439,821
22	2016	665992	121,210,544	73,464,196	1,938,471,838
23	2017	665997	121,211,454	73,464,747	1,938,486,391
24	2018	665999	121,211,818	73,464,968	1,938,492,213
25	2019	665999	121,211,818	73,464,968	1,938,492,213
26	2020	666000	121,212,000	73,465,078	1,938,495,123
27	2021	666000	121,212,000	73,465,078	1,938,495,123
28	2022	666000	121,212,000	73,465,078	1,938,495,123
29	2023	666000	121,212,000	73,465,078	1,938,495,123
30	2024	666000	121,212,000	73,465,078	1,938,495,123
31	2025	666000	121,212,000	73,465,078	1,938,495,123

	Year	Number of Units in Operation	Energy Savings by Fuel Type (million Btus)					
			Distillate Oil	Residual Oil	Natural Gas	Propane	Gasoline	Coking Coal
1	1990	-	-	-	-	-	-	-
2	1995	-	-	-	-	-	-	-
3	2000	68,224	-	-	-	-	-	12,416,768
4	2005	589,683	-	-	-	-	-	107,322,306
5	2010	664,729	-	-	-	-	-	120,980,678
6	2015	665,981	-	-	-	-	-	121,208,542
7	2020	666,000	-	-	-	-	-	121,212,000
8	2025	666,000	-	-	-	-	-	121,212,000

	Year	Number of Units in Operation	Steam Coal	Electricity	Other	Total Energy Savings	
						million Btus	1994 \$
9	1990	-	-	-	-	-	-
10	1995	-	-	-	-	-	-
11	2000	68,224	-	-	-	12,416,768	18,997,655
12	2005	589,683	-	-	-	107,322,306	164,203,128
13	2010	664,729	-	-	-	120,980,678	185,100,437
14	2015	665,981	-	-	-	121,208,542	185,449,069
15	2020	666,000	-	-	-	121,212,000	185,454,360
16	2025	666,000	-	-	-	121,212,000	185,454,360

		Waste Reduction by Waste Type (tons)								
		***** Non-Combustion Related *****								
Year	Number of Units In Operation	Non-hazardous (RCRA)	Toxic (TRI)	Hazardous (non-TRI)	CFCs	VOCs	SHH	Other 2	Other 3	Other 4
1	1990	-	-	-	-	-	-	-	-	-
2	1995	-	-	-	-	-	-	-	-	-
3	2000	68,224	6,208,384	-	-	-	-	-	-	-
4	2005	589,683	53,661,153	-	-	-	-	-	-	-
5	2010	664,729	60,490,339	-	-	-	-	-	-	-
6	2015	665,981	60,604,271	-	-	-	-	-	-	-
7	2020	666,000	60,606,000	-	-	-	-	-	-	-
8	2025	666,000	60,606,000	-	-	-	-	-	-	-

		Waste Reduction by Waste Type (tons)					TOTAL WASTE REDUCTION (tons)
		***** Combustion Related *****					
Year	Number of Units In Operation	Particulates	VOCs	Sulfur Dioxides	Nitrogen Oxides	Carbon Dioxide	
9	1990	-	-	-	-	-	-
10	1995	-	-	-	-	-	-
11	2000	4,470	31	15,521	5,898	1,291,344	7,525,648
12	2005	38,636	268	134,153	50,978	11,161,520	65,046,708
13	2010	43,553	302	151,226	57,466	12,581,991	73,324,877
14	2015	43,635	303	151,511	57,574	12,605,688	73,462,982
15	2020	43,636	303	151,515	57,576	12,606,048	73,465,078
16	2025	43,636	303	151,515	57,576	12,606,048	73,465,078

**Economic Comparison of a
Conventional Asphalt, 12-Year Pavement
with a
Superior Asphalt, 24-Year Pavement**

OIT Project Benefit Analysis Worksheet Version 2.1

Project Name:

Dvlopmtnt of Superior Asphalt Recycling Agents

Filename:

saf95_b.xls

Analyst:

Charles Glover

This system of spreadsheets was developed to aid in the financial, market, and benefit analysis of OIT projects. The user is asked for a number of inputs relating to both the new and existing technologies for a certain project, such as: capital costs, annual costs, energy use, waste reduction, equipment lifetime, discount rate and market information. The system will calculate the following project statistics: initial capital investment, total annual costs, project financial information, market penetration information, net energy savings and net waste reduction. The spreadsheets are designed in such a way that the user can change information in the cells with green text only. The cells with red text contain formulas and are locked.

Industrial Partner: Texas Department of Transportation

Comparison between a) a conventional pavement placement (having an assumed life of 12 years) with b) a superior asphalt pavement placement (with an assumed life of 24 years). Also, it is assumed that the annual cost in both cases equals the (total capital cost)/(yrs service)/4. In addition to this baseline cost, the conventional pavement has added cost of replacement (12 years capital cost prorated over the 24 years). Under these assumptions, the internal rate of return is 95.5% and the discounted payback period is 1.2 years.

4/2/96

Sheet A

Capital Investment Worksheet

Dvlopmnt of Superior Asphalt Recycling Agents

	Conventional Unit	New Unit	Incremental Capital Costs	Incremental Savings	Net Cost Increment
1 First Cost of Equipment	\$ 31,883	\$ 37,806	\$ 5,723	\$ -	\$ 5,723
2 Site Preparation and Engineering	\$ -	\$ -	\$ -	\$ -	\$ -
3 Installation	\$ 66,217	\$ 66,217	\$ -	\$ -	\$ -
4 Contingency Allowance	\$ -	\$ -	\$ -	\$ -	\$ -
5 Construction Indirect Costs	\$ -	\$ -	\$ -	\$ -	\$ -
6 Interest During Construction	\$ -	\$ -	\$ -	\$ -	\$ -
7 Start-up Expenses	\$ -	\$ -	\$ -	\$ -	\$ -
8 Working Capital	\$ -	\$ -	\$ -	\$ -	\$ -
9 Other:	\$ -	\$ -	\$ -	\$ -	\$ -
10 TOTAL: Initial Capital Investment	\$ 98,100	\$ 103,823	\$ 5,723	\$ -	\$ 5,723

Costs should be entered in 1994 dollars.

Equipment Cost Index			
1986	797.6	1991	930.6
1987	813.6	1992	943.1
1988	852.0	1993	964.2
1989	895.1	1994	993.4
1990	915.1	1995	1015.3

Source: Marshall & Swift Equipment Cost Index
 Chemical Engineering Magazine; McGraw-Hill, Inc. New York, NY.
 (1995 index is estimated.)

Sheet B

Annual (non-energy) Cost Worksheet

Development of Superior Asphalt Recycling Agents

	Annual Cost Component	Conventional Unit	New Unit	Incremental Annual Costs	Incremental Savings	Net Cost Increment
1	Payroll plus Labor Indirects			\$ -	\$ -	\$ -
2	Operating Supplies		\$ -	\$ -	\$ -	\$ -
3	Maintenance Supplies	\$ -	\$ -	\$ -	\$ -	\$ -
4	Transportation	\$ -	\$ -	\$ -	\$ -	\$ -
5	Pollution Control and Waste Disposal			\$ -	\$ -	\$ -
6	Other Costs/Credits	\$ 6,130	\$ 1,081	\$ -	\$ 5,049	\$ (5,049)
7	TOTAL: Annual (non-energy) Costs	\$ 6,130	\$ 1,081	\$ -	\$ 5,049	\$ (5,049)

Costs should be entered in 1994 dollars.

Sheet C

Energy Savings Worksheet

Dvlopmt of Superior Asphalt Recycling Agents

180

	Annual Unit Energy Use (Million Btu/year)		Net Energy Saved
	Conventional Technology	New Technology	
	1 Distillate Oil	-	
2 Residual Oil	-	-	-
3 Natural Gas	-	-	-
4 Propane	-	-	-
5 Gasoline	-	-	-
6 Coking Coal	545	272	273
7 Steam Coal	-	-	-
8 Electricity	-	-	-
9 Other	-	-	-
10 Use by Others	-	-	-
11 TOTAL	545	272	273

1994 Fuel Prices (\$ per million Btu)		Default 1994 Fuel Prices* (\$ per million Btu)	
12 Distillate Oil	4.12	Distillate Oil	4.12
13 Residual Oil	2.35	Residual Oil	2.35
14 Natural Gas	2.96	Natural Gas	2.96
15 Propane	5.66	Propane	5.66
16 Gasoline	5.89	Gasoline	5.89
17 Coking Coal	1.53	Coking Coal	1.53
18 Steam Coal	1.36	Steam Coal	1.36
19 Electricity	4.50	Electricity	4.50
20 Other	2.00	Other	2.00

Express end-use electricity use as primary equivalent (10,500 Btu/kWh)

* Source: Energy Information Administration, Monthly Energy Review, April 1995; Energetics, Inc. estimates.

Energy Savings: Only net savings were provided for the analysis.

Sheet D

Waste Reduction Worksheet

	Annual Unit Waste Production (Tons/Year)		Net Waste Reduction	
	Conventional Technology	New Technology		
	<u>Non-combustion Related</u>			
1	Non-hazardous (RCRA)	273	137	136
2	Toxic (TRI)	-	-	-
3	Hazardous (non-TRI)	-	-	-
4	CFCs	-	-	-
5	VOCs	-	-	-
6	SHH	-	-	-
7	Other 2	-	-	-
8	Other 3	-	-	-
9	Other 4	-	-	-
<u>Combustion Related</u>				
10	Particulates	0	0	0
11	VOCs	0	0	0
12	Sulfur Dioxides	1	0	0
13	Nitrogen Oxides	0	0	0
14	Carbon Dioxide	57	28	28
15	TOTAL	330.8	165.9	165.0

SHH = Solid, hydrocarbon/organic, regulated under hazardous.

Development of Superior Asphalt Recycling Agents

Combustion Emission Rates (lbs/million Btu)						
	Particulates	VOCs	SOx	NOx	CO2	
16	Distillate Oil	0.010	0.002	0.160	0.140	161.000
17	Residual Oil	0.080	0.009	1.700	0.370	161.000
18	Natural Gas	0.003	0.006	0.000	0.140	113.000
19	Propane	0.003	0.006	0.000	0.140	113.000
20	Gasoline	0.000	0.090	0.000	0.140	162.000
21	Coking Coal	0.720	0.005	2.500	0.950	208.000
22	Steam Coal	0.720	0.005	2.500	0.950	208.000
23	Electricity	0.400	0.004	1.450	0.550	134.000
24	Other 1					

Electricity use expressed as primary equivalent (10,500 Btu/kWh)

Sheet E

Financial Worksheet**Unit Technology Inputs**

1	Discount rate:	10%
2	Equipment lifetime (yrs.):	24
3	Initial capital investment:	\$5,723
4	Annual costs:	(\$5,049)

Development of Superior Asphalt Recycling Agents**User's Unit Summary Financial Results**

5	Annual energy income:	\$418
6	Annual net income:	\$5,467
7	Total Life Cycle Cost:	\$5,723
8	Total Life Cycle Benefit:	\$49,117
9	Net Present Value:	\$43,394
10	Benefit-Cost Ratio:	8.58
11	Internal Rate of Return:	95.52%
12	Rate of Return:	95.52%
13	Uniform Capital Recovery Factor:	0.1113
14	Levelized Cost of Energy (per mil. Btu):	-\$16.16
15	Annual Production Cost Savings:	\$4,830
16	Discounted Payback Period:	1.20

Express cost inputs as 1994\$

Sheet F

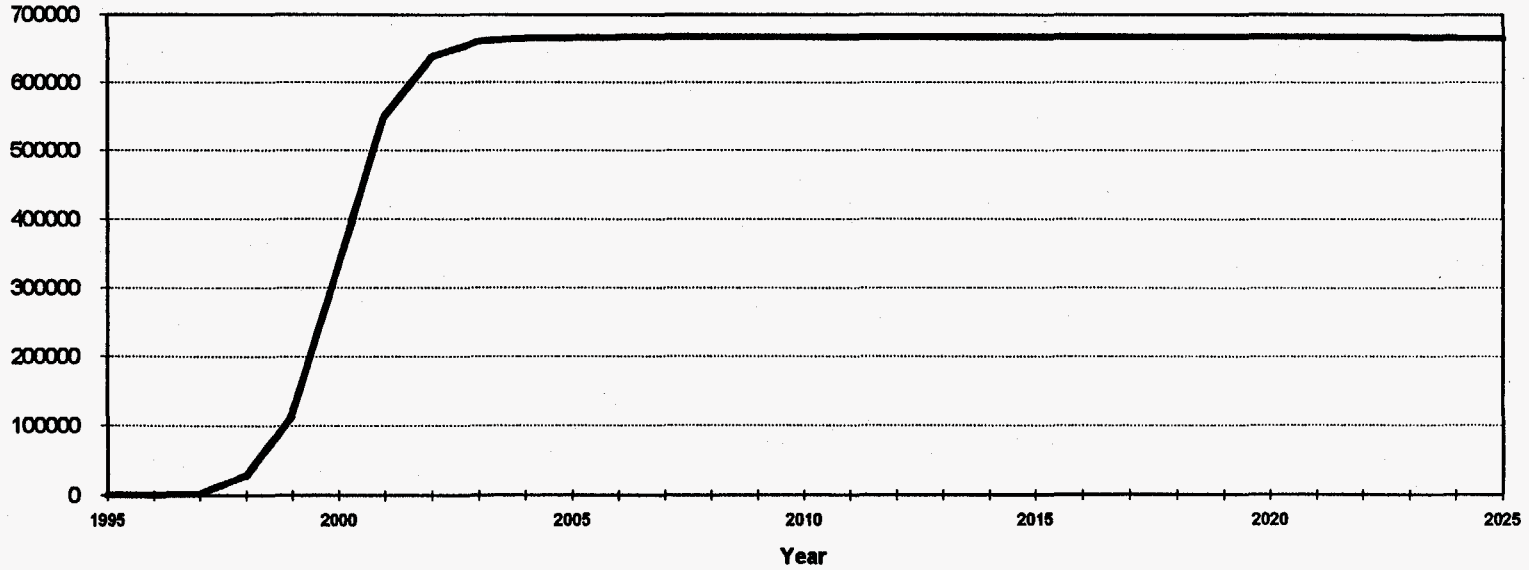
Market Penetration Worksheet

Development of Superior Asphalt Recycling Agents

Inputs		
1	Hurdle rate IRR (%):	25%
2	Year of introduction:	1997
3	Number of units at introduction:	2000
4	Total potential market (# units):	2,000,000.00
5	Maximum market penetration (fraction):	0.33
6	Number of years at market saturation:	10

Market Penetration		
25	Internal Rate of Return:	96%
26	Market share at introduction:	0%

Number of Units in Operation



Sheet G

Market Penetration Results

Dvlopmt of Superior Asphalt Recycling Agents

	Year	Units in Operation	Energy Savings <i>million Btu/year</i>	Waste Reduction <i>tons/year</i>	Prod. Cost Savings <i>(\$/Year)</i>
1	1995	-	-	-	-
2	1996	-	-	-	-
3	1997	2000	546,000	329,924	9,659,443
4	1998	27718	7,567,014	4,572,414	133,870,217
5	1999	114320	31,209,360	18,858,443	552,133,748
6	2000	331134	90,399,582	54,624,490	1,599,284,959
7	2001	549541	150,024,693	90,653,321	2,654,129,917
8	2002	637681	174,086,913	105,193,061	3,079,821,559
9	2003	659859	180,141,507	108,851,586	3,186,935,120
10	2004	664704	181,464,192	109,650,826	3,210,335,120
11	2005	665728	181,743,744	109,819,747	3,215,280,755
12	2006	665943	181,802,439	109,855,214	3,216,319,145
13	2007	665988	181,814,724	109,862,638	3,216,536,482
14	2008	665997	181,817,181	109,864,122	3,216,579,950
15	2009	665999	181,817,727	109,864,452	3,216,589,609
16	2010	666000	181,818,000	109,864,617	3,216,594,439
17	2011	666000	181,818,000	109,864,617	3,216,594,439
18	2012	666000	181,818,000	109,864,617	3,216,594,439
19	2013	666000	181,818,000	109,864,617	3,216,594,439
20	2014	666000	181,818,000	109,864,617	3,216,594,439
21	2015	666000	181,818,000	109,864,617	3,216,594,439
22	2016	666000	181,818,000	109,864,617	3,216,594,439
23	2017	666000	181,818,000	109,864,617	3,216,594,439
24	2018	666000	181,818,000	109,864,617	3,216,594,439
25	2019	666000	181,818,000	109,864,617	3,216,594,439
26	2020	666000	181,818,000	109,864,617	3,216,594,439
27	2021	665997	181,817,181	109,864,122	3,216,579,950
28	2022	665988	181,814,724	109,862,638	3,216,536,482
29	2023	665943	181,802,439	109,855,214	3,216,319,145
30	2024	665728	181,743,744	109,819,747	3,215,280,755
31	2025	664704	181,464,192	109,650,826	3,210,335,120

Total Energy Savings

Development of Superior Asphalt Recycling Agents

Year	Number of Units in Operation	Energy Savings by Fuel Type (million Btus)					
		Distillate Oil	Residual Oil	Natural Gas	Propane	Gasoline	Coking Coal
1990	-	-	-	-	-	-	-
1995	-	-	-	-	-	-	90,399,582
2000	331,134	-	-	-	-	-	181,743,744
2005	665,728	-	-	-	-	-	181,818,000
2010	668,000	-	-	-	-	-	181,818,000
2015	668,000	-	-	-	-	-	181,818,000
2020	668,000	-	-	-	-	-	181,818,000
2025	664,704	-	-	-	-	-	181,464,192

1
2
3
4
5
6
7
8

Year	Number of Units in Operation	Total Energy Savings			
		Steam Coal	Electricity	Other	1994 \$
1990	-	-	-	-	-
1995	-	-	-	-	-
2000	331,134	-	-	-	138,311,360
2005	665,728	-	-	-	278,067,928
2010	668,000	-	-	-	278,181,540
2015	668,000	-	-	-	278,181,540
2020	668,000	-	-	-	278,181,540
2025	664,704	-	-	-	277,640,214

9
10
11
12
13
14
15
16

Total Waste Reduction

Development of Superior Asphalt Recycling Agents

Year	Number of Units in Operation	Waste Reduction by Waste Type (tons)								
		***** Non-Combustion Related *****								
		Non-hazardous (RCRA)	Toxic (TRI)	Hazardous (non-TRI)	CFCs	VOCs	SHH	Other 2	Other 3	Other 4
1 1990	-	-	-	-	-	-	-	-	-	-
2 1995	-	-	-	-	-	-	-	-	-	-
3 2000	331,134	45,034,224	-	-	-	-	-	-	-	-
4 2005	665,728	90,539,008	-	-	-	-	-	-	-	-
5 2010	666,000	90,576,000	-	-	-	-	-	-	-	-
6 2015	666,000	90,576,000	-	-	-	-	-	-	-	-
7 2020	666,000	90,576,000	-	-	-	-	-	-	-	-
8 2025	664,704	90,399,744	-	-	-	-	-	-	-	-

Year	Number of Units in Operation	Waste Reduction by Waste Type (tons)					TOTAL WASTE REDUCTION (tons)
		***** Combustion Related *****					
		Particulates	VOCs	Sulfur Dioxides	Nitrogen Oxides	Carbon Dioxide	
9 1990	-	-	-	-	-	-	-
10 1995	-	-	-	-	-	-	-
11 2000	331,134	32,544	226	112,999	42,940	9,401,557	54,624,490
12 2005	665,728	65,428	454	227,180	86,328	18,901,349	109,819,747
13 2010	666,000	65,454	455	227,273	86,364	18,909,072	109,864,617
14 2015	666,000	65,454	455	227,273	86,364	18,909,072	109,864,617
15 2020	666,000	65,454	455	227,273	86,364	18,909,072	109,864,617
16 2025	664,704	65,327	454	226,830	86,195	18,872,276	109,650,826